UNIVERSIDADE FEDERAL DE UBERLÂNDIA
INSTITUTO DE BIOTECNOLOGIA
PÓS-GRADUAÇÃO EM GENÉTICA E BIOQUÍMICA

APLICAÇÕES DA TECNOLOGIA DO PHAGE DISPLAY NA SELEÇÃO DE ANTICORPOS E LIGANTES PARA FINS TERAPÊUTICOS EM INFECÇÕES, INFLAMAÇÃO E OFIDISMO

Aluna: Jessica Brito de Souza

Orientadora: Profª. Drª. Belchiolina Beatriz Fonseca / IBTEC-UFU

Coorientadora: Drª. Emília Rezende Vaz / IBTEC-UFU

UBERLÂNDIA – MG
2022

UNIVERSIDADE FEDERAL DE UBERLÂNDIA
INSTITUTO DE BIOTECNOLOGIA
PÓS-GRADUAÇÃO EM GENÉTICA E BIOQUÍMICA

APLICAÇÕES DA TECNOLOGIA DO PHAGE DISPLAY NA SELEÇÃO DE ANTICORPOS E LIGANTES PARA FINS TERAPÊUTICOS EM INFECÇÕES, INFLAMAÇÃO E OFIDISMO

Aluna: Jessica Brito de Souza

Orientadora: Profª. Drª. Belchiolina Beatriz Fonseca

Coorientadora: Drª. Emília Rezende Vaz

> **Tese apresentada à Universidade Federal de Uberlândia como parte dos requisitos para obtenção do Título de Doutora em Genética e Bioquímica (Área Genética)**

UBERLÂNDIA – MG

2022

UNIVERSIDADE FEDERAL DE UBERLÂNDIA

Coordenação do Programa de Pós-Graduação em Genética e Bioquímica

Av. Pará 1720, Bloco 2E, Sala 244 - Bairro Umuarama, Uberlândia-MG, CEP 38400-902

Telefone: +55 (34) 3225-8438 - www.ppggb.ibtec.ufu.br - ppggb@ufu.br

ATA DE DEFESA - PÓS-GRADUAÇÃO

Programa de Pós-Graduação em:	Genética e Bioquímica
Defesa de:	Doutorado Acadêmico/PPGGB.

Data:	Vinte e sete de julho de dois mil e vinte e dois.	Hora de início:	14:00h	Hora de encerramento:	18:00

Matrícula do Discente:	11723GBI003
Nome do Discente:	Jéssica Brito de Souza
Título do Trabalho:	Aplicações da tecnologia do *Phage Display* na seleção de anticorpos e ligantes para fins terapêuticos em infecções, inflamação e ofidismo.
Área de concentração:	Genética
Linha de pesquisa:	Nanobiotecnologia.
Projeto de Pesquisa de vinculação:	INCT em Teranóstica e Nanobiotecnologia (INCT-TeraNano).

Aos vinte e sete dias do mês de julho de dois mil e vinte e dois, às 14:00 horas, reuniu-se via web conferência pela Plataforma *Google Meet*, em conformidade com a Portaria nº 36, de 19 de março de 2020 da Coordenação de Aperfeiçoamento de Pessoal de Nível Superior – CAPES, Resolução de nº 06/2020 e Resolução nº 19/2022 do Conselho de Pesquisa e Pós-graduação pela Universidade Federal de Uberlândia, a Banca Examinadora, designada pelo Colegiado do Programa de Pós-graduação em Genética e Bioquímica, assim composta: Dr. Vasco Ariston de Carvalho Azevedo, Dr. Álvaro Ferreira Junior, Drª. Hebréia Oliveira Almeida Souza, Dr. Foued Salmen Espindola e Drª. Belchiolina Beatriz Fonseca, orientadora da candidata e demais convidados presentes conforme lista de presença. Iniciando os trabalhos a presidente da mesa, Drª. Belchiolina Beatriz Fonseca apresentou a Comissão Examinadora e a candidata, agradeceu a presença do público, e concedeu à Discente a palavra para a exposição do seu trabalho. A duração da apresentação da Discente e o tempo de arguição e resposta foram conforme as normas do Programa de Pós-graduação em Genética e Bioquímica. A seguir a senhora presidente concedeu a palavra, pela ordem sucessivamente, aos examinadores, que passaram a arguir a candidata. Ultimada a arguição, que se desenvolveu dentro dos termos regimentais, a Banca, em sessão secreta, atribuiu os conceitos finais. Em face do resultado obtido, a Banca Examinadora considerou a candidata:

APROVADA.

Esta defesa de Tese de Doutorado é parte dos requisitos necessários à obtenção do título de Doutor. O competente diploma será expedido após cumprimento dos demais requisitos, conforme as normas do Programa, a legislação pertinente e a regulamentação interna da UFU. Nada mais havendo a tratar foram encerrados os trabalhos. Foi lavrada a presente ata que após lida e achada conforme foi assinada pela Banca Examinadora.

Documento assinado eletronicamente por **Belchiolina Beatriz Fonseca**, **Professor(a) do Magistério Superior**, em 27/07/2022, às 18:21, conforme horário oficial de Brasília, com fundamento no art. 6º,

§ 1º, do Decreto nº 8.539, de 8 de outubro de 2015.

Documento assinado eletronicamente por **Foued Salmen Espíndola**, **Professor(a) do Magistério Superior**, em 27/07/2022, às 18:42, conforme horário oficial de Brasília, com fundamento no art. 6º, § 1º, do Decreto nº 8.539, de 8 de outubro de 2015.

Documento assinado eletronicamente por **Hebreia Oliveira Almeida Souza**, **Usuário Externo**, em 27/07/2022, às 18:49, conforme horário oficial de Brasília, com fundamento no art. 6º, § 1º, do Decreto nº 8.539, de 8 de outubro de 2015.

Documento assinado eletronicamente por **Álvaro Ferreira Júnior**, **Usuário Externo**, em 27/07/2022, às 19:02, conforme horário oficial de Brasília, com fundamento no art. 6º, § 1º, do Decreto nº 8.539, de 8 de outubro de 2015.

Documento assinado eletronicamente por **Vasco Ariston de Carvalho Azevedo**, **Usuário Externo**, em 28/07/2022, às 10:52, conforme horário oficial de Brasília, com fundamento no art. 6º, § 1º, do Decreto nº 8.539, de 8 de outubro de 2015.

A autenticidade deste documento pode ser conferida no site https://www.sei.ufu.br/sei/controlador_externo.php? acao=documento_conferir&id_orgao_acesso_externo=0, informando o código verificador **3722761** e o código CRC **B06CB6FA**.

Referência: Processo nº 23117.046178/2022-17 SEI nº 3722761

UNIVERSIDADE FEDERAL DE UBERLÂNDIA
INSTITUTO DE BIOTECNOLOGIA
PÓS-GRADUAÇÃO EM GENÉTICA E BIOQUÍMICA

APLICAÇÕES DA TECNOLOGIA DO PHAGE DISPLAY NA SELEÇÃO DE ANTICORPOS E LIGANTES PARA FINS TERAPÊUTICOS EM INFECÇÕES, INFLAMAÇÃO E OFIDISMO

Aluna: Jessica Brito de Souza

COMISSÃO EXAMINADORA

Presidente: Profª. Drª. Belchiolina Beatriz Fonseca (orientadora)

Examinadores: Prof. Dr. Vasco Ariston de Carvalho Azevedo
Prof. Dr. Álvaro Ferreira Junior
Prof.ª Drª. Hebréia Oliveira Almeida Souza
Prof. Dr. Foued Salmen Espindola

Data da defesa: 27/07/2022

As sugestões da Comissão Examinadora e as Normas PPGGB para o formato da Tese foram contempladas.

_____

Profª. Drª. Belchiolina Beatriz Fonseca

"A persistência é o menor caminho do êxito"

(Charles Chaplin)

DEDICATÓRIA

Dedico esse trabalho ao meu eterno orientador **Prof. Dr. Luiz Ricardo Goulart Filho**! Você foi grandioso, e seu legado será para sempre.

AGRADECIMENTOS

Às **Agências de Fomento CAPES, CNPq, FAPEMIG e INCT-Teranano**, pelo auxílio financeiro concedido nessa pesquisa.

A **todos** que colaboraram conosco e auxiliaram no desenvolvimento desse trabalho!

AGRADECIMENTOS ESPECIAIS

Agradeço à **Deus** pela vida e por sempre conduzir o meu caminho.

Agradeço aos meus pais, **Henrique** e **Lúcia**, por todo o carinho e apoio oferecidos diariamente. Obrigada pela compreensão e por sempre me ensinarem a ver o lado bom de tudo e por me mostrarem o quanto é importante ser resiliente. Vocês são tudo na minha vida e o maior motivo de todas as minhas conquistas. Gratidão imensa por tê-los como pais e por sempre me motivarem. Essa conquista é para vocês!

A minha irmã, **Clara**, sou extremamente grata pelo companheirismo, parceria e carinho em todos os momentos. Obrigada pela compreensão nos dias mais difíceis e pela companhia diária. Aprendo todos os dias com você.

A minha avó **Nina** que representa, fisicamente, todos os meus outros avós eu agradeço pelas orações e por todo o afeto transmitido.

À **família Brito e família Souza e Marra**, agradeço por todo o carinho e apoio durante todas as fases da minha vida. Vocês são o significado real de que quem tem família tem tudo.

Aos meus amigos **Adriele, Aline, Camila, Felipe, Gabriel, Hiago, Luiza, Mariana, Radif, Tamiris, Victor,** agradeço por todo apoio e amizade. Vocês tornam a minha caminhada mais leve e feliz.

Ao **Prof. Dr. Luiz Ricardo Goulart Filho**, que nos deixou de forma precoce, eu agradeço imensamente pela oportunidade de crescimento profissional e pessoal. Foram muitos aprendizados, dentre o maior deles foi sempre mostrar a importância do trabalho em equipe e que juntos vamos sempre mais longe. É uma honra ter sido sua orientada e saber que o seu legado é eterno. Você foi e sempre será referência em qualquer lugar do mundo.

APOIO FINANCEIRO

SUMÁRIO

LISTA DE FIGURAS

LISTA DE ABREVIATURAS

PD	Phage Display
PLA$_2$	Fosfolipase A$_2$
CMSP	Células mononucleares do sangue periférico
scFv	Fragmentos variáveis de cadeia simples
SP	*Salmonella* Pullorum
IL-1β	Interleucina 1-beta
TNF-α	Fator de necrose tumoral alfa
LPS	Lipopolissacarídeo
IFN-γ	Interferon-gama
OMS	Organização Mundial da Saúde
DNA	Ácido Desoxirribonucleico
ELISA	Ensaio de imunoabsorção enzimática
PCR	Reação em cadeia da polimerase
kDa	quilodalton
VH	Domínio variável
CH	Domínio constante
Fab	Fragmento de ligação ao antígeno
Fc	Região constante
Fv	Região variável
VL	Domínio variável de cadeia leve
VH	Domínio varivável de cadeia pesada
NK	*Natural Killer*
SVMP	Metaloproteinases de veneno de cobra
PAF	Ativador de plaquetas

RESUMO

A técnica de Phage Display (PD) é bastante utilizada para a descoberta e desenvolvimento de medicamentos. Uma das suas grandes aplicabilidades, é conseguir aprimorar os estudos imunológicos. Tendo isso em vista, o objetivo desse trabalho foi utilizar o PD para selecionar moléculas com atividades antiveneno e anti-inflamatória, além disso propor um modelo *in vivo* para validações. Para isso, nós selecionamos anticorpos neutralizantes do veneno da *Bothrops pauloensis (B. pauloensis)* pela tecnologia do PD que, posteriormente, foi expresso em plantas para avaliar a atividade enzimática do anticorpo. A fim de propor um modelo para inflamação e infecção útil para testar fagos e peptídeos selecionados pela tecnologia do PD, nós padronizamos um modelo *in vivo* de inflamação e infecção sistêmica a partir do embrião de galinhas para que fagos selecionados pelo PD possam ser usados em testes preliminares. E, finalmente, a partir da tecnologia do PD um inibidor de fosfolipase A$_2$ (PLA$_2$) selecionado a partir do veneno da *B. pauloensis*, nomeado como F7, foi testado para ação anti-inflamatória em células mononucleares do sangue periférico (CMSP) e modelo de embrião de galinha. Os ensaios proteolíticos mostraram a capacidade das moléculas de fragmentos variáveis de cadeia simples (scFv) em inibir as ações danosas do veneno da *B. pauloensis* e verificamos que o anticorpo neutralizou os efeitos tóxicos do envenenamento, principalmente aqueles relacionados a processos sistêmicos, interagindo com uma das classes enzimáticas predominantes, as metaloproteinases. Um modelo para infecção e inflamação sistêmica foi padronizado em embriões de galinhas infectados pela *Salmonella* Pullorum (SP). Esse é um modelo interessante de infecção e inflamação sistêmica e fagos selecionados por PD podem ser testados nesse modelo desde que purificado sem a presença da *Escherichia coli (E.coli).* O inibidor da PLA$_2$ selecionado (F7) foi capaz de modular a secreção de citocinas inflamatórias (IL-1β e TNF-α) em CMSP tratados com lipopolissacarídeo (LPS) mostrando os efeitos anti-inflamatórios do F7. No embrião, o fago F7 também apresentou as mesmas propriedades para as citocinas IL-1β e IFN-γ embora não tenha contido a mortalidade dos embriões. Esse trabalho apresenta duas moléculas potenciais para a terapia antiofídica e anti-inflamatória, sendo elas um

scFv e o F7, respectivamente. Em especial, o peptídeo F7 deve ser testado em outros modelos de inflamação branda e localizada para viabilizar sua aplicação *in vivo*.

Palavras-chave: anti-veneno; bacteriófago; *biopanning*; imunomodulação

ABSTRACT

Phage Display (PD) technique is widely used for drug discovery and development. One of its great applications is to improve immunological studies. The objective of this work was to select by PD molecules with antivenom and anti-inflammatory activities, besides proposing an *in vivo* model for validations. For this, we selected neutralizing antibodies from *B. pauloensis* venom by PD technology that was subsequently expressed in plants to evaluate the enzymatic activity of the antibody. To propose a model for inflammation and infection useful for testing phages and peptides selected by PD technology, we standardized an *in vivo* model of systemic inflammation and infection from chicken embryo so that phages selected by PD can be used in preliminary tests. And finally, from the PD technology a phospholipase A_2 (PLA_2) inhibitor selected from *B. pauloensis* venom, named as F7, was tested for anti-inflammatory action in peripheral blood mononuclear cells (PBMC) and chicken embryo model. Proteolytic assays showed the ability of single chain variable fragment (scFv) molecules to inhibit the damaging actions of *B. pauloensis* venom and we found that the antibody neutralized the toxic effects of the envenomation, mainly those related to systemic processes, by interacting with one of the predominant enzyme classes, the metalloproteinases. A model for systemic infection and inflammation has been standardized in chicken embryos infected by *Salmonella* Pullorum (SP). This is an interesting model for infection and systemic inflammation and phages selected by PD can be tested in this model provided they are purified without the presence of *Escherichia coli* (*E.coli*). The selected PLA_2 inhibitor (F7) was able to modulate the secretion of inflammatory cytokines (IL-1β and TNF-α) in lipopolysaccharide (LPS)-treated PBMCs showing the anti-inflammatory effects of F7. In the embryo the phage F7 also showed the same properties for the cytokines IL-1β and IFN-γ although it did not contain embryo mortality. This work presents two potential molecules for antiviral and anti-inflammatory therapy, being a scFv and F7, respectively. In particular, the F7 peptide should be tested in other models of mild and localized inflammation to enable its application *in vivo*.

Keywords: anti-venom; bacteriophage; biopanning; immunomodulation.

APRESENTAÇÃO

O Phage Display (PD) é uma técnica de seleção eficiente que expressa peptídeos, proteínas ou fragmentos de anticorpos na superfície de partículas de fagos, podendo ser extremamente útil para o tratamento e prevenção de uma série de doenças. O ofidismo é considerado pela Organização Mundial da Saúde (OMS) uma doença tropical negligenciada de grande importância pelo número de acidentes e óbitos. As principais classes enzimáticas responsáveis pelos efeitos locais dos venenos botrópicos são as metaloproteases e as fosfolipases A_2 (PLA_2s), e por isso se tornaram alvo do PD para tentar desenvolver moléculas seguras, a fim de diminuir o número de óbitos. As PLA_2s vêm ganhando relevância cada vez maior nos processos inflamatórios, de forma que elas estão relacionadas em várias condições patológicas. Dessa forma, torna importante desenvolver mecanismos para regular sua atividade e desenvolver inibidores como potenciais agentes farmacêuticos para tratar doenças inflamatórias.

Baseado na importância do ofidismo no Brasil e na necessidade de desenvolver novas moléculas inflamatórias, o objetivo geral desse trabalho foi selecionar e caracterizar por PD ligantes de componentes do veneno da *Bothrops pauloensis* (*B. pauloensis*) para fins terapêuticos contra o ofidismo e a inflamação. Além disso, avaliar um modelo de infecção e inflamação *in vivo* para testes com fagos ou peptídeos selecionados por PD.

No Capítulo I, realizamos uma revisão geral da literatura sobre o PD, as propriedades dos componentes do veneno da *B. pauloensis* e o uso de ligantes dos componentes para fins de terapia no ofidismo e na inflamação.

No Capítulo II, apresentamos três artigos científicos. O primeiro artigo (DOI: 10.1016/j.ijbiomac.2020.02.028) descreve a seleção de anticorpos neutralizantes do veneno da *B. pauloensis* pela tecnologia do PD que, posteriormente, foi expresso em plantas para avaliar a atividade enzimática do anticorpo. Nós avaliamos, por ensaios proteolíticos, a capacidade das moléculas de fragmentos variáveis de cadeia simples (scFv) em inibir as ações danosas do veneno da *B. pauloensis* e após, verificamos que o anticorpo neutralizou os efeitos tóxicos do envenenamento, principalmente aqueles relacionados a

processos sistêmicos, interagindo com uma das classes predominantes de metaloproteinases.

No segundo artigo, descrevemos a padronização de um modelo *in vivo* de inflamação e infecção sistêmica, a partir do embrião de galinhas para que fagos selecionados pelo PD possam ser usados em testes de validação. Esse artigo mostra que embriões de galinhas infectados pela *Salmonella* Pullorum são um modelo interessante de infecção e inflamação sistêmica e que o fago selecionado por PD pode ser usado nesse modelo desde que purificado sem a presença da *Escherichia coli (E.coli).*

O terceiro artigo descreve a seleção de fagos ligantes da PLA$_2$ do veneno da *B. pauloensis* e sua ação anti-inflamatória em células mononucleares do sangue periférico (CMSP) e modelo de embrião de galinha. O inibidor da PLA$_2$ selecionado (F7) foi capaz de modular a secreção de citocinas inflamatórias (IL-1β e TNF-α) em CMSP tratados com lipopolissacarídeo (LPS) mostrando os efeitos anti-inflamatórios do F7. No embrião, o fago F7 também apresentou as mesmas propriedades para as citocinas IL-1β e IFN-γ embora não pode conter a mortalidade dos embriões.

Esse trabalho apresenta duas moléculas potenciais para a terapia antiofídica e anti-inflamatória. Em especial, o peptídeo F7 deve ser testado em outros modelos de inflamação para que sua aplicação *in vivo* seja reconhecida e aplicada.

Capítulo 1

Fundamentação Teórica

1. Phage Display

1.1.   Técnica

O Phage Display (PD) é uma técnica de biologia molecular que consiste na expressão de peptídeos, proteínas ou fragmentos de anticorpos na superfície de partículas de fagos (WILLATS, 2002). Essa técnica foi descrita pela primeira vez em 1985 por George Smith, considerada inovadora por conseguir ligar um genótipo e um fenótipo fisicamente em uma única partícula viral e amplificá-los bilhões de vezes em bactérias (SMITH, 1985). De forma mais detalhada, fragmentos de ácido desoxirribonucleico (DNA) exógenos conseguem ser incorporados no genoma do fago de forma que o peptídeo ou proteína expressado fique exposto na superfície em fusão com uma proteína endógena (PARMLEY; SMITH, 1988). Essa exposição permite uma interação com uma ampla diversidade de moléculas-alvo externas, e, posteriormente, o isolamento desses ligantes exibidos na superfície do fago (SCOTT; SMITH, 1990).

1.2.   Aplicações do Phage Display

O PD é um método que apresenta alto rendimento e que apesar da seleção de proteínas ser a principal característica, ele tem sido utilizado em diversos outros campos da biotecnologia. Dentre eles, para o desenvolvimento de vacinas, interação proteína-proteína, seleção de substratos e inibidores e mapeamento de epítopos (EBRAHIMIZADEH; RAJABIBAZL, 2014). Pelo reconhecimento das novas descobertas por meio dessa técnica, contribuindo de forma revolucionária e significativa para a química e o desenvolvimento de biofarmacêuticos, os criadores George P. Smith e Sir Gregory P. Winter foram concedidos com parte do Prêmio Nobel de Química de 2018 (BARDERAS; BENITO-PEÑA, 2019).

1.3.   Tipos de bacteriófagos

Bacteriófagos ou fagos consistem em vírus que infectam uma bactéria hospedeira e utilizam o seu sistema para replicar o próprio DNA e expressar vários peptídeos ou proteínas no capsídeo do bacteriófago. O sistema de PD pode ser classificado de acordo com o tipo de vetor de expressão que é utilizado. Os 4 tipos de fagos principais existentes são T7, lambda, T4 ou M13. O fago T7 é um vírus de DNA que apresenta ciclo de vida lítico, sendo montado no citoplasma e liberado pela lise das bactérias. O lambda é constituído por um dsDNA linear e duas proteínas de revestimento principais (proteína D e proteína PV). O T4 tem um genoma de DNA de fita dupla e infecta *E.coli* (TAN et al., 2016).

Dentre os fagos filamentosos, o grupo mais explorado e estudado é o fago específico do pilus F ou Ff, conhecido como f1, fd e M13 (FOULADVAND et al., 2020). O fago utilizado com maior frequência no PD é o M13, por conter regiões não essenciais que possibilitam inserções de genes exógenos (DENG et al., 2018). Ele é um fago filamentoso específico de *E.coli*, que apresenta uma forma cilíndrica com cerca de 930 nm de comprimento e 6 nm de diâmetro (ANAND et al., 2021). Possui DNA de fita simples cercado por um revestimento proteico. Esse revestimento contém 5 proteínas diferentes. Nas extremidades da partícula estão localizadas as proteínas de revestimento menores, pIII e pVI em uma extremidade, e pVII e pIX na outra extremidade. Há quatro ou cinco cópias de cada uma dessas proteínas no fago. A predominante que cobre todo o comprimento da partícula é a pVIII (SIDHU, 2001) (Figura 1). Por sua vez, a proteína pIII é a responsável pela ligação do fago à célula hospedeira, que consiste no primeiro passo da infecção.
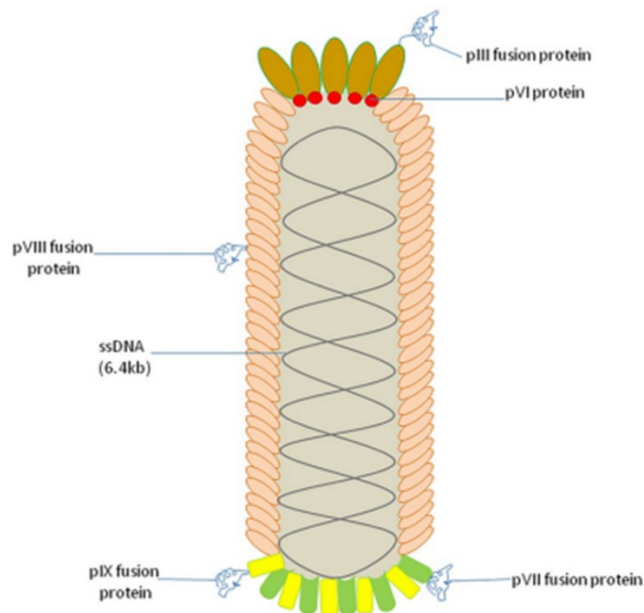
Figura 1. Representação do fago M13. Fonte: ANAND et al (2021).

1.4. Processo de infecção

O processo de infecção começa quando a pIII se liga ao pilus F na superfície da *E.coli* e em seguida, insere o ssDNA no citoplasma da bactéria. No interior dela, a fita simples do DNA viral é transformada em fita dupla, através da utilização da maquinaria da bactéria pelo genoma do fago. Esse material genético duplicado é usado de modelo para produzir todas as proteínas do fago. O genoma do fago apresenta duas regiões de codificação, sendo que tem um promotor mais forte que faz a síntese de proteínas mais utilizadas como a pVIII, e um promotor menos eficiente que codifica proteínas usadas com menor frequência (WEIGEL; SEITZ, 2006; WILSON; FINLAY, 1998). Alguns fatores são utilizados para categorizar o PD com o fago do tipo M13, dentre eles a proteína de revestimento, a expressão da proteína de revestimento e os vetores, podendo ser por exemplo do tipo 3, 33, 8 ou 88. No caso da exibição do tipo 3, o gene de interesse é inserido a jusante do gene pIII no genoma do M13, fazendo com que todas as proteínas pIII sejam expressas de forma recombinante e carregando a proteína de fusão (EBRAHIMIZADEH; RAJABIBAZL, 2014). Em virtude da baixa

quantidade da pIII comparada com a pVIII, as bibliotecas de peptídeos sintéticos em fusão com a pIII são mais indicadas para a seleção de ligantes com alta afinidade do que as bibliotecas ligadas a pVIII (BRIGIDO; MARANHÃO, 2002).

O *biopanning* é um processo *in vitro* em que a seleção de sequências ocorre por meio da afinidade de ligação do fago a uma molécula alvo. Em primeiro lugar, é feito a imobilização do alvo em algum tipo de meio sólido, seja em placas de Ensaio de imunoabsorção enzimática (ELISA), em microesferas magnéticas ou de afinidade, resinas ou membranas. Depois de imobilizado, a biblioteca de peptídeos expostos em fagos é incubada contra o alvo. São realizadas lavagens sucessivas para eliminar os fagos que não se ligaram. Os fagos específicos permanecem ligados e depois serão eluidos, para que sejam amplificados para os ciclos posteriores de seleção biológica ou *biopanning*. Dessa forma, ao final do processo há um maior número de fagos com sequências específicas contra o alvo e eles podem ser caracterizados por sequenciamento de DNA, *western blotting* ou ELISA (SMITH, 1985) (Figura 2).
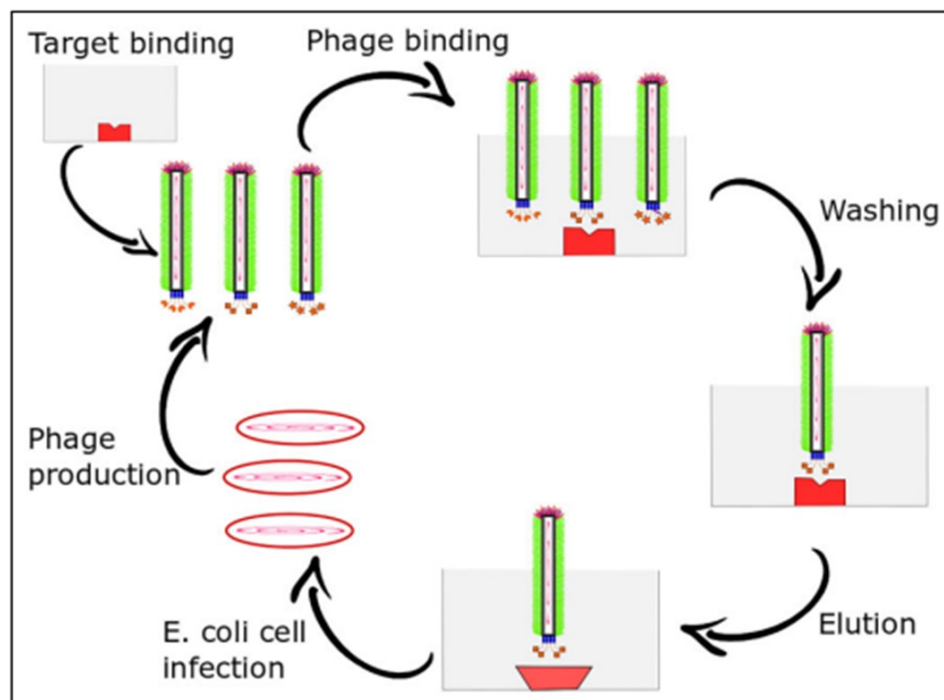
Figura 2. Esquema do *biopanning*. Técnica de seleção por afinidade utilizada para selecionar os fagos-alvo. No início do processo, as bibliotecas de PD são incubadas com o alvo que está imobilizado em uma placa sólida. Em seguida, as partículas de

fago são ligadas, enquanto os fagos que não se ligaram são eliminados durante as lavagens sucessivas. As partículas de fago que apresentaram afinidade e se ligaram ao alvo são posteriormente eluídas e amplificadas por infecção de bactérias. Fonte: ZAMBRANO-MILA et al (2020).

1.5.   Tipos de Phage Display

1.5.1. Phage Display de Peptídeos

Na década de 1990, a técnica de PD foi aprimorada e tornou-se possível utilizar uma biblioteca de epítopos para selecionar milhões de peptídeos curtos que apresentam uma forte ligação a um anticorpo (DEVLIN; PANGANIBAN; DEVLIN, 1990). Isto ocorre a partir de uma proteína de ligação que purifica, por afinidade, aqueles fagos que exibem peptídeos de ligações mais fortes. Eles são propagados em *E.coli* e depois há o sequenciamento da região de codificação correspondente aos DNAs virais, para obter as sequências de aminoácidos dos peptídeos exibidos no fago (SCOTT; SMITH, 1990). A construção de bibliotecas de PD que expressam peptídeos é extremamente relevante porque a partir dos peptídeos selecionados por afinidade, é possível descobrir miméticos de epítopos ou mesmo predizer epítopos (RYVKIN et al., 2018). Recentemente, uma grande biblioteca com mais de 2 x 10^{10} clones foi gerada por autoligação de produto de reação em cadeia da polimerase (PCR) com plasmídeo inteiro (KONG et al., 2020). A obtenção de bibliotecas cada vez maiores permite aos pesquisadores expandir os possíveis alvos das aplicações do PD.

Este tipo de PD permite a seleção de peptídeos que são agonistas ou antagonistas de receptores, peptídeos usados como antibióticos ou peptídeos que desempenham função de inibidores enzimáticos (LADNER et al., 2004). Dessa forma, apresentam várias aplicações médicas, dentre elas no câncer e lesões metastáticas, em doenças infecciosas parasitárias, doenças infecciosas virais, distúrbios degenerativos da articulação, doenças cardíacas, lesões cerebrais (ZAMBRANO-MILA; BLACIO; VISPO, 2020).

1.5.2. Phage Display de Anticorpos

O anticorpo é uma proteína heterodimérica com 150 quilodalton (kDa), composto por duas cadeias pesadas (50 kDa) e duas leves (25 kDa), ambas idênticas. Estas últimas apresentam um domínio variável (VH) e três domínios constantes (CH1, CH2 e CH3). Do ponto de vista funcional, o anticorpo tem dois fragmentos de ligação ao antígeno (Fabs) e uma região constante (Fc) sendo que estas estruturas ficam unidas por uma região flexível. Os antígenos se ligam à região variável (Fv) que é formada pelas regiões dos domínios variáveis nas cadeias leve (VL) e pesada (VH) (KIM; PARK; HONG, 2005) (Figura 3).
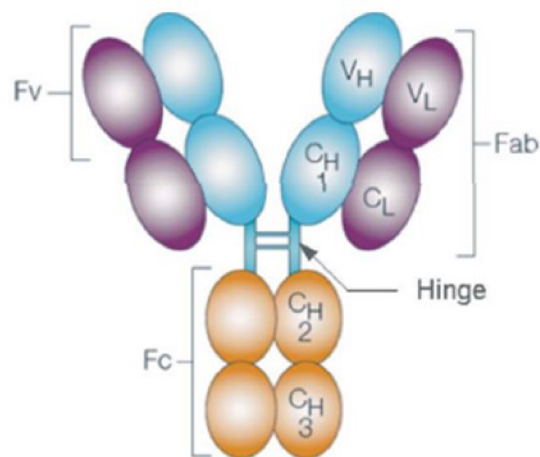
Figura 3. Estrutura da molécula de anticorpo. Fonte: KIM et al (2005), com modificações.

Pelo fato da molécula de anticorpo apresentar um tamanho maior, a sua exposição na superfície do fago se torna mais desafiadora. O Fab e o fragmento variável de cadeia única (scFv) têm tido êxito no processo de exibição em fagos por serem menores, ~50 kDa e ~28 kDa, respectivamente (BARBAS et al., 2001; HOOGENBOOM et al., 1991; WINTER et al., 1994). Os Fabs consistem em uma região variável de uma imunoglobulina, apresentando um domínio VL, um domínio VH, um CL e um CH1. O scFv é um polipeptídeo mimético da região Fv do anticorpo, em que os segmentos VH e VL estão unidos por um linker

polipeptídico flexível que confere estabilidade a molécula (HOLLIGER; HUDSON, 2005).

MCCAFFERTY et al (1990) foram os primeiros a descreverem a seleção de PD de anticorpos, quando conseguiram fusionar genes responsáveis por codificar um domínio inteiro de ligação de anticorpo (scFv) ao gene III. Na maioria das vezes, esses fragmentos de anticorpos estão fusionados na pIII do fago M13 e muitas bibliotecas de anticorpos podem ser geradas a partir da clonagem de muitos genes que codificam um fragmento de anticorpo (SCHOFIELD et al., 2007). Como alternativa para uma exibição multivalente de proteínas de fusão anticorpo-pIII, pode ser utilizado vetores de fago baseados em "plasmídeos mínimos", denominados fagemídeos. Eles apresentam 3 elementos principais: marcador de antibiótico para seleção e propagação do plasmídeo; gene codificante da proteína fusionada anticorpo-pIII e presença das regiões de origem da replicação do fago e síntese da fita de DNA. Nesse caso, a *E.coli* contendo o vetor fagemídeo é infectada por um "fago helper" que contém o genoma do M13 completo (Figura 4). Este vetor é mais usado na construção de bibliotecas pela maior eficiência de transformação (LEDSGAARD et al., 2018). Pelo tipo de anticorpo podem existir vários tipos de bibliotecas, dentre elas *naive*, sintéticos ou semi-sintéticos (ALMAGRO et al., 2019).
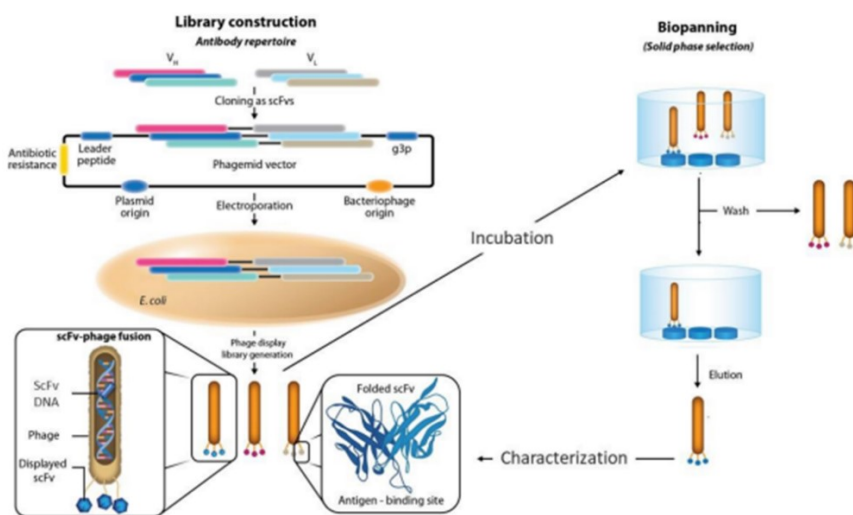
Figura 4. Construção da biblioteca e seleção pelo Phage Display. O método engloba a construção de uma biblioteca (painel esquerdo) de peptídeos ou variantes

proteicos ou, como demonstrado, de anticorpos. É feita uma seleção por afinidade de um repertório de genes de anticorpos (painel direito), onde o anticorpo está fusionado com o fago e ocorre ligações específicas por afinidade com o alvo de interesse. Neste caso, exemplifica uma biblioteca de anticorpos que normalmente é construída a partir de um vetor fagemídeo fusionado a uma das proteínas de revestimento do fago. Fonte: ALMAGRO et al (2019).

2. Inflamação

A inflamação é caracterizada como uma resposta complexa do organismo a alguma injúria tecidual, podendo ser infecciosa ou não. Do ponto de vista clínico, as quatro características que são observadas e indicam um processo inflamatório são: dor, calor, vermelhidão e inchaço. Essas características surgem devido à ação dos mediadores nos tecidos locais (MUNN, 2017). A partir da lesão primária ocorre também alguns processos como alteração de pH, desnaturação de macromoléculas e liberação de substâncias que causam alterações bioquímicas celulares e vasculares no local inflamado (SOUZA et al., 2014). Diversos tipos de estímulos podem causar a inflamação, dentre eles agentes biológicos (bactérias, vírus, fungos e parasitas), substâncias químicas (carragenina, formaldeído), agentes físicos (temperaturas extremas, radiação) e/ou má formação do tecido (MUNN, 2017).

No processo inflamatório, as PLA2's realizam a hidrólise dos fosfolipídios, liberando ácido araquidônico. Este é modificado em compostos chamados eicosanóides, que incluem prostaglandinas e leucotrienos, que são os principais mediadores da inflamação (KHAN; HARIPRASAD, 2020).

A resposta inflamatória pode ser considerada aguda ou crônica, sendo que na primeira há o predomínio de mediadores liberados pelas células residentes que incluem os mediadores pré-formados (histamina, serotonina e heparina) e pós-formados (citocinas e as espécies reativas de oxigênio) (FEGHALI; WRIGHT, 1997). Em decorrência disso, ocorre o aumento da permeabilidade vascular e do fluxo sanguíneo, de modo que os leucócitos e proteínas plasmáticas transitem de forma mais fácil (HIRANO, 2021).

As citocinas consistem em polipeptídeos ou glicoproteínas extracelulares, com tamanho que varia entre 8 e 30 kDa. Elas podem ser produzidas por vários tipos de células no local lesionado e por células do sistema imune a partir da ativação de proteinoquinases ativadas por mitógenos. Sua atuação pode ser, principalmente, por mecanismos parácrino (células vizinhas) e autócrino (próprias células produtoras). Podem ter uma ação de cascata, em que uma citocina estimula suas células-alvo a produzir maior quantidade de citocinas. Sendo assim, a célula imunológica tem a sua atividade, diferenciação, proliferação e sobrevida diretamente relacionada com a ação das citocinas. Caso as citocinas aumentem a resposta inflamatória, são chamadas de pró-inflamatórias (Th1), e as principais são interleucinas (IL-1, 2, 6 e 7) e fator de necrose tumoral (TNF). Caso elas diminuam a resposta, recebem o nome de anti-inflamatórias dentre elas IL-4, IL-10 e IL-13 (Th2) (DE OLIVEIRA et al., 2011).

A resposta imune inata corresponde a resposta mais rápida, responsável pela defesa inicial contra as infecções. Os seus componentes são principalmente barreiras químicas, físicas e biológicas e algumas células especializadas, dentre elas macrófagos, neutrófilos, células dendríticas e células *Natural Killer* (NK) (ABBAS, 2007). Nesse tipo de resposta ocorre fagocitose, ativação do sistema complemento e liberação de mediadores da inflamação. O outro tipo de resposta existente é a adaptativa que se desenvolve de modo mais tardio, sendo mais eficiente contra as infecções. As principais células envolvidas nesse caso, são os linfócitos, formados pela imunidade humoral e celular. Na humoral participam anticorpos específicos, produzidos pelos linfócitos B maduros e que estão presentes no plasma sanguíneo. Já a imunidade celular é mediada pelos linfócitos T citotóxicos (CRUVINEL et al., 2010).

3. Ofidismo e enzimas presentes nos venenos

Os acidentes ofídicos ou ofidismo consiste no quadro clínico decorrente da mordedura de serpentes (SOUZA et al., 2021). Em 2009, a Organização Mundial da Saúde (OMS) incluiu o ofidismo na lista de Doenças Tropicais Negligenciadas, dando uma estimativa de que ocorrem, anualmente, no planeta

1.841.000 casos de envenenamento resultando em 94.000 óbitos (MENDES et al., 2020). A identificação da serpente envolvida no acidente é extremamente importante para que a produção do soro antiofídico seja realizada conforme o gênero, sendo o soro um tipo de imunização que tem a finalidade de proteger o organismo contra a ação de agentes infecciosos (LEITE et al., 2017).

Os gêneros *Bothrops* e *Crotalus* estão associados com a maioria dos acidentes ofídicos no Brasil (DE AZEVEDO-MARQUES; CUPO; HERING, 2003). Os venenos das serpentes apresentam substâncias complexas, sendo que mais de 90% de seu peso seco é formado por enzimas, toxinas não enzimáticas, proteínas e proteínas não tóxicas (SCHULZ et al., 2016). Do ponto de vista biológico, as serpentes apresentam estas moléculas com o intuito de paralisar, matar, digerir a presa ou para se defender de predadores. No caso de envenenamento em seres vivos, há desde alterações locais, como neurotoxicidade, dermonecrose, hemorragia, edema e dor, até alterações sistêmicas, como coagulopatias, hemorragias, choque cardiovascular e insuficiência renal aguda (MOREIRA et al., 2012). Nesse caso de evolução da fisiopatologia, a reação imunológica direta causada pelos antígenos presentes no veneno e a ativação indireta gerada em resposta ao dano tecidual pode evoluir para choque anafilático (SOUZA et al., 2021).

Na composição dos venenos das serpentes do gênero *Bothrops*, destacam-se três grandes classes de enzimas, as metaloproteases, as fosfolipases A_2 (PLA$_2$s) e as serinoproteases. Essas são as principais responsáveis pelos efeitos locais dos venenos botrópicos (QUEIROZ et al., 2008).

3.1.   Metaloproteases

As metaloproteinases de veneno de cobra (SVMPs) podem ser agrupadas em três classes principais, de acordo com a composição do seu domínio P-I, P-II e P-III. Na classe P-I, a proteína madura é formada apenas pelos domínios das metaloproteinases (domínio catalítico). A classe P-II é composta pelo domínio metaloproteinase e um domínio desintegrina e a classe P-III tem ambos os

domínios, além de um domínio adicional rico em cisteína (OLAOBA et al., 2020). Na literatura, já é bem descrito que essas enzimas desempenham um papel fundamental no envenenamento em decorrência da sua atividade proteolítica, papel digestivo e provocação de uma miotoxicidade local, hemorragia, sangramento sistêmico e alterações hemostáticas (GUTIÉRREZ; RUCAVADO, 2000; SALVADOR et al., 2020). Dessa forma, ela consegue ativar o fator X de coagulação e protrombina ocasionando a estimulação da ação fibrinogenolítica. Ainda participam da degradação da matriz extracelular, gerando uma reação inflamatória (AMÉLIO et al., 2021).

3.2.   Fosfolipases A$_2$

As fosfolipases fazem parte de uma ampla classe de enzimas (A1, A2, C e D), e especificamente, a PLA$_2$ (EC 3.1.1.4) é uma das toxinas enzimáticas mais estudadas em venenos de serpentes (MACKESSY, 2002). São responsáveis por catalisar a hidrólise de 2-*sn*-fosfolipídeos em ácidos graxos e lisofosfolipídeos que são mediadores em vários processos biológicos (KINI, 2003). Para a catálise enzimática, é necessário a presença do cofator Ca^{2+} sendo sua estrutura de ligação altamente conservada na maior parte dos venenos (SCOTT et al., 1990). Os quatro principais resíduos envolvidos na regulação do Ca^{2+} são His48, Asp49, Tyr52 e Asp99 (SHUKLA et al., 2015). De acordo com a localização das ligações dissulfeto, as PLA$_2$s podem ser classificadas em dois grandes grupos, Grupo I PLA$_2$ (GIPLA$_2$) e Grupo II PLA$_2$ (GIIPLA$_2$). No primeiro, a cadeia polipeptídica é única e contém de 6 a 8 ligações dissulfeto. O segundo grupo apresenta de 120-125 resíduos de aminoácidos e sete ligações dissulfeto (SIX; DENNIS, 2000).

Além da classificação em grupos, as variantes de PLA$_2$s podem ser classificadas em D49 PLA$_2$ ácida (Asp-49), K49 PLA$_2$ básica (presença de Lys-49 no lugar de Asp-49) e S49 PLA$_2$ (presença de Ser-49). Os homólogos básicos (K49 e S49) são cataliticamente inativos e por isso são responsáveis por muitas atividades biológicas independentes de Ca^{2+} (WARD et al., 2002). A PLA$_2$ apresenta atividade e relevância na miotoxicidade sistêmica ou local (ANDRIÃO-ESCARSO et al., 2000; GUTIÉRREZ et al., 2008), inibição da agregação plaquetária (SATISH et al., 2004), anticoagulante (ZHAO; ZHOU; LIN, 2000),

neurotoxicidade pré-sináptica ou pós-sináptica (PRAŽNIKAR; PETAN; PUNGERČAR, 2009; ROUAULT et al., 2006), cardiotoxicidade (ZHANG et al., 2002) e atividades indutoras de edema (YAMAGUCHI et al., 2001).

A PLA_2 de mamíferos é uma enzima chave na liberação de ácido araquidônico e ácido lisofosfatídico, e estes são substratos para a síntese de vários mediadores inflamatórios lipídicos (TEIXEIRA et al., 2003). Dentre as PLA_2s de mamífero, a PLA_2 secretada ($sPLA_2$) é uma das mais estudadas (DORE; BOILARD, 2019). Após a enzima $sPLA_2$ realizar hidrólise e liberar ácido araquidônico, este é convertido em mediadores inflamatórios (tromboxano, leucotrieno, prostaglandinas e prostaciclinas). O outro produto da hidrólise, ácido lisofosfatídico é catalisado a um fator ativador de plaquetas (PAF) que intensifica a atividade inflamatória. Além disso, ainda é produzido espécies reativas de oxigênio (ROS) que colaboram para a função defensiva (Figura 5). No entanto, a permanência desses ROS são maléficos, pois causa complicações deletérias e desempenham função importante em algumas doenças inflamatórias, dentre elas bronquite crônica, asma, artrite reumatóide e doença de Alzheimer (GIRESHA et al., 2022). Recentemente, foi descoberto que as $sPLA_2$s conseguem hidrolisar eficientemente as membranas bacterianas e produzir efeitos sistêmicos no sistema imunológico por meio da sua atividade na microbiota e em seu lipidoma (DORÉ et al., 2022).
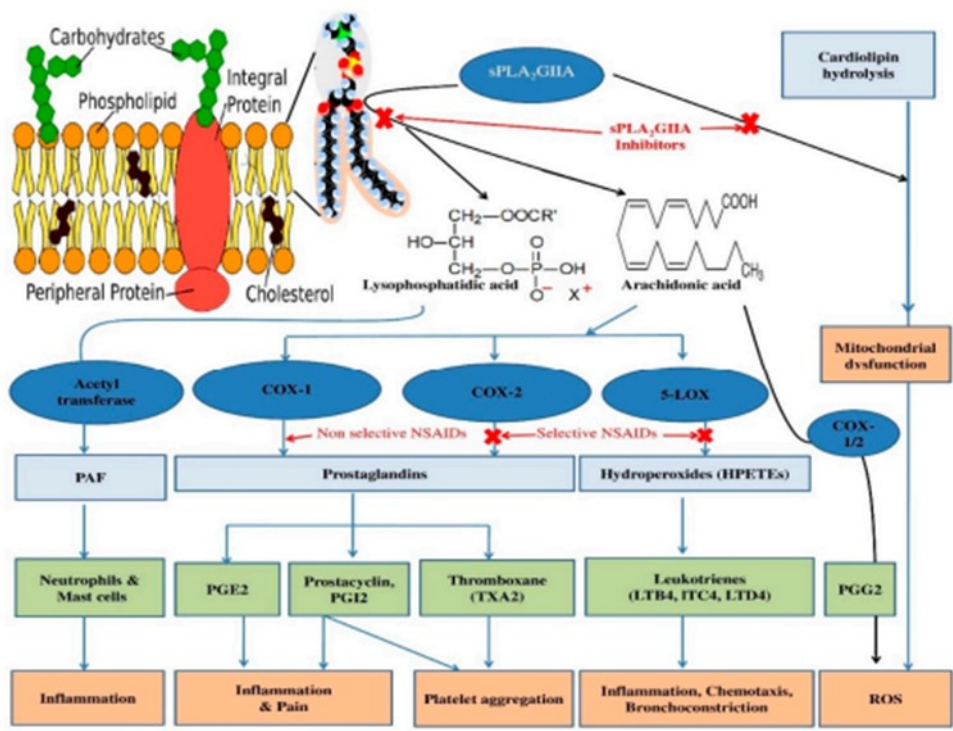
Figura 5. Esquema das vias inflamatórias que são mediadas pela enzima PLA$_2$-IIA, produção de ROS e pontos de controle de moléculas/drogas anti-inflamatórias. Fonte: GIRESHA et al (2022).

As PLA$_2$s vêm ganhando relevância cada vez mais nos processos inflamatórios, de forma que elas estão relacionadas em várias condições patológicas, como artrite, doenças cardiovasculares e diabetes (BATSIKA et al., 2021). Dessa forma, torna importante desenvolver mecanismos para regular sua atividade e desenvolver inibidores como potenciais agentes farmacêuticos para tratar doenças inflamatórias.

REFERÊNCIAS

ABBAS, A. K. Imunologia básica. [s.l.] **Elsevier Brasil**, 2007.

ALMAGRO, J. C. et al. Phage Display Libraries for Antibody Therapeutic Discovery and Development. **Antibodies**, v. 8, n. 3, p. 44, 2019. https://doi.org/10.3390/antib8030044

D'AMÉLIO et al. *Bothrops moojeni* venom and its components-na overview. **Journal of Venom Research**, v. 11, p. 26, 2021.

ANAND, T. et al. Phage Display Technique as a Tool for Diagnosis and Antibody Selection for Coronaviruses. **Current Microbiology**, v. 78, n. 4, p. 1124–1134, 2021. https://doi.org/10.1007/s00284-021-02398-9

ANDRIÃO-ESCARSO, S. H. et al. Myotoxic phospholipases A2 in Bothrops snake venoms: Effect of chemical modifications on the enzymatic and pharmacological properties of bothropstoxins from Bothrops jararacussu. **Biochimie**, v. 82, n. 8, p. 755–763, 2000. https://doi.org/10.1016/S0300-9084(00)01150-0

BARBAS, C. et al. Phage display: a laboratory manual. **New York: Cold Spring Harbor Laboratory Press**, 2001.

BARDERAS, R.; BENITO-PEÑA, E. The 2018 Nobel Prize in Chemistry: phage display of peptides and antibodies. **Analytical and Bioanalytical Chemistry**, v. 411, n. 12, p. 2475–2479, 2019. https://doi.org/10.1007/s00216-019-01714-4

BATSIKA, C. S. et al. The design and discovery of phospholipase A2 inhibitors for the treatment of inflammatory diseases. **Expert Opinion on Drug Discovery**, v. 16, n. 11, p. 1287–1305, 2021. https://doi.org/10.1080/17460441.2021.1942835

BRIGIDO, M. M.; MARANHÃO, A. Q. Bibliotecas apresentadas em fagos. **Biotecnologia Ciência & Desenvolvimento**, v. 26, p. 44–51, 2002.

CAROLINE BABETO SOUZA, F. DE et al. Controle Do Processo Inflamatório Na Odontologia Com Anti-Inflamatorios Não-Esteroidais Control of Inflammatory

Process in Dentistry With Nonsteroidal Anti-Inflammatory. v. 20, n. 2, p. 35–42, 2014.

CRUVINEL, W. M. et al. Immune system - part I fundamentals of innate immunity with emphasis on molecular and cellular mechanisms of inflammatory response. **Revista Brasileira de Reumatologia**, v. 50, n. 4, p. 443–461, 2010.

DE AZEVEDO-MARQUES, M. M.; CUPO, P.; HERING, S. E. Envenomation caused by poisonous animals: Poisonous snakes. **Medicina**, v. 36, n. 2–4, p. 480–489, 2003. https://doi.org/10.11606/issn.2176-7262.v36i2/4p480-489

DE OLIVEIRA, C. et al. Citocinas y dolor. **Revista Brasileira de Anestesiologia**, v. 61, n. 2, p. 137–142, 2011.

DENG, X. et al. Advances in the T7 phage display system (Review). **Molecular Medicine Reports**, v. 17, n. 1, p. 714–720, 2018. https://doi.org/10.3892/mmr.2017.7994

DEVLIN, J. J.; PANGANIBAN, L. C.; DEVLIN, P. E. Random peptide libraries: A source of specific protein binding molecules. **Science**, v. 249, n. 4967, p. 404–406, 1990. https://doi.org/10.1126/science.2143033

DORÉ, E. et al. The interaction of secreted phospholipase A2-IIA with the microbiota alters its lipidome and promotes inflammation. **JCI Insight**, v. 7, n. 2, p. 1–19, 2022. https://doi.org/10.1172/jci.insight.152638

DORE, E.; BOILARD, E. Roles of secreted phospholipase A 2 group IIA in inflammation and host defense. **Biochimica et Biophysica Acta - Molecular and Cell Biology of Lipids**, v. 1864, n. 6, p. 789–802, 2019. https://doi.org/10.1016/j.bbalip.2018.08.017

EBRAHIMIZADEH, W.; RAJABIBAZL, M. Bacteriophage vehicles for phage display: Biology, mechanism, and application. **Current Microbiology**, v. 69, n. 2, p. 109–120, 2014. https://doi.org/10.1007/s00284-014-0557-0

FEGHALI, C. A.; WRIGHT, T. M. Cytokines in acute and chronic inflammation. **Frontiers in Bioscience-Landmark**, v. 2, n.4, p. 12–26, 1997. https://doi.org/10.2741/A171

FOULADVAND, F. et al. A review of the methods for concentrating M13 phage.

Journal of Applied Biotechnology Reports, v. 7, n. 1, p. 7–15, 2020.

GIRESHA, A. S. et al. Sinapicacid Inhibits Group IIA Secretory Phospholipase A2 and Its Inflammatory Response in Mice. **Antioxidants**, v. 11, n. 7, p. 1251, 2022. https://doi.org/10.3390/antiox11071251

GUTIÉRREZ, J. M. et al. Systemic and local myotoxicity induced by snake venom group II phospholipases A2: Comparison between crotoxin, crotoxin B and a Lys49 PLA2 homologue. **Toxicon**, v. 51, n. 1, p. 80–92, 2008. https://doi.org/10.1016/j.toxicon.2007.08.007

GUTIÉRREZ, J. M.; RUCAVADO, A. Snake venom metalloproteinases: Their role in the pathogenesis of local tissue damage. **Biochimie**, v. 82, n. 9–10, p. 841–850, 2000. https://doi.org/10.1016/S0300-9084(00)01163-9

HIRANO, T. IL-6 in inflammation, autoimmunity and cancer. **International immunology**, v. 33, n. 3, p. 127–148, 2021. https://doi.org/10.1093/intimm/dxaa078

HOLLIGER, P.; HUDSON, P. J. Engineered antibody fragments and the rise of single domains. **Nature Biotechnology**, v. 23, n. 9, p. 1126–1136, 2005. https://doi.org/10.1038/nbt1142

HOOGENBOOM, H. R. et al. Multi-subunit proteins on the surface of filamentous phage: Methodologies for displaying antibody (Fab) heavy and light chains. **Nucleic Acids Research**, v. 19, n. 15, p. 4133–4137, 1991. https://doi.org/10.1093/nar/19.15.4133

KHAN, M. I.; HARIPRASAD, G. Human secretary phospholipase a2 mutations and their clinical implications. **Journal of Inflammation Research**, v. 13, p. 551–561, 2020. https://doi.org/10.2147/JIR.S269557

KIM, S. J.; PARK, Y.; HONG, H. J. Antibody engineering for the development of therapeutic antibodies. **Molecules and Cells**, v. 20, n. 1, p. 17–29, 2005.

KINI, R. M. Excitement ahead: Structure, function and mechanism of snake venom phospholipase A2 enzymes. **Toxicon**, v. 42, n. 8, p. 827–840, 2003. https://doi.org/10.1016/j.toxicon.2003.11.002

KONG, X. D. et al. Generation of a large peptide phage display library by self-

ligation of whole-plasmid PCR product. **ACS Chemical Biology**, v. 15, n. 11, p. 2907–2915, 2020. https://doi.org/10.1021/acschembio.0c00497

LADNER, R. C. et al. Phage display-derived peptides as therapeutic alternatives to antibodies. **Drug Discovery Today**, v. 9, n. 12, p. 525–529, 2004. https://doi.org/10.1016/S1359-6446(04)03104-6

LEDSGAARD, L. et al. Basics of antibody phage display technology. **Toxins**, v. 10, n. 6, 2018. https://doi.org/10.3390/toxins10060236

LEITE, J. E. DE F. et al. Epidemiologia Dos Acidentes Ofídicos Notificados Em Um Centro De Assistência Toxicológica De 2011 a 2015. **Revista Baiana de Saúde Pública**, v. 40, n. 4, p. 862–875, 2017. https://doi.org/10.22278/2318-2660.2016.v40.n4.a2090

MACKESSY, S. P. Biochemistry and pharmacology of colubrid snake venoms. **Journal of Toxicology - Toxin Reviews**, v. 21, n. 1–2, p. 43–83, 2002. https://doi.org/10.1081/TXR-120004741

MCCAFFERTY, J. et al. Phage antibodies: filamentous phage displaying antibody variable domains. **Nature**, 1990. https://doi.org/10.1038/348552a0

MENDES, J. DA S. et al. Aspectos epidemiológicos dos acidentes ofídicos ocorridos no município de Vitória da Conquista- Bahia, Brasil. **Brazilian Applied Science Review**, v. 4, n. 3, p. 1607–1625, 2020. https://doi.org/10.34115/basrv4n3-070

MOREIRA, V. et al. Local inflammatory events induced by Bothrops atrox snake venom and the release of distinct classes of inflammatory mediators. **Toxicon**, v. 60, n. 1, p. 12–20, 2012. https://doi.org/10.1016/j.toxicon.2012.03.004

MUNN, L. L. Cancer and inflammation. **Wiley Interdisciplinary Reviews: Systems Biology and Medicine**, v. 9, n. 2, 2017.

OLAOBA, O. et al. Snake venom metalloproteinases (SVMPs): a structure-function update. **Toxicon: X**, v. 7, n. 100052, 2020. https://doi.org/10.1016/j.toxcx.2020.100052

PARMLEY, S. F.; SMITH, G. P. Antibody-selectable filamentous fd phage vectors: affinity purification of target genes. **Gene**, v. 73, n. 2, p. 305–318, 1988.

https://doi.org/10.1016/0378-1119(88)90495-7

PRAŽNIKAR, Z. J.; PETAN, T.; PUNGERČAR, J. A neurotoxic secretory phospholipase A2 induces apoptosis in motoneuron-like cells. **Annals of the New York Academy of Sciences**, v. 1152, p. 215–224, 2009. https://doi.org/10.1111/j.1749-6632.2008.03999.x

QUEIROZ, G. P. et al. Interspecific variation in venom composition and toxicity of Brazilian snakes from Bothrops genus. **Toxicon**, v. 52, n. 8, p. 842–851, 2008. https://doi.org/10.1016/j.toxicon.2008.10.002

ROUAULT, M. et al. Neurotoxicity and other pharmacological activities of the snake venom phospholipase A2 OS2: The N-terminal region is more important than enzymatic activity. **Biochemistry**, v. 45, n. 18, p. 5800–5816, 2006. https://doi.org/10.1021/bi060217r

RYVKIN, A. et al. Phage display peptide libraries: Deviations from randomness and correctives. **Nucleic Acids Research**, v. 46, n. 9, 2018. https://doi.org/10.1093/nar/gky077

SALVADOR, G. H. M. et al. Biochemical, pharmacological and structural characterization of BmooMP-I, a new P–I metalloproteinase from Bothrops moojeni venom. **Biochimie**, v. 179, p. 54–64, 2020. https://doi.org/10.1016/j.biochi.2020.09.001

SATISH, S. et al. Purification of a Class B1 platelet aggregation inhibitor phospholipase A2 from Indian cobra (Naja Naja) venom. **Biochimie**, v. 86, n. 3, p. 203–210, 2004. https://doi.org/10.1016/j.biochi.2004.02.003

SCHOFIELD, D. J. et al. Application of phage display to high throughput antibody generation and characterization. **Genome Biology**, v. 8, n. 11, 2007. https://doi.org/10.1186/gb-2007-8-11-r254

SCHULZ, R. DA S. et al. Tratamento da ferida por acidente ofídico: caso clínico. **Cuidarte Enfermagem**, v. 10, n. 2, p. 172–179, 2016.

SCOTT, D. L. et al. Interfacial catalysis: The mechanism of phospholipase A2. **Science**, v. 250, n. 4987, p. 1541–1546, 1990. https://doi.org/10.1126/science.2274785

SCOTT, J. K.; SMITH, G. P. Searching for Peptide Ligands with an Epitope Library. **Science**, v. 249, n. 4967, p. 386–390, 1990. https://doi.org/10.1126/science.1696028

SHUKLA, P. K. et al. Structures and binding studies of the complexes of phospholipase A2 with five inhibitors. **Biochimica et Biophysica Acta - Proteins and Proteomics**, v. 1854, n. 4, p. 269–277, 2015. https://doi.org/10.1016/j.bbapap.2014.12.017

SIDHU, S. S. Engineering M13 for phage display. **Biomolecular Engineering**, v. 18, n. 2, p. 57–63, 2001. https://doi.org/10.1016/S1389-0344(01)00087-9

SIX, D. A.; DENNIS, E. A. The expanding superfamily of phospholipase A2 enzymes: Classification and characterization. **Biochimica et Biophysica Acta - Molecular and Cell Biology of Lipids**, v. 1488, n. 1–2, p. 1–19, 2000. https://doi.org/10.1016/S1388-1981(00)00105-0

SMITH, G. P. Filamentous Fusion Phage: Novel Expression Vectors That Display Cloned Antigens on the Virion Surface. **Science**, v. 228, n. 4705, 1985. https://doi.org/10.1126/science.4001944

SOUZA, F. DOS S. et al. Manejo clínico na emergência para acidentes ofídicos: envenenamentos podem evoluir para choque anafilático? / Emergency clinical management for official accidents: can poisons evolve in anaphylactic shock? **Brazilian Journal of Health Review**, v. 4, n. 1, p. 1454–1461, 2021. https://doi.org/10.34119/bjhrv4n1-122

TAN, Y. et al. Advance in phage display technology for bioanalysis. **Biotechnology Journal**, v. 11, n. 6, p. 732–745, 2016. https://doi.org/10.1002/biot.201500458

TEIXEIRA, C. F. P. et al. Inflammatory effects of snake venom myotoxic phospholipases A2. **Toxicon**, v. 42, n. 8, p. 947–962, 2003. https://doi.org/10.1016/j.toxicon.2003.11.006

WARD, R. J. et al. Active-site mutagenesis of a Lys49-phospholipase A2: Biological and membrane-disrupting activities in the absence of catalysis. **Biochemical Journal**, v. 362, n. 1, p. 89–96, 2002. https://doi.org/10.1042/bj3620089

WEIGEL, C.; SEITZ, H. Bacteriophage replication modules. **FEMS Microbiology Reviews**, v. 30, n. 3, p. 321–381, 2006. https://doi.org/10.1111/j.1574-6976.2006.00015.x

WILLATS, W. G. T. Phage display: Practicalities and prospects. **Plant Molecular Biology**, v. 50, n. 6, p. 837–854, 2002. https://doi.org/10.1023/A:1021215516430

WILSON, D. R.; FINLAY, B. B. Phage display: Applications, innovations, and issues in phage and host biology. **Canadian Journal of Microbiology**, v. 44, n. 4, p. 313–329, 1998. https://doi.org/10.1139/w98-015

WINTER, G. et al. Making antibodies by phage display technology. **Annual Review of Immunology**, v. 12, p. 433–455, 1994. https://doi.org/10.1146/annurev.iy.12.040194.002245

YAMAGUCHI, Y. et al. Characterization, amino acid sequence and evolution of edema-inducing, basic phospholipase A2 from Trimeresurus flavoviridis venom. **Toxicon**, v. 39, n. 7, p. 1069–1076, 2001. https://doi.org/10.1016/S0041-0101(00)00250-6

ZAMBRANO-MILA, M. S.; BLACIO, K. E. S.; VISPO, N. S. Peptide Phage Display: Molecular Principles and Biomedical Applications. **Therapeutic Innovation and Regulatory Science**, v. 54, n. 2, p. 308–317, 2020. https://doi.org/10.1007/s43441-019-00059-5

ZHANG, H. L. et al. Structure of a cardiotoxic phospholipase A2 from Ophiophagus hannah with the "pancreatic loop". **Journal of Structural Biology**, v. 138, n. 3, p. 207–215, 2002. https://doi.org/10.1016/S1047-8477(02)00022-9

ZHAO, K.; ZHOU, Y.; LIN, Z. Structure of basic phospholipase A2 from Agkistrodon halys Pallas: Implications for its association, hemolytic and anticoagulant activities. **Toxicon**, v. 38, n. 7, p. 901–916, 2000. https://doi.org/10.1016/S0041-0101(99)00193-2

Capítulo 2

Artigos Científicos

Generation and *In-planta* expression of a recombinant single chain antibody with broad neutralization activity on *Bothrops pauloensis* snake venom

Jessica B. Souza [a],[*],[1], Rone Cardoso [a],[1], Hebréia O. Almeida-Souza [a], Camila P. Carvalho [b],
Lucas Ian Veloso Correia [a], Paula Cristina B. Faria [a], Galber R. Araujo [a], Mirian M. Mendes [a],
Renata Santos Rodrigues [a], Veridiana M. Rodrigues [a], Abhaya M. Dandekar [c],
Luiz Ricardo Goulart [a],[*], Rafael Nascimento [a]

[a] *Institute of Biotechnology, Federal University of Uberlandia, Av. Amazonas, Bloco 2E, Campus Umuarama, 38400-902 Uberlandia, MG, Brazil*
[b] *Department of Plant Pathology, University of Sao Paulo, Av. Padua Dias 11, 13418-310 Piracicaba, SP, Brazil*
[c] *Plant Sciences Department, University of California, Davis, 1 Shields Ave, Davis, CA 95616, USA*

ARTICLE INFO

ABSTRACT

The main systemic alterations present in bothropic envenomation are hemostasis disorders, for which the conventional treatment is based on animal-produced antiophidic sera. We have developed a neutralizing antibody against *Bothrops pauloensis* (*B. pauloensis*) venom, which is member of the genus most predominant in snakebite accidents in Brazil. Subsequently, we expressed this antibody in plants to evaluate its enzymatic and biological activities. The ability of single-chain variable fragment (scFv) molecules to inhibit fibrinogenolytic, azocaseinolytic, coagulant and hemorrhagic actions of snake venom metalloproteinases (SVMPs) contained in *B. pauloensis* venom was verified through proteolytic assays. The antibody neutralized the toxic effects of envenomation, particularly those related to systemic processes, by interacting with one of the predominant classes of metalloproteinases. This novel molecule is a potential tool with great antivenom potential and provides a biotechnological antidote to snake venom due to its broad neutralizing activity.

© 2020 Elsevier B.V. All rights reserved.

1. Introduction

Epidemiological data estimates 421,000 to two million snakebite envenomations per year, resulting in 81,000 to 138,000 deaths worldwide [1]. According to the World Health Organization (WHO), snakebite accidents are included in the list of neglected tropical diseases, with a greater incidence in tropical and/or developing countries. The people most affected by such accidents are low-income populations living in rural areas [2]. In 2018, Brazil had 633.7 cases per 100,000 inhabitants and in 2019, there were 106 deaths (Fig. 1A). The state with the highest death rate was Bahia, with 15 deaths in 2019 (Fig. 1B) [3]. Snakes in the genus *Bothrops* (family Viperidae, subfamily Crotalinae) are implicated in 85% of snakebite accidents in Brazil [4].

Toxins present in snake venom cause severe pathology and toxicity to victims of bites [5]. Among pathological symptoms of *Bothrops* spp. venom are local pain, swelling, bruising and blisters, followed by

systemic manifestations such as bleeding and coagulatory activity [6]. Metalloproteinases and phospholipases A_2 (PLA_2) are enzymes responsible for emergence of these pathological disorders [7]. Snake venom metalloproteinases (SVMPs) are zinc-dependent endoproteolytic enzymes and are the most expressed in bothropic venoms [8,9]. In this genus, metalloproteinases are linked to proteolytic degradation of endothelial surface proteins, inflammatory action and proteolytic, hemorrhagic and procoagulant activities [10]. PLA_2 are a family of enzymes that catalyze phospholipid hydrolysis [11]. A primary effect in *Bothrops* venom is anticoagulant action, myotoxic activity and edema generation [12]. Due to their action, these enzymes present great potential as targets for envenomation treatment.

The most effective treatment for snakebite envenomation is still conventional serum therapy [13]. Antiserum production is accomplished by hyperimmunization of large host mammals, usually horses, with sublethal doses of one or more venoms [14]. To increase efficiency, purified total IgG solutions or immunoglobulin fragments from F(ab')2 or Fab have been used [15]. However, no antivenom is free of the risk of causing anaphylactic reactions and/or serum sickness [16]. Production of high quality, affordable and regionally suitable antivenom is needed in highly endemic areas, but commercial

---

A

B
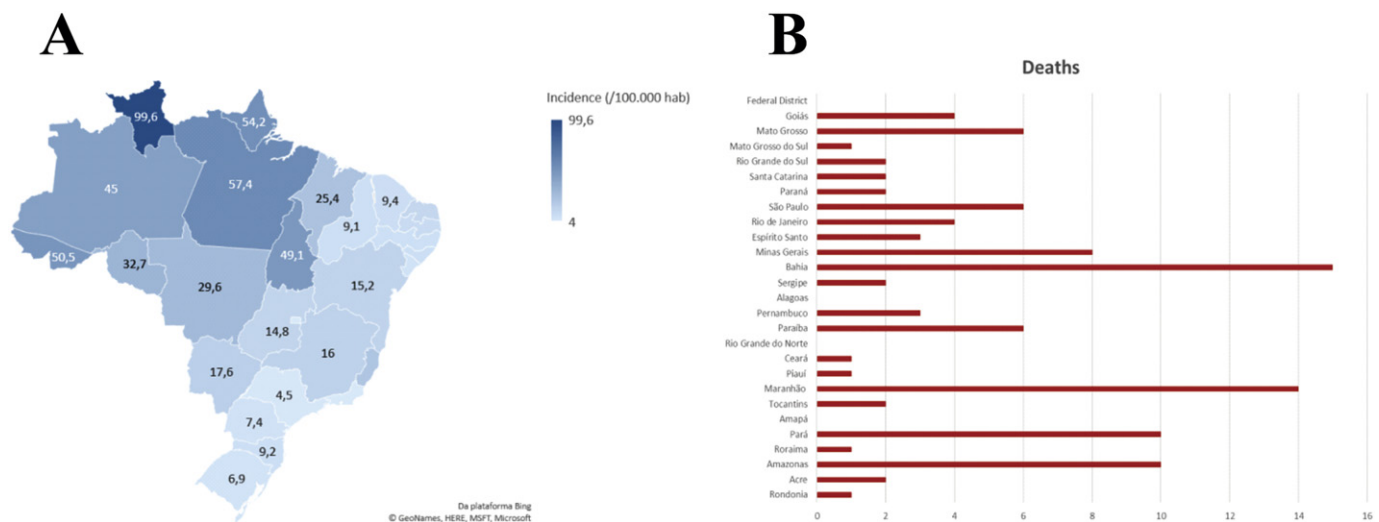
Fig. 1. Epidemiology of snakebite cases in Brazil in 2018. A: Geographic distribution by the incidence of snakebite accidents per 100.000 inhabitants. B: Number of deaths from snakebite for each Brazilian state.

and financial factors increase the problem, directly affecting many communities [17]. Biotechnological advances could allow a different type of antivenom, with greater potency and availability and reduced side effects and treatment costs [18].

Plant biofactories are used widely to produce antibodies of pharmaceutical interests because of several advantages: easy production scale-up [19]; lower risk of contamination with adventitious pathogens and the absence of bacterial endotoxins, improving safety and reducing the risk of anaphylactic shock [20]; and high yield and low cost of production due to the few requirements required to construct facilities [21]. The first plant-produced drug was approved by the Food and Drug Administration (FDA) for human use in 2012, to treat patients with Gaucher disease [22]. Currently, several drugs are in preclinical tests and others in phase 1 or 2 of human clinical trials [23,24].

An alternative strategy to produce antiserum for treating envenomation is to obtain recombinant monoclonal antibodies from combinatorial libraries. One of the most used is the scFv combinatorial library obtained by the phage display [25], due to smaller size (~25 kDa), lower immunogenicity, higher biodistribution and greater tissue permeability, ensuring faster neutralization of toxins [26,27].

A recombinant scFv (scFvBaP1) was developed from mRNA derived from BaP1-8 (MABaP1-8) monoclonal antibody-producing cells [28]. BaP1 is a metalloproteinase present abundantly in *Bothrops asper* (*B. asper*) venom. The produced fragment showed neutralizing activities against hemorrhage, fibrinolysis, myotoxicity and proinflammatory properties present in the venom. However, this technique resulted in low yields, which would make large-scale production inviable [28]. The efficiency of a transgenic plant system as a transient expression tool to increase yield of the scFvBaP1 fragment has been demonstrated [29]. The modified scFvBaP1 antibodies produced by *Nicotiana benthamiana* cells retained neutralizing activities similar to those of the original scFvBaP1. Moreover, this molecule still displayed activities against distinct toxins present in other *Bothrops* snake species [29].

Unlike in previous studies [28,29], we selected an scFv against *B. pauloensis* crude venom from a combinatorial library through Phage Display. This strategy led us to develop a dominant scFv with broad neutralizing activity against anti-snake venom metalloproteinases, which was then expressed in transgenic plants. The development of this novel antibody is discussed in detail herein.

2. Experimental procedures

2.1. Venom and toxin isolation

B. pauloensis, *B. moojeni*, *B. leucurus*, *B. jararaca*, *B. jararacussu* and *Crotalus durissus collilineatus* snake venoms were donated by Pentapharm serpentarium, Minas Gerais, Brazil. *Neuwiedase* is a metalloproteinase that was isolated from *Bothrops neuwiedi* venom as described [30].

2.2. Animals

The animals were housed at the animal facility of the Federal University of Uberlândia with free access to food and water. Two-week-old White Leghorn chickens were kept at a controlled temperature. Male Swiss mice (22.5 ± 2.5 g) were kept at 22 ± 1 °C on a 12 h light/dark cycle. The experimental protocols involving animals were approved by an institutional Committee for Ethics in Animal Use (CEUA/UFU, protocol no. 063/08).

2.3. Antigen preparation and immunizations

Four three-month-old White Leghorn chickens were used for immunizations. Two chickens were immunized at 14-day intervals with *B. pauloensis* crude venom and two others were used as negative controls (immunized with adjuvant and phosphate-buffered saline-PBS) as described [31]. For the first dose, 200 µg *B. pauloensis* snake venom in complete Freund's adjuvant was administrated. For the two following doses, 100 µg snake venom and incomplete Freund's adjuvant were used. After the third immunization, blood was taken from each animal and titrated by enzyme-linked immunosorbent (ELISA) assay to determine the presence of an antigen-specific immune response.

2.4. Total RNA extraction and cDNA synthesis

After ensuring satisfactory antibody titer, chickens were sacrificed and their spleens immediately removed, frozen in liquid nitrogen and stored at −80 °C. The spleens were macerated in liquid nitrogen and total RNA was extracted using TRIzol reagent (Invitrogen), following manufacturer's instructions. Approximately 20 µg total RNA was used for cDNA synthesis using the Access Quick RT-PCR System kit (Promega), oligo(dT)$_{12-18}$ primer and AMV reverse transcriptase

(Invitrogen). The reaction products were used directly as cDNA templates to construct the scFv gene sublibrary.

2.5. Construction of the recombinant antibody library

All procedures were performed as described [31]. To amplify fragments from the light and heavy antibody chains, five PCR reactions were carried out using 10 μL cDNA as template. Each reaction had a final volume of 100 μL, using 60 pmoles of primer sets CSCVHo-F (forward)/CSCG-B (reverse) and CSC-VK (forward)/CKJo-B (reverse) for VH and VL gene amplification, respectively. PCR reactions were performed according to the following conditions: 94 °C for 5 min, then 30 cycles of 94 °C for 45 s, 56 °C for 1 min and 72 °C for 2 min. Final extension was conducted at 72 °C for 10 min.

The amplified VH and VL gene segments were separated by electrophoresis in a 2% agarose gel, purified with a Wizard SV Gel up-System kit (Promega) and joined *via* overlapping sequences present in oligonucleotides CSC-B and CSC-F. Ten PCR reactions were performed using 500 ng of VH and VL genes and 60 pmoles of each primer, under the following conditions: melting gradient of 5 min at 94 °C, 1 min at 80 °C, 1 min at 70 °C, a stop for the addition of Taq polymerase, followed by 30 cycles of 15 s at 56 °C, 15 s at 72 °C and 15 s at 94 °C. The final annealing and final extension were carried out for 15 s at 56 °C and 10 min at 72 °C, respectively. The scFv gene products were purified as described for VH and VL and then ligated into the display vector pComb3XSS, both digested with *Sfi*I restriction enzyme. Three identical ligation systems were used to increase the variability of the antibody library using 1400 ng phagemid pComb3XSS mixed with 700 ng scFv in 40 μL 5× T4 DNA Ligase Reaction Buffer and 10 μL T4 DNA Ligase (both from Invitrogen), followed by incubation at 16 °C for 20 h. To obtain the recombinant viral particles, XL1-Blue (Stratagene) eletrocompetent cells were transformed with the aforementioned ligation system. To ensure the efficiency of ligation, two reactions were pooled for the library construction. Three μL portions were used to transform electrocompetent XL1-Blue cells. Phagemid particles from the library were prepared by rescue with VCS-M13 helper phage (Stratagene) as described previously [31]. After the library construction, colonies were grown on agar plates with 100 μg/mL carbenicillin and 40 mM glucose, isolated and sequenced to assess library integrity and diversity.

2.6. Phage preparation and selection

Phage from the scFv library were panned against *B. pauloensis* crude venom using a solid-phase protocol. For each cycle of selection, 50 μg antigen diluted in 100 μL carbonate buffer (0.1 M, pH 8.6) was coated in triplicate wells of an MaxiSorp plate (NUNC, NY, USA). The plate was coated overnight at 4 °C with TBS-BSA 3%, followed by incubation with 100 μL freshly prepared phage-scFv library at 37 °C for 2 h to allow phage binding. The unbound phages were discarded and wells were washed with TBS-Tween 0,5% by vigorously pipeting and incubating at room temperature for 5 min. The wells were washed five times in the first cycle of selection and 10 and 15 times in the subsequent two cycles of selection, respectively. The bound phages were eluted with 50 μL glycine-HCl (pH 2.2) and neutralized with 3 μL Tris-base (2 M). Eluted phage from triplicate wells were combined and added directly to 2 mL fresh XL1-Blue bacterial culture for infection and phage amplification. The cells were incubated at room temperature for 15 min, after which the culture volume was increased to 6 mL with pre-warmed SB. The output phage titer was determined by plating 0.1 μL, 1 μL and 10 μL on LB/cabenicillin plates. The cultures were then supplemented with 20 μg/mL carbenicillin and incubated at 37 °C and 270 rpm. The carbenicillin concentration was then increased to 50 μg/mL and the culture was incubated for an additional hour. The culture volumes were increased to 100 mL with pre-warmed SB supplemented with 50 μg/mL cabenicillin and 1 mL VCSM13 helper phage (~10^{12} PFU/mL). After incubation for 2 h, the culture was supplemented with 70 μg/mL kanamycin and

incubated overnight. Phage particles were precipitated with PEG-NaCl; three cycles of selection were carried out using this protocol. Following the third cycle of selection, phage were precipitated from culture supernatants and phagemid DNA was extracted from the bacterial pellet. In each selection cycle, the input and output titer of eluted phages were determined as described previously to evaluate the enrichment.

2.7. DNA sequencing analysis

The sequencing reaction was carried out using a DyEnamic ET Dye Terminator Cycle Sequencing Kit (GE Healthcare), following manufacturer's instructions. The reaction was performed with 400 ng plasmidial DNA and the MMB4/MMB5 primer set. DNA sequences were analyzed using Blastx [32] and protein sequences were aligned using ClustalW [33].

2.8. Expression and purification of soluble scFv antibodies

Plasmid DNA was extracted from *Escherichia coli* (*E. coli*) XL1 Blue cells previously infected with phages from the third selection cycle and then used to transform by thermal shock [34] the non-suppressing *E. coli* TOP 10 strain (Invitrogen), which was induced to express the soluble form of scFvs. Ninety-six random clones were inoculated into 1 mL SB medium with 100 μg carbenicillin and 20 mM MgCl₂ in a deep-well plate, following by incubation overnight at 37 °C with 300 rpm. The culture was centrifuged at 3000 ×g for 10 min and the sedimented cells were used for plasmid DNA extraction and sequencing. In another deep well plate, 50 μL of the culture was inoculated into 1 mL SB medium supplemented with 50 μg carbenicillin and 20 mM MgCl₂ and incubated for 2 to 3 h at 37 °C and 255 rpm agitation until the O.D.$_{600nm}$ equaled 1. Antibody expression was induced with IPTG addition for a final concentration of 1 mM. The plate was incubated for hours under the conditions described above. After induction, the plate was centrifuged at 3000 ×g for 20 min and the culture supernatant was transferred to a new plate and stored at 4 °C. Clones that expressed scFv in solution were tested for their reactivity against *B. pauloensis* crude venom and the *neuwiedase* metalloproteinase. After induction, soluble expressed scFv molecules were purified from culture supernatant by immobilized metal affinity chromatography using a HisTrap HP (GE Healthcare) column. The proteins were separated in 10% SDS-PAGE and their expression and purification was detected by western blotting using HRP-conjugated anti-HA (1:5000).

2.9. Plasmid construction and plant transformation

The coding sequences of single-chain, variable-fragment snake venom metalloproteinase (scFv-Svmp) was codon-optimized (Fig. S1), chemically synthesized and directionally cloned into our CaMV35S cassette-containing vector, pDU.99.2215, using *Sma*I and *Xho*I. This binary vector was introduced into a disarmed *Agrobacterium tumefaciens* (*A. tumefaciens*) strain to create functional plant transformation systems. *A. tumefaciens* vectors carrying the binary plasmid were provided to the Ralph M. Parsons Plant Transformation facility at the University of California Davis. *Nicotiana tabacum* (*N. tabacum*) L. cv. SR1 callus cultures were transformed. Fifteen independent transgenic lines were obtained and confirmed by PCR analysis of their DNA. Transgenic tobacco plants were confirmed by GUS (β-glucuronidase) activity and by sequencing to check for the presence of the incorporated gene.

2.10. Plant growth conditions

We used Petit Havana SR1 *N. tabacum* plants to created transgenic *N. tabacum* plants overexpressing scFv-Svmp antibody. *N. tabacum* seeds were germinated in vases containing commercially manufactured Bioplant substrate and fertilizer and kept in a germination chamber with controlled temperature (28 °C), humidity (55%) and luminosity

(16 h of light and 8 h of dark). After germination, plants ~2 cm in size were transferred to a greenhouse.

2.11. Protein extraction and purification of N. tabacum leaves

The leaves of *N. tabacum* plants were collected and frozen in liquid nitrogen. Extraction was done in a 1:3 ratio (g plant material: mL extraction buffer). The material was macerated in liquid nitrogen and extraction buffer (50 mM Tris-HCl pH 7.5, 75 mM NaCl, 1% Triton X-100, 5% glycerol, 2 mM EDTA, 0.4 mM benzamidine and 4 mM PMSF) added. The material was vortexed 10 min with ice breaks, then sonicated (six 30-second pulses). The material was then centrifuged at 8000 rpm at 4 °C for 30 min and the supernatant was purified by immobilized metal affinity chromatography using a HisTrap HP (GE Healthcare) column. The proteins were separated in 12% SDS-PAGE and their expression and purification was detected by western blotting using the HRP-conjugated anti-HA (1:2500). The protein expressed in plants was called scFv-Svmp1.

2.12. ELISA assay

A 96 well Maxisorp microtiter plate (NUNC, NY, USA) was coated with 10 μg of each crude venom (*B. pauloensis*; *B. moojeni*; *B. leucurus*; *B. jararaca*; *B. jararacussu* and *Crotalus durissus collilineatus*) in 50 mM NaHCO₃, pH 8.6, followed by incubation overnight at 4 °C. The wells were washed three times with PBS-T 0.05% and blocked with 3% BSA (w/v) in PBS-T 0.05% for 1 h at 37 °C. One hundred μL of the induced bacterial culture supernatant expressing scFv-Svmp and 9 μg purified scFv-Svmp1 were added, followed by incubation for 2 h at room temperature under low agitation. The supernatants were discarded and the plate washed three times with 0.05% PBS-T, followed by incubation with HRP-conjugated rat anti-HA (Roche Applied Science) diluted (1:1000) in 3% PBS-BSA for 1 h at 37 °C. The plate was washed three times in 0.05% PBS-T, revealed with 0.4 mg/mL *o*-phenylenodiamine dihydrochloride (OPD) dissolved in 0.05 M of phosphate-citrate buffer (0.2 M dibasic sodium phosphate, 0.1 M citric acid and 50 mL deionized water, pH 5.0), and 40 μL 30% H_2O_2 (3%). Reactions were stopped by adding 30 μL 4 N H_2SO_4 per well. The optical density of each well at 492 nm was determined using a microplate reader (Titertek Multiskan Plus, Flow Laboratories, USA).

2.13. Protein preparation and mass spectrometry analysis

B. pauloensis snake venom scFv-Svmp binding proteins were isolated using a NHS HiTrap NHS-Activated HP affinity column (GE Healthcare Life Sciences) following manufacturer's instructions. Isolated proteins were precipitated using a ProteoExtract protein precipitation kit (Calbiochem) followed by dehydration overnight in a sterile fume hood. The protein pellet was resuspended in 50 mM ammonium bicarbonate (pH 8.0) and subjected to an in-solution tryptic digestion. Digested peptides were then desalted and subjected to LC/MSMS. The digested peptides were analyzed using a QExactive mass spectrometer (Thermo Fisher Scientific) coupled with an Easy-LC (Thermo Fisher Scientific) and a nanospray ionization source. The peptides were loaded onto a trap (100 μm, C18 100 Å 5 U) and desalted online before separation using a reverse phased column (75 μm, C18 200 Å 3 U). The gradient duration for separation of peptides was 60 min using 0.1% formic acid and 100% ACN for solvents A and B, respectively. Data were acquired using a data-dependent ms/ms method with a full scan range of 300 to 1600 Da and a resolution of 70,000. The ms/ms method's resolution was 17,500, with an isolation width of 2 *m/z* with normalized collision energy of 27. The nanospray source was operated using 2.2 KV spray voltage and a heated transfer capillary temperature of 250 °C. Raw data was analyzed using X!Tandem and visualized using Scaffold Proteome Software (Version 3.01). Samples were searched against Uniprot databases appended with the cRAP database, which recognizes common laboratory contaminants. Reverse decoy databases were also applied to the database prior to the X!Tandem searches.

2.14. PLA₂ activity assays

The PLA₂ activity of scFv-Svmp was measured using an indirect hemolytic test in agarose gel. As substrate, a mixture containing mice red cells and an emulsion of egg yolk was used. Ten μg crude venom was incubated with antibody samples scFv-Svmp (1/0, 1/1 and 1/5 w/w) at 37 °C for 30 min.

The PLA₂ assay was performed as described [35]. Previously, purified plant scFv-Svmp1 at different proportions [1/5, 1/25, or 1/40 (w/w)] was incubated 1 h at 37 °C with 5 μg crude venom. Egg yolk was used as the substrate in the presence of 0.03 M sodium deoxycholate and 0.6 M CaCl₂. Results were expressed as mEq/mg/min. The positive control was *B. pauloensis* crude venom. The enzyme activity was expressed as a percentage, where 100% represents the absence of venom activity.

2.15. Fibrinogenolytic activity assay

The fibrinogenolytic activity of scFv-Svmp and scFv-Svmp1 was performed as described [30], with modifications. Fifty μg bovine fibrinogen samples in PBS at pH 7.8 were incubated with scFv-Svmp at the proportions [w/w] of 1/3, 1/5 or 1/10 of venom/scFv and with scFv-Svmp1 at the proportions [w/w] of 1/10, 1/25 or 1/50 of venom/scFv for 1 h at 37 °C. The reaction was stopped with 25 μL 0.06 M Tris–HCl, pH 6.8, containing 10% (v/v) glycerol, 10% (v/v) β-mercaptoethanol, 2% (w/v) SDS and 0.05% (w/v) bromophenol blue. The samples were then heated at 100 °C for 4 min and analyzed by 12.5% SDS-PAGE.

2.16. Azocaseinolytic and coagulant activities

The enzymatic characterization of purified scFv-Svmp1 was determined using azocasein as substrate as originally described [36] and later modified [37]. Samples containing 800 μL azocasein (1 mg/mL) in 0,05 M Tris-HCl and 0,15 M NaCl, pH 7,0, were incubated 30 min at 37 °C with metalloproteinase (negative control of inhibition), phenanthroline 10 mM (positive control of inhibition), purified plant scFv-Svmp1 and purified protein extract of wild-type *N. tabacum* (SR1) at different proportions [1/5, 1/25, or 1/40 (w/v)] in the wells of polystyrene 96-well plates (NUNC MaxiSorp). Next, 100 μL 20% (m/v) trichloroacetic acid was added to each sample. The plate was incubated at room temperature for 30 min, then centrifuged at 1856 $\times g$ for 20 min. The absorbance of the supernatant at 405 nm was determined using an EL800-Biotek reader. One unit (U) of azocaseinolytic activity was defined as an increase of 0.01 absorbance units at 405 nm under standard assay conditions. All assays were performed in triplicate and plotted on a graph.

Inhibition of coagulant activity on bovine plasma was performed as described [38], with modifications. One hundred fifty μL bovine plasma was incubated with metalloproteinase (negative control of coagulation), phenanthroline 10 mM (positive control of coagulation – inhibitor of metalloproteinase), purified plant scFv-Svmp1 or protein extract of wild type *N. tabacum* (SR1) purified at 37 °C. The samples were kept under constant and gentle stirring. The time required to start formation of the fibrin network was recorded by a photometric system in the coagulometer Quick Timer II (Draker – BR) and compared with the positive and negative control groups. Clotting time durations >240 s were considered indicative of a non-coagulant sample.

2.17. Hemorrhagic assay

To determine whether scFv-Svmp was potentially capable of interfering with the venom hemorrhagic effect, 10 μg *B. pauloensis* crude venom diluted in 50 μL PBS was inoculated intradermally in the back of six Swiss mice (18 to 22 g). For the test groups,

crude venom was pre-incubated with scFv-Svmp1 antibody for 30 min at 37 °C in venom/scFv ratios of 1/5 or 1/10. After 3 h, animals were sacrificed and had their skins removed. The hemorrhagic activity was evidenced by the presence and measure (average area in cm²) of hemorrhagic halos essentially as described [39]. For positive and negative controls, animals were inoculated with 10 μg *B. pauloensis* crude venom and 50 μL PBS, respectively.

2.18. Statistical analysis

Significant differences among experimental group values were determined by two-way ANOVA, followed by a Sidak test (*p* values <0.0005 were considered significant). Except for the values of hemorrhagic activity, the significance of the differences in group values was determined by one-way ANOVA, followed by a Tukey test (*p* values <0.05 were considered significant).
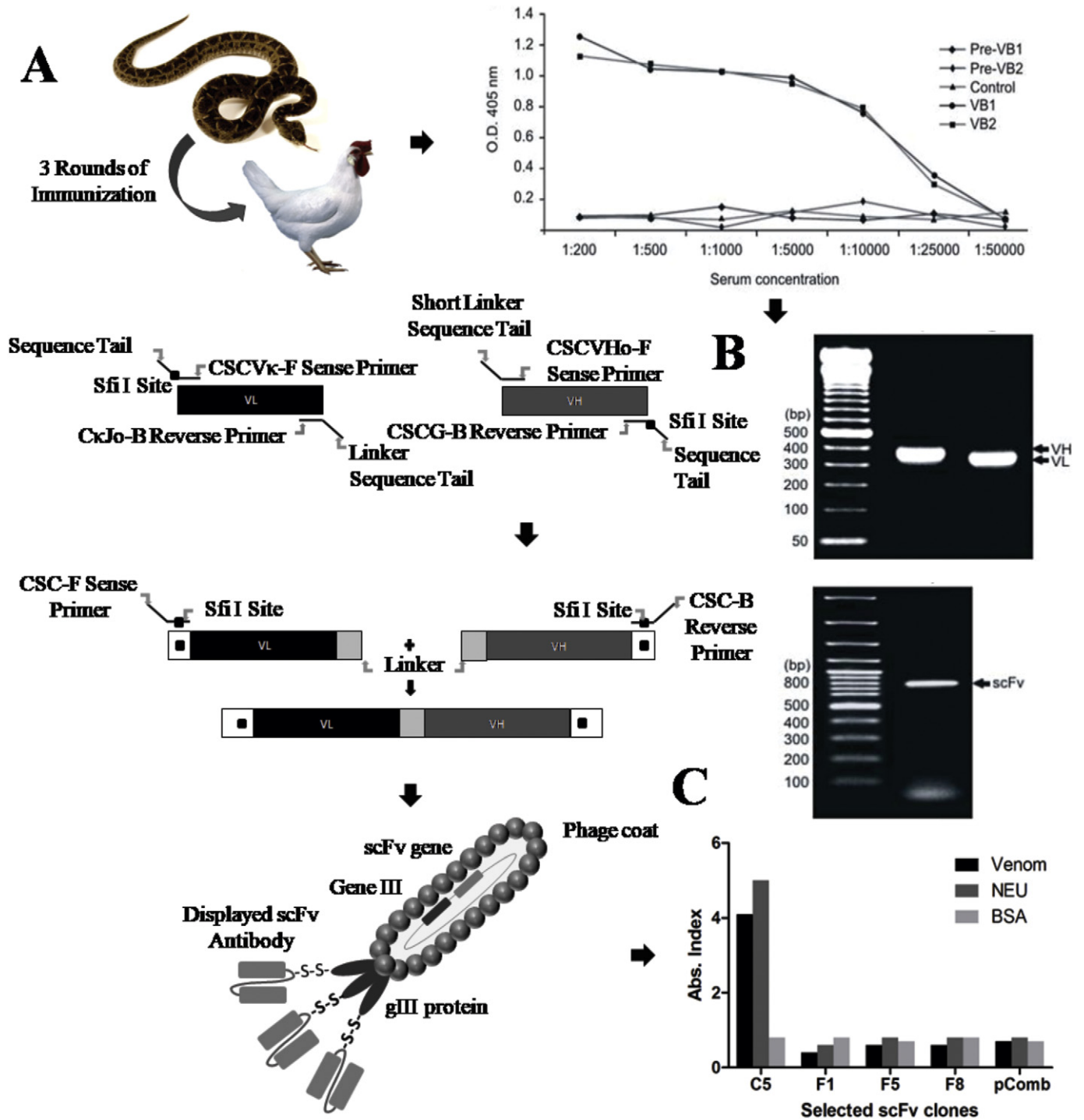
Fig. 2. Antibody library construction. A: Evaluation of immunization efficiency by sera titration of chickens immunized with *Bothrops pauloensis* crude venom. Pre-VB1 and Pre-VB2: pre-immune sera of immunized chickens. Control: chicken immunized with PBS and Freund adjuvant. VB1 and VB2: immune sera of immunized chickens after the third round of immunization. B: Agarose gel electrophoresis showing the amplified VL, VH and scFv fragments of 350, 400 and 800 bp, respectively. C: Evaluation of the specificity of four selected clones (C5, F1, F5 and F8) and empty vector (pComb) to crude and metalloproteinase-purified *neuwiedase* venoms, determined by ELISA.

3. Results

3.1. Antibody library construction and selection of phage-displayed antibody fragments

Chickens were immunized with *B. pauloensis* crude venom to select antibodies capable of neutralizing toxin activity. The generation of an antigen-specific immune response against crude venom in immunized chickens was certified by titration of specific IgY antibodies. After the third immunization, antibody titer reached 1:25,000 in both immunized chickens (VB1 and VB2; Fig. 2A). Titers above 1:1000 are sufficient to generate antibody libraries [31]. After obtaining the appropriate titer, animals were sacrificed and RNA was extracted from their spleens.

The amplification products of immunoglobulin light (VL) and heavy (VH) chain variable genes corresponded to the expected sizes of 350 bp and 400 bp, respectively (Fig. 2B). All PCR amplicons in the first round were purified in agarose gel, quantified and used as template for overlap reactions, which produced 800 bp scFv fragments. Following construction and transformation of the library into XL1-Blue electrocompetent cells, the library size was 2×10^8 independent transformants.

The VH and VL genes from the library were sequenced and translated to investigate its variability. Among 57 sequences, 17 VH genes presented different amino acid compositions and of 40 VL genes, only one was found twice, indicating high variability of the constructed library. After expressing the scFv library in phage particles, selection of specific antibodies was carried out by panning against *B. pauloensis* crude venom. The enrichment of eluted clones from the first to the third round was observed, despite increased stringency between rounds.

3.2. Characterization of selected clones

To assess the selected clones, *E. coli* cells were transformed with phagemid from the third selection cycle and used to express scFv molecules in solution, free of viral pIII protein. Following induction and expression in solution using a deep well system, an anti-HA antibody was used to detect heterologous proteins in culture supernatants by dot blot immunoassay (data not shown). Four clones with greater signal intensity were selected for further analysis. The specificity of these selected clones (C5, F1, F5 and F8) to *B. pauloensis* crude venom and metalloproteinase purified *neuwiedase* was determined by ELISA (Fig. 2C). There was much greater immunoreactivity to both antigens in the antibody present in clone C5 supernatant than in the other antibodies. These others had responses similar to negative controls, which correspond to the induced supernatant of a clone containing empty PComb3X in bovine serum albumin (BSA)-coated wells. This justified the choice of clone C5, called scFv-Svmp, for further testing.

3.3. Stable expression and purification of scFv-Svmp and scFv-Svmp1 proteins

The transgenic *N. tabacum* plants were obtained from stable transformation with scFv-Svmp sequence expression and did not vary phenotypically from the untransformed plant (Fig. 3A). Confirmation of scFv-Svmp1 protein expression was performed by western blot. The detectable band represents a fragment of ~ 30 kDa, indicating the fragment size of the recombinant scFv-Svmp1 antibody (Fig. 3B).

The bacterial culture supernatant expressing scFv-Svmp and leaf protein extract of the transgenic plants expressing scFv-Svmp1 were subjected to HPLC purification. Western blot analysis confirmed the presence of purified proteins with bands at ~ 30 kDa (Fig. 3C and D).

3.4. Antigen recognition of recombinant antibodies

To confirm whether the scFv-Svmp antibody recognized protein components from the venom, the spectrum of antigens recognized by the scFv-Svmp antibody in *B. pauloensis* venom was analyzed by western blot (Fig. 3E). The detected proteins ranged from low to high molecular weights. At least two different bands between 40 and 80 kDa (arrow 1) were recognized, with increasing intensity with increased concentrations of scFv (lanes 2 to 5). Two other bands are indicated by second and third arrows; the second indicates molecular weights ranging between 17 and 30 kDa and the third arrow highlights a band below 17 kDa.

3.5. scFv-Svmp interactome

To verify the interaction of scFv-Svmp with *B. pauloensis* venom proteins, the antibody was immobilized in a NHS affinity column and the eluted venom proteins were analyzed. The antibody interacted exclusively with two protein classes: PLA$_2$ and metalloproteinases (Table 1).

3.6. Cross-reactivity recognition of recombinant antibodies

To verify whether scFv-Svmp and scFv-Svmp1 show immunoreactivity to different snake venoms, these antibodies were subjected to ELISA analyses using *B. pauloensis*, *B. moojeni*, *B. leucurus*, *B. jararaca*, *B. jararacussu* and *C. durissus collilineatus* crude venoms. ScFv-Svmp and scFv-Svmp1 cross-reacted with venoms of different species (Fig. 4). The greatest reactivities of these antibodies were with *B. pauloensis* crude venom for scFv-Svmp and with *B. jararacussu* crude venom for scFv-Svmp1.

3.7. In vitro assay

3.7.1. Phospholipase activity

Recombinant antibodies scFv-Svmp and scFv-Svmp1 did not inhibit the phospholipase A$_2$ activities of *B. pauloensis* venom. Enzymes maintained the same activity as crude venom without antibodies (Fig. S2).

3.7.2. Proteolytic activity on fibrinogen

The ability of scFv-Svmp and scFv-Svmp1 to inhibit fibrinogenolytic activity of *B. pauloensis* crude venom was determined (Fig. 5A and B, respectively). Incubation of fibrinogen with crude venom previously associated with scFv-Svmp (1:3; 1:5 and 1:10, w/w) or scFv-Svmp1 (1:10; 1:25 and 1:50, w/w) resulted in a progressive increase in fibrinogen β chain protection (lanes 3 to 6), evidencing neutralization of some toxins present in the venom.

3.7.3. Proteolytic activity on azocasein and coagulant activity

Purified scFv-Svmp1 inhibited the proteolytic activity of the snake venom against azocasein as a substrate, compared to purified wild plant protein extract SR1. Inhibition of azocaseinolytic activity by the recombinant antibody was proportional to the concentration, with maximum inhibition of ~50% (Fig. 6A).

The effect of scFv-Svmp1 coagulation on the venom enzymes was evaluated. Inhibition caused by the antibody at all concentrations was greater than those caused by phenanthroline, a compound used as a positive coagulation control (Fig. 6B).

3.8. In vivo assay

3.8.1. Hemorrhagic activity

Venom toxins cause rupture of blood vessels (hemorrhage "per rexis"); however, animals inoculated with venom/antibody at 1:5 or 1:10 proportions have small bleeding halos (Fig. 7A). Variations in scFv-Svmp concentrations led to different degrees of inhibition of hemorrhagic activity at 1:10 (venom/antibody, w/w) there was partial neutralization of bleeding, an effect that increased with more concentrated antibodies (Fig. 7B). This finding demonstrates the protective effect of the antibody.
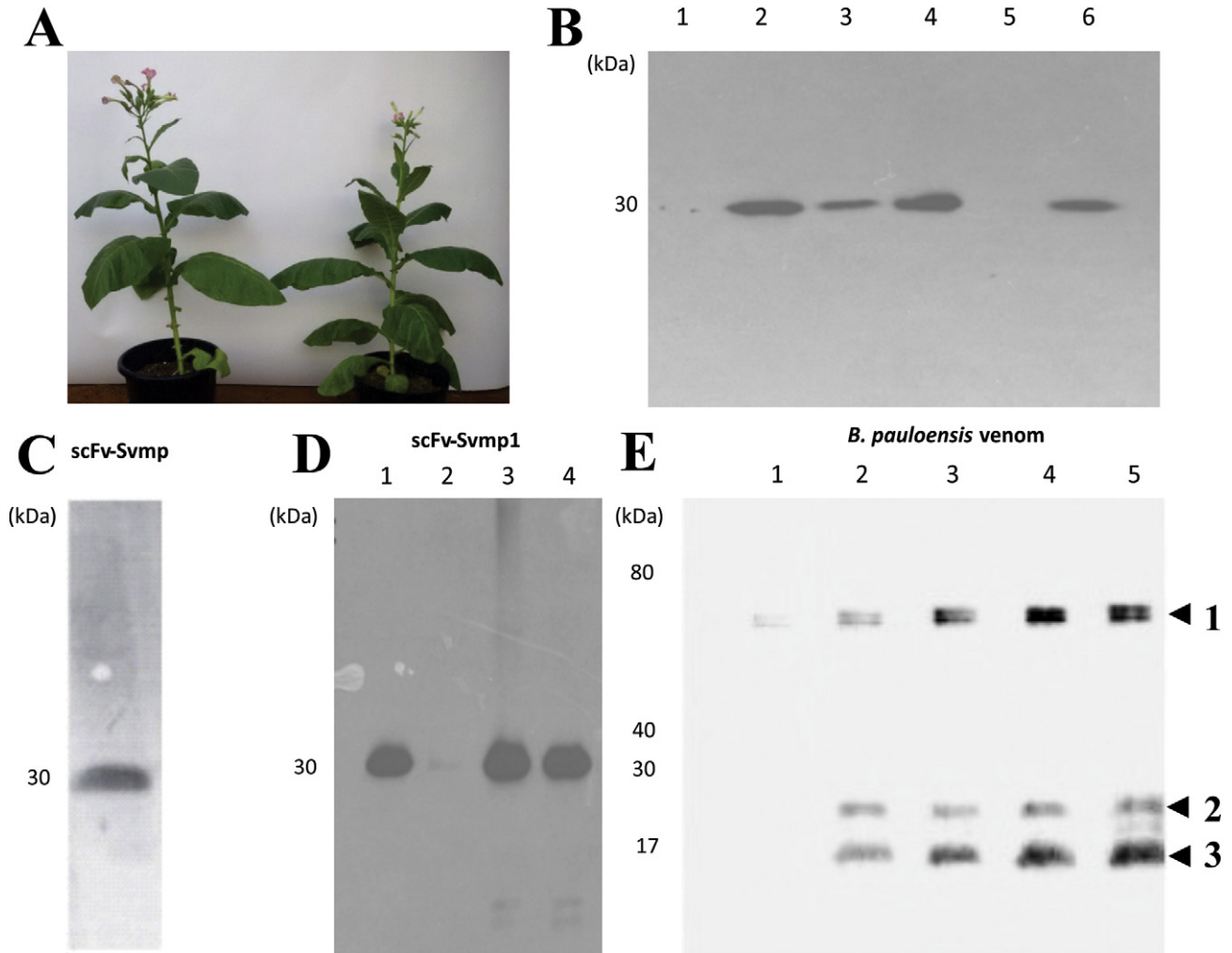
Fig. 3. Western blot analysis. A: Plant phenotype analysis. Wild *N. tabacum* plant (SR1 - left) and transgenic plant expressing scFv-Svmp1 (right). B: Transgenic confirmation. Western blot of protein samples extracted from leaves of wild plants (line 1) and five clones of transgenic plants (lines 2 to 6) of *N. tabacum*. C: Purification of scFv-Svmp. The antibody scFv-Svmp purified using His-tag column and HPLC system. D: Purification of scFv-Svmp1. Western blot anti-HA (1:2000 dilution) of *N. tabacum* crude extract scFv-Svmp1 (line 1) and three purified fractions of scFv-Svmp1 using His-tag column (lines 2 to 4). E: Antigenic profile of *B. pauloensis* crude venom recognized by scFv-Svmp antibody. Lanes 1–5: 15 μg *B. pauloensis* crude venom followed by its recognition by the scFv-Svmp antibody incubated in crescent concentrations (1/3000, 1/2000, 1/1500, 1/1000 and 1/800, respectively). The arrows show: 1- class III metalloproteinases (SVMPs-PIII); 2- class II and I metalloproteinases (SVMPs-PII and SVMPs-PI); 3- phospholipases A_2 (PLA$_2$).

4. Discussion

This investigation demonstrates the development of a novel scFv antibody anti-SVMPs with broad neutralizing activity against venoms from different snake species. Our strategy was based on phage display selections of an scFv combinatorial library, which led us to dominant clones with high reactivity against crude venoms. This novel clone prevented envenomation in a murine model due to its broad activity and was expressed in transgenic plants with great stability for large-scale production.

The scFv-Svmp interacted with different classes of metalloproteinases and PLA$_2$ present in *B. pauloensis* crude venom. The interaction of the antibody with the main classes of toxins present in *B. pauloensis* venom, the SVMPs (38%) and PLA$_2$ (32%) [40], can be explained by the fact that we used the crude venom in the construction of the library in which we identified the scFv-Svmp antibody (clone C5). Among the SVMPs classes, the interaction with class III metalloproteinases (SVMPs-PIII) had a molecular mass >50 kDa, which corresponded to one band (arrow 1 in Fig. 3E). This class is characterized by the presence of the disintegrin-like and cysteine-rich domains [41,42]. The scFv-

Table 1
Proteins identified in the *B. pauloensis* venom elution, with scFv-Svmp immobilized.

Sequence ID[a]	Description	Molecular weight (kDa)[b]	% Coverage	Number of peptides
AAF66703.1	Phospholipase A2 homolog, partial [*Bothrops pauloensis*]	13,51	87	4
ADO21505.1	MP_I2 SVMP precursor, partial [*Bothrops neuwiedi*]	27,18	79	10
ADO21501.1	MP_III1 SVMP precursor, partial [*Bothrops neuwiedi*]	49,81	56	15
ADO21502.1	MP_III2 SVMP precursor, partial [*Bothrops neuwiedi*]	49,63	65	8
ADO21506.1	MP_IIb1 SVMP precursor, partial [*Bothrops neuwiedi*]	36,08	65	4
ADO21511.1	MP_IIa SVMP precursor, partial [*Bothrops neuwiedi*]	34,9	62	5
ADO21503.1	MP_III3 SVMP precursor, partial [*Bothrops neuwiedi*]	49,31	30	9

[a] Protein Access Number on NCBI Platform (https://www.ncbi.nlm.nih.gov/).
[b] Theoretical molecular weight of the protein in kDa.
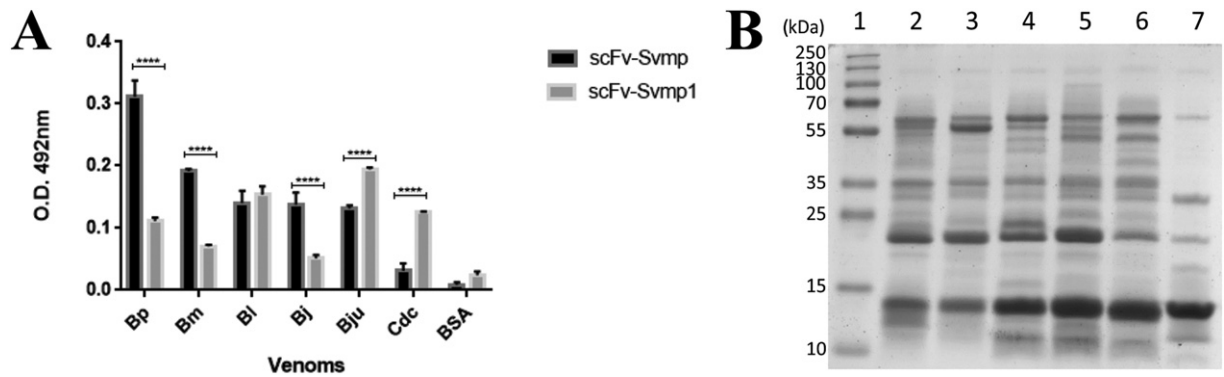
Fig. 4. Screening of scFv antibodies that bind to different snake venoms. A: The wells were coated with crude venom or BSA, then incubated with scFv-Svmp antibody (black bars) and scFv-Svmp1 antibody (grey bars). Bound scFv antibodies were detected with HRP-conjugated rat anti-HA and OPD substrate. The evaluated venoms were Bp: *Bothrops pauloensis*; Bm: *Bothrops moojeni*; Bl: *Bothrops leucurus*; Bj: *Bothrops jararaca*; Bju: *Bothrops jararacussu*; Cdc: *Crotalus durissus collilineatus*. ****$p < 0.0001$ compared with two groups. B: Protein profile of 10 μg of each evaluated venoms. Lane 1: Page Ruler Plus Prestained Protein Ladder (Thermo Scientific); 2: Bp; 3: Bm; 4: Bl; 5: Bj; 6: Bju; 7: Cdc. The gel was stained with Coomassie Blue G-250.

Svmp also interacted with SVMPs-PII (arrow 2), with a molecular mass between 25 and 50 kDa, with metalloproteinase and disintegrin domains. These bands may correspond to SVMPs-PI having an approximate molecular mass of 25 kDa and only the metalloproteinase domain [41,42]. In addition to SVMPs, there was also recognition of PLA$_2$, bands (arrow 3), which have molecular mass between 13 and 18 kDa [43]. Similar to the western blot results, the proteomic analysis of *B. pauloensis* venom eluate also showed that scFv-Svmp has an exclusive interaction with the same two protein families, metalloproteinases and phospholipases (Table 1). There was high affinity of scFv-Svmp for metalloproteinases, where there is a predominance of hits on PIII and PI classes, which are contained in the SVMPs of this species.

The scFv-Svmp and scFv-Svmp1 molecules reacted with venoms of the six species evaluated, five from the genus *Bothrops* and one from *Crotalus*. The interaction was species-specific. ScFv-Svmp was selected against crude venom of *B. pauloensis* and, as expected, showed greater reactivity against this venom, while scFv-Svmp1 showed greater reactivity against *B. jararacussu*. This difference in reactivity can be explained by the different heterologous protein expression systems used to produce these molecules. ScFv-Svmp was produced in *E. coli*, a prokaryotic system that lacks post-translational modification machinery [44]. ScFv-Svmp1 was produced in *N. tabacum*, a eukaryotic system that can perform post-translational modifications, folding and protein processing [45]. These structural differences probably explain the different reactivity observed. ScFv-Svmp binding was greater in those species with more SVMPs (Table 2). In contrast, scFv-Svmp1 had greater interaction with venoms with higher PLA$_2$ content. Because metalloproteinases and PLA$_2$ are the major venom protein families [46], this difference

in reactivity may be associated with variations in the proportions of SVMP and PLA$_2$ present in venoms. The importance of this assessment is that these two families are primarily responsible for most of the toxic effects of ophidian venoms [47]. Examples of primary pharmacological and therapeutic effects of isolated components of *B. pauloensis* venom include myotoxicity, neurotoxicity, necrosis, cytotoxicity, antiplatelet aggregation and fibrinogenolytic, among others [43].

Antibodies scFv-Svmp and scFv-Svmp1 did not interfere with PLA$_2$ activity (Fig. S2). The interaction of antibody with PLA$_2$ probably occurs at a non-active site of these enzymes, thus not interfering with the activity of this enzyme class. The surface of large proteins is covered by a large number of cavities that make potential binding sites for ligands [48]. Antibodies scFv-Svmp and scFv-Svmp1 do not interfere with the mechanisms of action of phospholipases, acting only on metalloproteinase activity.

We performed proteolytic tests in which scFv-Svmp and scFv-Svmp1 inhibited venom fibrinogenolytic activity, as they conserved part of the fibrinogen β chain (Fig. 6A and B). This conservation profile is similar to that obtained by 1,10-phenanthroline, a metal chelator that strongly inhibits SVMPs [49]. Beta chain and alpha cleavage causes the formation of fibrin, whose action promotes blood coagulation [50]. Most proteolytic enzymes that act on fibrinogen and fibrin are metalloproteinases [51]. ScFv-Svmp1 also inhibited >50% of proteolytic activity measured on an azocasein substrate.

ScFv-Svmp1 inhibits coagulation by reducing the activity of SVMPs contained in the venom. The interference in the coagulatory processes by SVMPs and their various isoforms lets them act simultaneously against several stages of the blood coagulation cascade [47]. Coagulation
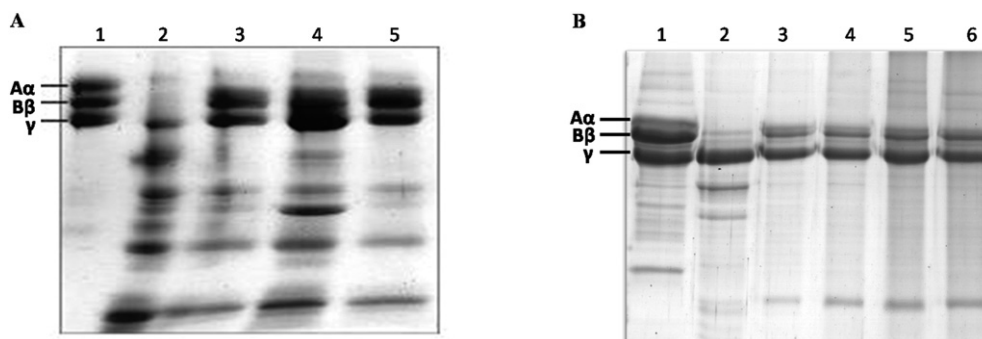
Fig. 5. Fibrinogenolytic activity inhibition by scFv's. Samples containing *B. pauloensis* crude venom were incubated with scFv-Svmp purified from bacteria (A) and scFv-Svmp1 from transgenic plants of *N. tabacum* (B) at 37 °C for 30 min, followed by incubation with bovine fibrinogen (1.5 mg/mL) for 2 h at 37 °C. A: lane 1: bovine fibrinogen (15 μg); lane 2: bovine fibrinogen incubated with *B. pauloensis* crude venom without scFv-Svmp; lines 3 to 5: *B. pauloensis* venom that was previously incubated with bacterial scFv-Svmp at venom/scFv (w/w) ratios of 1/3, 1/5 and 1/10, respectively. B: lane 1: bovine fibrinogen (15 μg); lane 2: metalloproteinase (5 μg) incubated with *B. pauloensis* crude venom without scFv-Svmp1 (negative control of inhibition); lane 3: 1–10 phenantroline (positive control of inhibition); lines 4 to 6: *B. pauloensis* venom that was previously incubated with purified plant scFv-Svmp1 at venom/scFv (w/w) ratios of 1/10, 1/25 and 1/50, respectively.
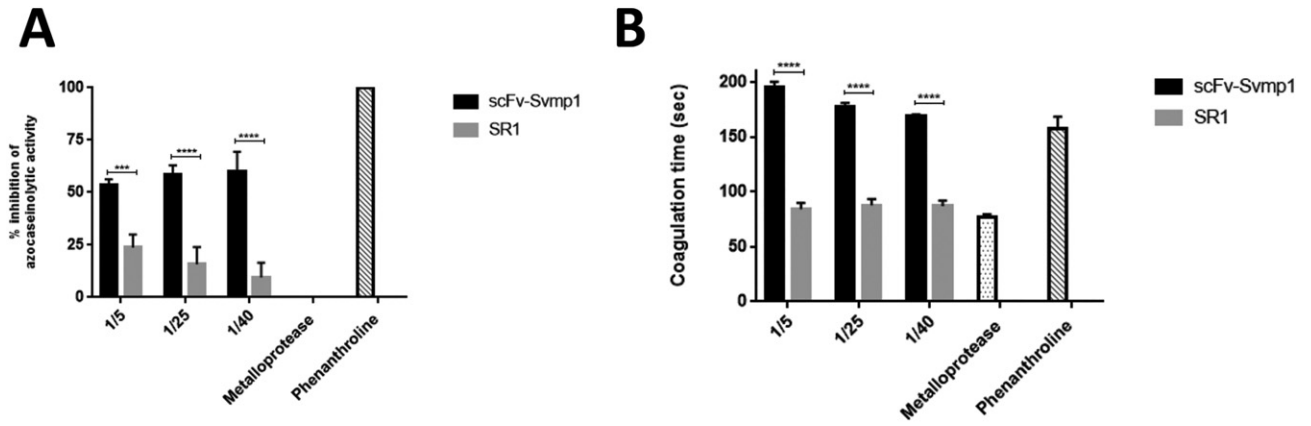
Fig. 6. Azocaseinolytic and coagulant activities of plant scFv-Svmp1. Samples enriched in metalloproteinase were preincubated with the samples to be evaluated for 30 min at 37 °C. A: Subsequently, azocasein (1 mg/mL) was added to samples with metalloproteinase (dotted bar; negative control of inhibition), 10 mM phenanthroline (striped bar; positive control of inhibition), purified plant scFv-Svmp1 (black bar) and protein extract of wild type *N. tabacum* (SR1) purified (grey bar) to measure azocaseinolytic activity. One unit (U) of azocaseinolytic activity was defined as an increase of 0.01 absorbance units at 405 nm under standard assay conditions. B: To evaluate coagulation activity, 150 μL bovine plasma was added to metalloproteinase (dotted bar; negative control of coagulation), 10 mM phenanthroline (striped bar; positive control of coagulation), purified plant scFv-Svmp1 (black bar) and purified protein extract of wild type *N. tabacum* (SR1; grey bar). The time required to start the formation of the fibrin network was recorded by a photometric system in the coagulometer. $***p = 0.0005$ compared with two groups. $****p < 0.0001$ compared with two groups.

time was prolonged by scFv-Svmp1 and, most of the time, the enzymes that advance coagulation in snake venoms are proteases. These are responsible for activating zymogen present in specific coagulation factors in the coagulation cascade and accelerating clot generation. In SVMPs, they can activate factor X and prothrombin [9]. Such activity causes these proteolytic enzymes to interfere directly with blood coagulation and platelet activity, leading to the occurrence of clinical manifestations [51]. Among them are microvascular thrombosis, extremity gangrene
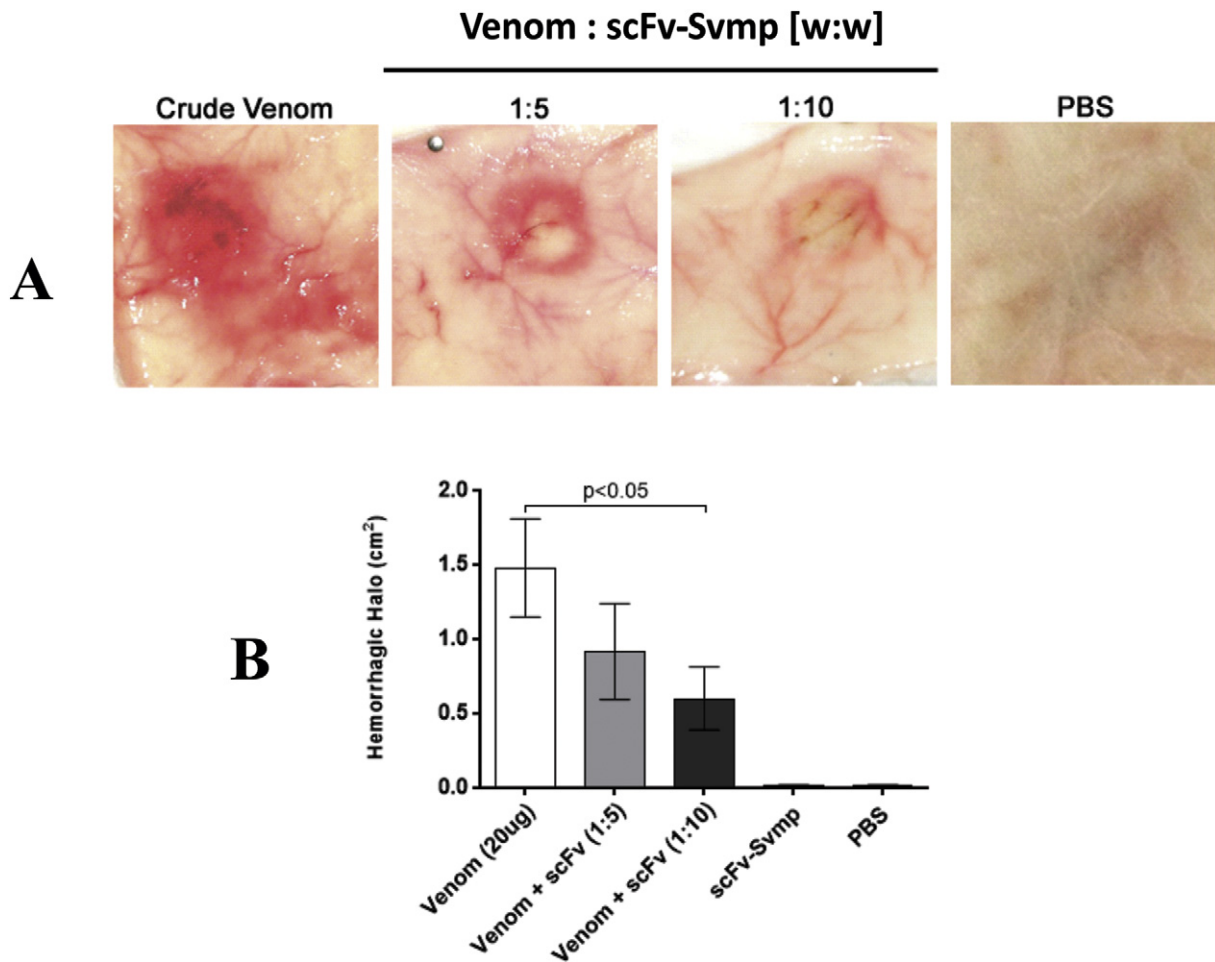
Fig. 7. Effect of the scFv-Svmp antibody on *B. pauloensis* venom activities. A: Hemorrhagic halos formed after inoculation with *B. pauloensis* snake venom previously incubated with bacterial scFv-Svmp in venom/scFv [w/w] ratios of 1/5 and 1/10. Crude venom: inoculation with two HMD (Hemorrhagic Minimal Dose, 16.3 μg) of venom diluted with phosphate buffer (positive control). PBS: inoculation with PBS (negative control). B: Measure of halo expressed in cm². Results are expressed by the mean ± S.D., $n = 6$.

Table 2
Percentage of the main toxin classes in the evaluated venoms.

Specie	Methodology	Sample	% SVMP	% Phospholipases	Reference
B. pauloensis	Proteomic	Crude venom	38.1	31.9	[40]
B. moojeni	Proteomic	Crude venom[a]	38.1	14.3	[4]
B. jararaca	Proteomic	Crude venom[b]	35.6	3.7	[55]
B. jararacussu	Transcriptome	Venomous gland	16.0	35.0	[56]
C. durissus terrificus	Proteomic	Crude venom	3.9	48.5	[57]

[a] Values refers to the average of male and female crude venom.
[b] Values refers to the crude venom of populations from Southeastern.

and hemorrhagic skin necrosis [52]. In addition to inhibiting coagulation, scFv-Svmp significantly neutralized the *in vivo* hemorrhagic effects caused by *B. pauloensis* crude venom in mice. This activity was dose-dependent, with the smallest halo obtained at a concentration of 1:10 (venom:scFv-Svmp; w:w). The variations in domain structures that comprise the different classes of SVMPs (Dis, Dis-like and Cys-rich) are responsible for the enzymes with distinct hemorrhagic activities [53]. The mechanism of action of hemorrhagic SVMPs is based on hydrolysis of the main substrates in the capillary basement membrane, causing wall weakening and consequent blood leakage [54]. However, despite the relevance of our findings, the replacement of antiophidic sera must be investigated.

5. Conclusion

We demonstrated control of hemorrhage caused by scFv-Svmp due to its high antigenic and neutralizing capacity against metalloproteinases present in venoms from different snake species. This reaffirms its potential use as a broad-spectrum immunobiological for treatment of snakebite envenomation.

Supplementary data to this article can be found online at https://doi.org/10.1016/j.ijbiomac.2020.02.028.

CRediT authorship contribution statement

Jessica B. Souza: Investigation, Methodology, Writing - original draft, Writing - review & editing. **Rone Cardoso:** Investigation, Methodology, Conceptualization, Writing - original draft. **Hebréia O. Almeida-Souza:** Investigation, Methodology, Writing - original draft, Writing - review & editing. **Camila P. Carvalho:** Investigation, Methodology. **Lucas Ian Veloso Correia:** Investigation, Methodology. **Paula Cristina B. Faria:** Investigation, Methodology. **Galber R. Araújo:** Investigation, Methodology. **Mirian M. Mendes:** Investigation, Methodology. **Renata Santos Rodrigues:** Writing – review & editing. **Veridiana M. Rodrigues:** Writing – review & editing. **Abhaya M. Dandekar:** Investigation, Methodology, Writing – review & editing. **Luiz Ricardo Goulart:** Conceptualization, Funding acquisition, Supervision. **Rafael Nascimento:** Investigation, Methodology, Conceptualization, Writing - original draft.

References

[1] J. Longbottom, F.M. Shearer, M. Devine, G. Alcoba, F. Chappuis, D.J. Weiss, S.E. Ray, N. Ray, D.A. Warrell, R. Ruiz de Castañeda, D.J. Williams, S.I. Hay, D.M. Pigott, Vulnerability to snakebite envenoming: a global mapping of hotspots, Lancet 392 (2018) 673–684.

[2] J.P. Chippaux, Snakebite envenomation turns again into a neglected tropical disease! J. Venom. Anim. Toxins Incl. Trop. Dis. 23 (2017) 1–2.

[3] Ministério da Saúde, (n.d.) Acidentes por animais peçonhentos: o que fazer e como evitar, http://www.saude.gov.br/saude-de-a-z/acidentes-por-animais-peconhentos (accessed August 9, 2019).

[4] F.G. Amorim, T.R. Costa, D. Baiwir, E. De Pauw, L. Quinton, S.V. Sampaio, Proteopeptidomic, functional and immunoreactivity characterization of Bothrops moojeni snake venom: influence of snake gender on venom composition, Toxins (Basel) 10 (2018) 1–18.

[5] S.E. Gasanov, R.K. Dagda, E.D. Rael, Snake venom cytotoxins, phospholipase A2s, and Zn2+dependent metalloproteinases: mechanisms of action and pharmacological relevance, J Clin Toxicol 4 (2014) 34.

[6] S.S. Oliveira, E.C. Alves, A.S. Santos, J.P.T. Pereira, L.K.S. Sarraff, E.F. Nascimento, J.D. De-Brito-sousa, V.S. Sampaio, M.V.G. Lacerda, J.A.G. Sachett, I.S. Sano-Martins, W.M. Monteiro, Factors associated with systemic bleeding in bothrops envenomation in a tertiary hospital in the brazilian amazon, Toxins (Basel) 11 (2019).

[7] C.M. Sant'Ana Malaque, J.M. Gutiérrez, Snakebite Envenomation in Central and South America, Springer International Publishing, Brent J, Switzerland, 2016.

[8] T. Tasoulis, G.K. Isbister, A review and database of snake venom proteomes, Toxins (Basel) 9 (2017).

[9] R.M. Kini, C.Y. Koh, Metalloproteases affecting blood coagulation, fibrinolysis and platelet aggregation from snake venoms: definition and nomenclature of interaction sites, Toxins (Basel) 8 (2016) 1–27.

[10] B.C. Prezoto, E.E. Kato, L.R.C. Gonçalves, S.C. Sampaio, I.S. Sano-Martins, Elevated plasma levels of hepatocyte growth factor in rats experimentally envenomated with Bothrops jararaca venom: role of snake venom metalloproteases, Toxicon 162 (2019) 9–14.

[11] C. Möller, W.C. Davis, E. Clark, A. DeCaprio, F. Marí, Conodipine-P1–3, the First Phospholipases A 2 Characterized from Injected Cone Snail Venom, 2019.

[12] J.C. Sobrinho, A.M. Kayano, R. Simões-Silva, J.J. Alfonso, A.F. Gomez, M.C.V. Gomez, F.B. Zanchi, L.A. Moura, V.R. Souza, A.L. Fuly, E. de Oliveira, S.L. da Silva, J.R. Almeida, J.P. Zuliani, A.M. Soares, Anti-platelet aggregation activity of two novel acidic Asp49-phospholipases A 2 from Bothrops brazili snake venom, Int. J. Biol. Macromol. 107 (2018) 1014–1022.

[13] F.F. Cardoso, R.J. Borges, T.R. Dreyer, G.H.M. Salvador, W.L.G. Cavalcante, M.D. Pai, M. Gallacci, M.R.M. Fontes, Structural basis of phospholipase A2-like myotoxin inhibition by chicoric acid, a novel potent inhibitor of ophidian toxins, Biochim. Biophys. Acta - Gen. Subj. 1862 (2018) 2728–2737.

[14] J.J. Calvete, Y. Rodríguez, S. Quesada-Bernat, D. Pla, Toxin-resolved antivenomics-guided assessment of the immunorecognition landscape of antivenoms, Toxicon 148 (2018) 107–122.

[15] J.M. Gutiérrez, G. Solano, D. Pla, M. Herrera, Á. Segura, M. Vargas, M. Villalta, A. Sánchez, L. Sanz, B. Lomonte, G. León, J.J. Calvete, Preclinical evaluation of the efficacy of antivenoms for snakebite envenoming: state-of-the-art and challenges ahead, Toxins (Basel) 9 (2017) 1–22.

[16] D.J. Williams, A.G. Habib, D.A. Warrell, Clinical studies of the effectiveness and safety of antivenoms, Toxicon 150 (2018) 1–10.

[17] A.G. Habib, N.I. Brown, The snakebite problem and antivenom crisis from a health-economic perspective, Toxicon 150 (2018) 115–123.

[18] A.H. Laustsen, K.H. Johansen, M. Engmark, M.R. Andersen, Recombinant snakebite antivenoms: a cost-competitive solution to a neglected tropical disease? PLoS Negl. Trop. Dis. 11 (2017) 1–14.

[19] D. De Martinis, E.P. Rybicki, K. Fujiyama, R. Franconi, E. Benvenuto, Editorial: plant molecular farming: fast, scalable, cheap, sustainable, Front. Plant Sci. 7 (2016) 2.

[20] E.N. Kosobokova, M.V. Piniugina, V.S. Kosorukov, Synthesis of biologically active human interferon α-2b in Nicotiana benthamiana, Appl. Biochem. Microbiol. 52 (2016) 705–713.

[21] M.J. Paul, H. Thangaraj, J.K.C. Ma, Commercialization of new biotechnology: a systematic review of 16 commercial case studies in a novel manufacturing sector, Plant Biotechnol. J. 13 (2015) 1209–1220.

[22] J. Yao, Y. Weng, A. Dickey, K.Y. Wang, Plants as factories for human pharmaceuticals: applications and challenges, Int. J. Mol. Sci. 16 (2015) 28549–28565.

[23] H.S. Loh, B.J. Green, V. Yusibov, Using transgenic plants and modified plant viruses for the development of treatments for human diseases, Curr. Opin. Virol. 26 (2017) 81–89.

[24] M. Sack, A. Hofbauer, R. Fischer, E. Stoger, The increasing value of plant-made proteins, Curr. Opin. Biotechnol. 32 (2015) 163–170.

[25] L.M. Alvarenga, M. Zahid, A. di Tommaso, M.O. Juste, N. Aubrey, P. Billiald, J. Muzard, Engineering Venom's toxin-neutralizing antibody fragments and its therapeutic potential, Toxins (Basel) 6 (2014) 2541–2567.

[26] M.B. Luiz, S.S. Pereira, N.D.R. Prado, N.R. Gonçalves, A.M. Kayano, L.S. Moreira-Dill, J.C. Sobrinho, F.B. Zanchi, A.L. Fuly, C.F. Fernandes, J.P. Zuliani, A.M. Soares, R.G. Stabeli, C.F.C. Fernandes, Camelid single-domain antibodies (VHHs) against crotoxin: a basis for developing modular building blocks for the enhancement of treatment or diagnosis of crotalic envenoming, Toxins (Basel) 10 (2018).

[27] G. Richard, A.J. Meyers, M.D. McLean, M. Arbabi-Ghahroudi, R. MacKenzie, J.C. Hall, In vivo neutralization of α-cobratoxin with high-affinity llama single-domain antibodies (VHHs) and a VHH-Fc antibody, PLoS One 8 (2013) 1–14.

[28] J.M.A. Castro, T.S. Oliveira, C.R.F. Silveira, M.C. Caporrino, D. Rodriguez, A.M. Moura-Da-Silva, O.H.P. Ramos, A. Rucavado, J.M. Gutiérrez, G.S. Magalhães, E.L. Faquim-Mauro, I. Fernandes, A neutralizing recombinant single chain antibody, scFv, against BaP1, A P-I hemorrhagic metalloproteinase from Bothrops asper snake venom, Toxicon 87 (2014) 81–91.

[29] M. Gomes, M.A. Alvarez, L.R. Quellis, M.L. Becher, J.M. de A. Castro, J. Gameiro, M.C. Caporrino, A.M. Moura-da-Silva, M. de Oliveira Santos, Expression of an scFv antibody fragment in Nicotiana benthamiana and in vitro assessment of its neutralizing potential against the snake venom metalloproteinase BaP1 from Bothrops asper, Toxicon 160 (2019) 38–46.

[30] V.M. Rodrigues, A.M. Soares, R. Guerra-Sá, V. Rodrigues, M.R.M. Fontes, J.R. Giglio, Structural and functional characterization of neuwiedase, a nonhemorrhagic fibrin (ogen)olytic metalloprotease from Bothrops neuwiedi snake venom, Arch. Biochem. Biophys. 381 (2000) 213–224.

[31] C.F. Barbas, G.J. Silverman, J.K. Scott, D.R. Burton, Phage Display: A Laboratory Manual, Cold Spring Harbor Laboratory Press, Cold Spring Harbor, New York, 2001.

[32] S.F. Altschul, T.L. Madden, A.A. Schäffer, J. Zhang, Z. Zhang, W. Miller, D.J. Lipman, Gapped BLAST and PSI-BLAST: a new generation of protein database search programs, Nucleic Acids Res. 25 (1997) 3389–3402.

[33] J.D. Thompson, D.G. Higgins, T.J. Gibson, CLUSTAL W: improving the sensitivity of progressive multiple sequence alignment through sequence weighting, position-specific gap penalties and weight matrix choice, Nucleic Acids Res. 22 (1994) 4673–4680.

[34] M. Azevedo, M. Felipe, M. Brígido, A. Maranhão, M. De-Souza, Técnicas básicas em biologia molecular, Universidade de Brasília, Brasília, DF, 2003.

[35] G.H. De Haas, N.M. Postema, W. Nieuwenhuizen, L.L.V. Deenen, Purification and properties of phospholipase A from porcine pancreas, Biochim. Biophys. Acta 159 (1968) 103–117.

[36] E. Mendonça, L. Visôtto, N.C. Costa, F. Ribeiro, J. Oliveira, M.G. Oliveira, Caracterização enzimática de isoformas de cisteíno protease de Anticarsia gemmatalis (HÜBNER, 1818), Ciência e Agrotecnologia 35 (2011) 446–454.

[37] D.L. Naves de Souza, M.S.R. Gomes, F.B. Ferreira, R.S. Rodrigues, D.C. Achê, M. Richardson, M.H. Borges, V.M. Rodrigues, Biochemical and enzymatic characterization of BpMP-I, a fibrinogenolytic metalloproteinase isolated from Bothropoides pauloensis snake venom, Comp. Biochem. Physiol. - B Biochem. Mol. Biol. 161 (2012) 102–109.

[38] M.T. Assakura, M. da G. Salomão, G. Puorto, F.R. Mandelbaum, Hemorrhagic, fibrinogenolytic and edema-forming activities of the venom of the colubrid snake Philodryas olfersii (green snake), Toxicon 30 (1992) 427–438.

[39] T. Nikai, N. Mori, M. Kishida, M. Tsuboi, H. Sugihara, Isolation and characterization of hemorrhagic toxin g from the venom of Crotalus atrox (western diamondback rattlesnake), Am. J. Trop. Med. Hyg. 34 (1985) 1167–1172.

[40] R.S. Rodrigues, J. Boldrini-França, F.P.P. Fonseca, P. de la Torre, F. Henrique-Silva, L. Sanz, J.J. Calvete, V.M. Rodrigues, Combined snake venomics and venom gland transcriptomic analysis of Bothropoides pauloensis, J. Proteome 75 (2012) 2707–2720.

[41] G.F.Ş. Andrei, G.F. Adriana, K. Hajnal, D.-L. Muntean, Snake Venom Metalloproteinases, Acta Medica Marisiensis 62 (2016) 106–111.

[42] J.W. Fox, S.M.T. Serrano, Structural considerations of the snake venom metalloproteinases, key members of the M12 reprolysin family of metalloproteinases, Toxicon 45 (2005) 969–985.

[43] V. Rodrigues, D. Lopes, L. Castanheira, S. Gimenes, D. Naves de Souza, D. Ache, I. Borges, K. Yoneyama, R. Rodrigues, Bothrops pauloensis snake venom toxins: the search for new therapeutic models, Curr. Top. Med. Chem. 15 (2015) 670–684.

[44] S. Sahdev, S.K. Khattar, K.S. Saini, Production of active eukaryotic proteins through bacterial expression systems: a review of the existing biotechnology strategies, Mol. Cell. Biochem. 307 (2008) 249–264.

[45] O. Khow, S. Suntrarachun, Strategies for production of active eukaryotic proteins in bacterial expression system, Asian Pac. J. Trop. Biomed. 2 (2012) 159–162.

[46] L.F. Sousa, C.A. Nicolau, P.S. Peixoto, J.L. Bernardoni, S.S. Oliveira, J.A. Portes-Junior, R.H.V. Mourão, I. Lima-dos-Santos, I.S. Sano-Martins, H.M. Chalkidis, R.H. Valente, A.M. Moura-da-Silva, Comparison of phylogeny, venom composition and neutralization by antivenom in diverse species of bothrops complex, PLoS Negl. Trop. Dis. 7 (2013).

[47] C.R. Ferraz, A. Arrahman, C. Xie, N.R. Casewell, R.J. Lewis, J. Kool, F.C. Cardoso, Multi-functional toxins in snake venoms and therapeutic implications: from pain to hemorrhage and necrosis, Front. Ecol. Evol. 7 (2019) 1–19.

[48] D. Suplatov, V. Švedas, Study of functional and allosteric sites in protein superfamilies, Acta Nat. 7 (2015) 34–45.

[49] J.B. Bjarnason, J.W. Fox, Hemorrhagic metalloproteinases from snake venoms, Pharmacol. Ther. 62 (1994) 325–372.

[50] M.W. Mosesson, Fibrinogen and fibrin structure and functions, J. Thromb. Haemost. 3 (2005) 1894–1904.

[51] E.F. Sanchez, R.J. Flores-Ortiz, V.G. Alvarenga, J.A. Eble, Direct fibrinolytic snake venom metalloproteinases affecting hemostasis: structural, biochemical features and therapeutic potential, Toxins (Basel) 9 (2017).

[52] S.M. Rezende, Disturbios da Hemostasia: doenças hemorrágicas, Rev Med Minas Gerais 20 (2010) 534–553.

[53] J.M. Gutiérrez, T. Escalante, A. Rucavado, C. Herrera, Hemorrhage caused by snake venom metalloproteinases: a journey of discovery and understanding, Toxins (Basel) 8 (2016).

[54] J.M. Gutiérrez, A. Rucavado, T. Escalante, C. Díaz, Hemorrhage induced by snake venom metalloproteinases: biochemical and biophysical mechanisms involved in microvessel damage, Toxicon 45 (2005) 997–1011.

[55] L. Gonçalves-Machado, D. Pla, L. Sanz, R.J.B. Jorge, M. Leitão-De-Araújo, M.L.M. Alves, D.J. Alvares, J. De Miranda, J. Nowatzki, K. de Morais-Zani, W. Fernandes, A.M. Tanaka-Azevedo, J. Fernández, R.B. Zingali, J.M. Gutiérrez, C. Corrêa-Netto, J.J. Calvete, Combined venomics, venom gland transcriptomics, bioactivities, and antivenomics of two Bothrops jararaca populations from geographic isolated regions within the Brazilian Atlantic rainforest, J. Proteome 135 (2016) 73–89.

[56] S. Kashima, P.G. Roberto, A.M. Soares, S. Astolfi-Filho, J.O. Pereira, S. Giuliati, M. Faria, M.A.S. Xavier, M.R.M. Fontes, J.R. Giglio, S.C. França, Analysis of Bothrops jararacussu venomous gland transcriptome focusing on structural and functional aspects: I-gene expression profile of highly expressed phospholipases A2, Biochimie 86 (2004) 211–219.

[57] D. Georgieva, M. Öhler, J. Seifert, M. Von Bergen, R.K. Arni, N. Genov, C. Betzel, Snake venomic of crotalus durissus terrificus-correlation with pharmacological activities, J. Proteome Res. 9 (2010) 2302–2316.

2

Use of phage M13 from phage display library in experimental chicken embryo model

5

6   Jessica Brito de Souza[1*], Simone Sommerfeld[2], Luiz Ricardo Goulart[1t], Emília Rezende

7   Vaz[1], Hebreia Oliveira Almeida Souza[1], Luciana Machado Bastos[1], Fabiana Almeida

8   Araújo Santos[1], Alessandra Castro Rodrigues[2], Alessandra Aparecida Medeiros-

9   Ronchi[2], Belchiolina Beatriz Fonseca[1,2]

10

11   1. Postgraduate Program in Genetics and Biochemistry, Institute of Biotechnology,

12   Federal University of Uberlândia, Brazil

13   2. Postgraduate Program in Veterinary Sciences, Faculty of Veterinary Medicine,

14   Federal University of Uberlândia, Brazil

15

16   *Corresponding author: souzajessicab34@gmail.com

17   Alternative corresponding author: biafonseca@ufu.br

18   ƚ: in memoriam

19

20

21

22

23

24

25

26

27   **ABSTRACT**

28

29   The filamentous bacteriophage M13 is the most used in phage display (PD) technology

30   and, like other phages, has been applied in several areas of medicine, agriculture, and the

31   food industry. One of the advantages is that they can modulate the immune response in

32   the presence of pathogenic microorganisms, such as bacteria and viruses. This study

33   evaluated the use of phage M13 in the chicken embryos model. We inoculated 13-day-

34   old chicken embryos with SP and then evaluated survival for the presence of phage M13

35   or *E.coli* ER2738 (ECR) infected with M13. We found that the ECR bacterium inhibits

36   SP multiplication and that the ECR-free phage M13 from the PD library can be used in

37   chicken embryo models. This work provides the use of the chicken embryo as a model to

38   study systemic infection and can be employed as an analysis tool for various peptides that

39   M13 can express from PD selection.

40

41   **KEYWORDS:** filamentous phage M13; bacterial infection; animal model.

42

43

44

45

46

47

48

49

50

51

52

53

1. INTRODUCTION

Phage Display (PD) technology consists of *in vitro* selection based on the presentation of peptides or proteins exposed on the surface of bacteriophages in the form of fusion proteins (Rahbarnia et al. 2017; Jiang et al. 2022). Bacteriophages are a type of virus that can carry out an infectious process in bacteria, fungi, actinomycetes, or spirochetes (Ge et al. 2020). PD applications are increasing and efficiently employed as phage therapy in veterinary medicine, agriculture, and food safety (Jamal et al. 2019).

Among the different types of bacteriophages used in PD, the most used is the filamentous phage M13, which receives this name due to its filamentous appearance and dependence on pilus F in the infection process (Ebrahimizadeh and Rajabibazl 2014). Some of its applications are already well described in the literature, such as its use to evaluate antiviral activity (Nakakido et al. 2022) and stimulate the immune system by activating antigen-presenting cells (Dong et al. 2020). Furthermore, it proved that phages and peptides expressed and selected by the PD modulate the immune response against bacterial and viral infections (díaz-Valdés et al. 2011; Van Belleghem et al. 2019).

Given the importance of better understanding infectious processes and the search for the feasibility of experimental models, the chicken embryo is considered an accessible, inexpensive, and low-maintenance *in vivo* model. Moreover, it is easy to manipulate and allows a non-invasive follow-up during its development (Rashidi and Sottile 2009). Given all these advantages, this model has recently been used in several areas, such as evaluation of drug toxicity and distribution (Zosen et al. 2021; Ghimire et al. 2022), epigenetics (Bednarczyk et al. 2021), teratology (Wachholz et al. 2021), analysis of snake venom effects (Polláková et al. 2021), and bacterial infections (Li et al. 2019; Kosecka-Strojek et al. 2021).

The chicken embryo (CE) is a good model for tests with infection since it is possible to determine the pathogenicity of different bacteria (Gibbs et al. 2003; Oh et al. 2012; Blanco et al. 2018; Rezaee et al. 2021). Given the importance of using the PD to select ligands in several processes and the use of chicken embryos as a good study model to understand such mechanisms, this work aims to propose an experimental model for the utilization of phage M13 from the PD library in tests in an experimental model of chicken embryos. It would be helpful to have the chick embryo as an experimental model of pathogen-binding phages or other molecules for disease control.

2. METHODOLOGY

Performed this research in the following laboratories of the Federal University of Uberlândia: Poultry Egg Incubation, Nanobiotechnology, Biochemistry, Laboratory of Infectious Diseases, and Animal Pathology. Project certified by the Ethics and Research with Animals Committee of the Federal University of Uberlândia (Nº 45/2022/CEUA/PROPP/REITO, process Nº23117.043271/2022-61).

2.1 Evaluation of the ability of *E.coli* ER2738 and phage M13 to inhibit S. Pullorum *in vitro*

We developed a test to understand the *S.* Pullorum infection in chicken embryos and then used this bacterium in the control group.

2.1.1 Phage Amplification and Purification

Amplification of wild phage M13 (New England Biolabs) was started by preparing a pre-inoculum containing one colony of *Escherichia coli* ER2738 (ECR) (New England Biolabs) at 37°C in 50mL of Luria Bertani (LB - Tryptone 10 g/L, yeast extract 5 g/L, NaCl 10 g/L) (Kasvi) culture medium with tetracycline (Sigma Chemical Co., 20 mg/mL) under stirring until reaching OD 600~0.3. After, 10 uL of phage M13 was added and incubated at 37°C overnight under shaking. Centrifuged the culture at 15,000×g for 10 minutes and transferred the supernatant to a tube containing PEG/NaCl (20% polyethylene glycol 8000, Fluka, and 2.5 M NaCl Neon-sterile solution) and incubated at 4°C overnight. Centrifuged the precipitate for 15 minutes at 15,000×g, discarded the supernatant, and resuspended the pellet in PBS. Subsequently, it was centrifuged again for 10 minutes at 15,000×g, supernatant was transferred to another tube containing PEG/NaCl when it was incubated for 1 hour on ice and centrifuged 10 minutes at 15,000×g. At last, resuspended the phage pellet with sterile PBS. After phage amplification, it was filtered on PES membrane with a pore size of 0.22 μm (K18-230, Kasvi) for further use during this work.

For bacterial inoculum, phage M13-infected and uninfected with ECR streaked on a plate containing LB enriched with IPTG (isopropyl β-d-1-thiogalactopyranoside-Ludwig Biotec) (0.5 mM) + X-gal (5-bromo4-chloro-3-indolyl β-d-galactopyranoside-

117 Ludwig Biotec) (40 µg/mL) and tetracycline (Sigma Chemical Co., 20 mg/mL). After a

118 24-hour incubation period at 37°C, 3 white colonies (not infected with the phage) were

119 diluted in 10mL of PBS and evaluated on the McFarland scale. In addition, inoculated 3

120 blue colonies (infected with the phage) into PBS. Both samples went through serial

121 dilutions until reaches the inoculum amount. The exact amount was evaluated and

122 confirmed by titrating the dilutions.

123

124 **2.2. Ability of ECR and M13 to inhibit S. Pullorum**

125 To propose an infection model, we used a SP isolated from free-range chickens

126 by the Laboratory of Infectious Diseases at the Federal University of Uberlândia. The SP

127 was cultured in nutrient agar (Kasvi) at 37°C for 24 hours. Before testing the embryos,

128 we performed an *in vitro* test to evaluate the interaction between ECR and/or M13

129 incubated with SP.

130 To evaluate whether phage M13 can invade SP or influence its multiplication,

131 incubated 500uL of SP containing ~4.34 log CFU/mL with 500 uL of ECR or ECR

132 infected with M13 (~4 log CFU/mL) at room temperature for ~ 20 minutes. Parallel,

133 inoculated 1 mL of PBS containing 4.34 log CFU/mL of SP with 50 uL 10 log UFP/uL

134 of phage M13 for ~20 minutes at room temperature. After this period, performed serial

135 dilution and plated the samples on LB agar containing 0.5mM IPTG, 40ug/mL X-gal, and

136 whether or not containing 20mg/mL tetracycline. The medium with tetracycline inhibits

137 the growth of SP but does not inhibit that of ECR. Performed SP colony count by the

138 difference between the tetracycline-enriched and non-enriched plates.

139

140 **2.3. Evaluation of the inhibition ability of ECR and M13 on S. Pullorum in a chicken**

141 **embryo model**

142

143 **2.3.1. Chicken Embryos**

144 The eggs line Hy-Line W36 were donated by Incubatório Novo Mundo

145 (Uberlândia, Brazil). Incubated the eggs in an artificial incubator (Premium Ecológica®)

146 at 37 °C, 58% humidity, and turned at a two-hour interval until 13 days of incubation (DI)

147 when the tests started.

2.3.2. Evaluation of the dose and age of SP inoculation in embryos

Since we know that SP leads to high mortality in embryos (Berhanu and Fulasa 2020), we did a pilot test to verify the best age and inoculation dose for them to suffer injury and for mortality to be equal to or lower than 60%. It is essential to evaluate the best age to work with the model. We used 13 and 14-day-old embryos inoculated with 6.13, 4.13, and 2.13 CFU/embryo via allantois. The choice of age is because the embryo at this age already has an active immune system (Seto 1981) which facilitates understanding of the response to a challenge. The embryos were monitored daily for viability by ovoscopy. Four days after inoculation, euthanized embryos via cervical dislocation and evaluated macroscopic lesions.

2.3.3. Evaluation of the effects of phage M13 and ECR on the embryo

To verify whether phage M13, phage M13 infected and phage M13 uninfected ECR can be used on embryos without causing mortality, we performed a test on embryos. For this purpose, inoculated the 13-day-old embryos via allantois with ~2.9 log CFU/embryo of M13-infected or uninfected ECR and 5 and 11 log CFU/embryo of purified phage M13. In parallel, a group of embryos received ~2.13 log CFU/embryo of SP, in addition to a negative control group. In each group, there were 5 embryos. The embryos were monitored daily by assessing viability by ovoscopy. After 4 days, euthanized the embryos via cervical dislocation and evaluated macroscopic lesions.

2.3.3.1. Evaluation of the inhibitory capacity of phage M13 free or infecting ECR on SP infecting chicken embryos

To assess whether phage M13-free or infecting ECR interferes with mortality or injury caused by SP, embryos were infected with ~2.13 log CFU/embryo of SP via allantoic fluid at 13 days of incubation. After 1 hour, we treated the embryos with ~2 log CFU/embryo of ECR, or ~2 log CFU/embryo of M13-infected ECR, or 11 log CFU/embryo of the M13 phage. We inserted SP-inoculated and negatives control groups were entered. Embryos were evaluated daily for viability by ovoscopy. At 17 days of incubation, we weighed the 21 surviving embryos, collected blood through the allantoic vessel, and performed macro- and microscopic analyses.

2.3.3.2. Weight of the Chicken embryos

Before the inoculation with SP, we numbered the eggs and recorded the weights. Then, at 17 DI, the CE were weighed immediately after collecting blood. As the embryo weight is related to the initial egg weight, we set the initial egg weight to 50 grams, according to Ribeiro et al. (2020).

2.3.3.3. Mortality and Macroscopic evaluations

After the determined evaluation time, we checked and counted the embryos that died and determined the date of death according to the degree of development of the embryo. For the animals that were alive, we noted whether the annexes had the presence of circulatory changes, malformation, and/or color changes. We also performed an external evaluation on the embryos and evaluated the internal organs for circulatory changes, malformation, and color changes. We compared the treated groups with their respective control group.

2.3.3.4. Histopathological changes

We performed a histopathological analysis of the liver and heart of all live embryos from the positive and negative groups in addition to 5 embryos from the SP-challenged and M13-infected ECR-treated group. The fragments of the liver and heart were fixed in 10% buffered formalin and processed for the preparation of histological slides stained with Haematoxylin and Eosin (HE)(Behmer and Tolosa 2003).

All slides from liver samples were analysed by two experienced pathologists without knowledge of the treatment group. After lesions were identified and scored for severity, the slides for the control group were identified and re-evaluated for normality. The control samples were used as a guide for the normal histological appearance and natural rate of lesion occurrence. All slides were re-examined in comparison with a normal slide to ensure accurate recognition and grading of lesions.

All liver slides were examined microscopically for histological evidence of degeneration, inflammation, and circulatory lesions (Molina et al. 2006). Severity scores

were based on a scale of 0 to 3, which corresponded to normal, mild, moderate, and severe, respectively.

Hepatic lipidosis was scored as follows: 0: no detectable cytoplasmic vacuolation; 1: scattered individual vacuoles or low numbers of vacuoles within the cytoplasm of some hepatocytes; 2: clusters of vacuoles within the cytoplasm of many hepatocytes; 3: clearing of the cytoplasm because of advanced vacuolation in nearly all hepatocytes. The control samples were used as a guide for the normal histological appearance and the natural rate of lesion occurrence.

2.3.3.4. ELISA

The levels of Interferon Gamma (IFN-γ), Interleukin-1 beta (IL-1β), and Interleukin 10 (IL-10) in the serum of chicken embryos were measured by Enzyme Linked Immunosorbent Assay (ELISA) technique. High binding plates (Greiner Bio-One) were sensitized with embryo serum diluted (1:1) in 50 mM bicarbonate buffer (pH 8.6) for 1 hour at 37°C. After 3 washes with PBS-T (PBS+Tween 20 at 0.05%), the plates were blocked with 3% BSA in PBS for 1 hour at 37°C. Then, they were rewashed with PBS-T for 4 times. Then, we incubate the plates with the antibodies, rabbit anti-chicken IFN-γ IgG antibody (BioRad), rabbit anti-chicken IL-1β IgG antibody (BioRad) or IL-10 Polyclonal IgG antibody (Thermo), diluted (1:500) in 3% BSA + PBS for 1 hour at 37°C. After 4 washes with PBS-T, all plates were incubated with secondary goat anti-rabbit IgG HRP (Sigma) diluted (1:5000) in 3% BSA + PBS. Following this, washed 4 times with PBS-T, and the binding of the antibody/antigen was detected by adding 3,3′,5,5′-tetramethylbenzidine (TMB) substrate (Thermo Scientific). The reaction was stopped by the addition of 2 N H_2SO_4. Reactivity was determined in a plate reader (Titertek Multiskan Plus, Flow Laboratories, USA) at a wavelength of 450 nm. During the reaction, we used different concentrations of recombinants IFN-γ, IL-1β, and IL-10 proteins (BD Biosciences, San Diego, CA) to construct the standard curve.

2.4. Statistical Analysis

Data from *in vitro* tests and embryo weight analysis were parametric, and we used ANOVA followed by the Tukey test. In mortality analysis, we perform the chi-square

243   test, followed by the binomial between two proportions comparing all groups inoculated

244   with SP. A relative standard curve was constructed from the absorbance values according

245   to the control (recombinant protein IFN-γ, IL-1β and IL-10). We interpolate the data using

246   Pade (1,1) or hyperbolic approximant. After, the ANOVA test was followed by the Tukey

247   test ($p<0.05$) (Graph pad prism 9.1).

248

249   **3.   RESULTS**

250

251   **3.1.   ECR can inhibit SP multiplication *in vitro***

252

253   The presence of the ECR bacterium, both alone and infected with phage M13,

254   significantly decreased the amount of SP. In contrast, we did not observe the same result

255   when only phage M13 was present (Table 1).

256

257   Table 1. Mean amount of SP (log CFU/mL) inoculated with ECR, ECR infected
258   with M13 and M13.

SP	SP (ECR)	SP (ECR+M13)	SP (M13)
4,34 (+/-0,08)a	3,9 (+/-0,12)b	4,02 (+/-0,06)b	4,37 (+/-0,13)a

259   SP: Group infected with SP. SP (ECR): Group of embryos challenged with *Salmonella* Pullorum
260   (SP) inoculated with *Escherichia coli* ER2738 (ECR) not infected with phage M13. ECR+M13:
261   Group of embryos infected with SP and inoculated with ECR infected with phage M13. M13:
262   Group of embryos challenged with SP and inoculated with phage M13. Different letters show a
263   statistical difference by ANOVA followed by Tukey's test ($p<0.05$).

264

265   **3.2.   The dose of 2 log CFU/embryo of SP leads to a 60% mortality in 13 and 14-**
266   **day-old embryos**

267   In the animal born SP causes inflammation and a vertically transmitted disease

268   that leads to lesions and mortality in old embryos. According to the pilot test performed,

269   the embryos inoculated with SP at the lowest dose tested, 2 log CFU/embryo, showed the

270   lowest mortality rate (Figure 1). And after 4 days of inoculation, the embryos showed

271   macroscopic lesions compared to the negative control, which suggests inflammation,

272   among them thickening and increased redness of blood vessels, and an excess of excreta.

273   Thus, we standardized on using 13-day-old embryos and 2 log CFU for the assays in this

274   study.

Figure 1. Percentage of embryos killed with different doses of SP at two different

276 ages
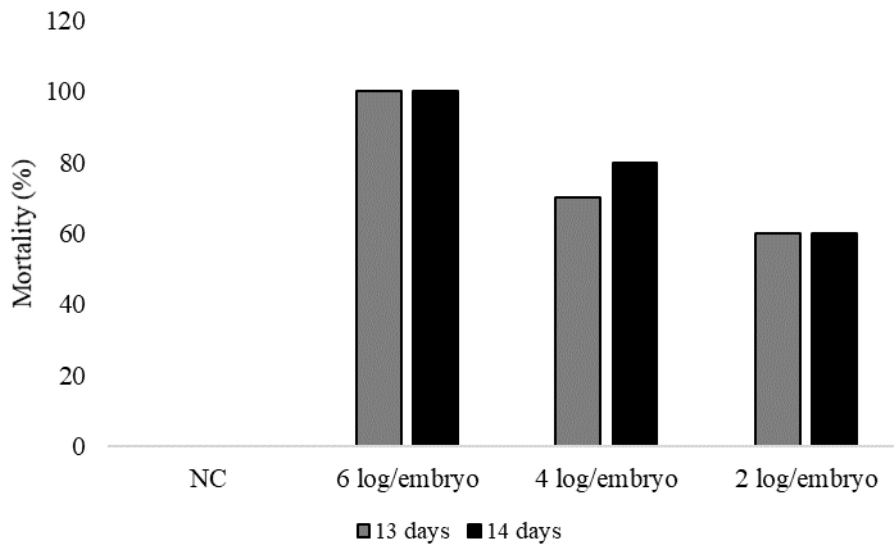
277
278
279 NC: Negative control group with PBS. 6 log/embryo: Group inoculated with 6 log/embryo of
280 SP. 4 log/embryo: Group inoculated with 4 log/embryo of SP. 2 log/embryo: Group inoculated
281 with 2 log/embryo of SP.

282
283

**284 3.3 Free phage M13 or infecting ECR does not lead to mortality or serious
285 lesions in embryos**

286 From Table 2, phage M13 infecting ECR or free did not cause any death in the
287 embryos. The only lesion found in the embryos treated with free phage or infecting ECR
288 was excess uric acid in the embryos.

289

290 Table 2. Number of dead and injured embryos after inoculated with two doses of
291 M13, M13-infected *E. coli* ER2738 and *E. coli* ER2738

	ECR+M13	**ECR**	**M13** (5 PFU/uL)	**M13** (11 PFU/uL)	**Nc**	**SP**
24 hours dead	0	0	0	0	0	1
Macroscopic alterations						Hemorrhagic embryo with membrane sticking
48 hours dead	0	0	0	0	0	1

Macroscopic alterations						Hemorrhagic embryo with membrane sticking
Dead after 48 hours	0	0	0	0	0	3
Macroscopic alterations	Excess uric acid in all	Excess uric acid in all	Excess uric acid in one embryo	Excess uric acid in all	All normal	Death 72 hours after inoculation. Hemorrhagic and small
Total Live	**5**	**5**	**5**	**5**	**5**	**0**

292 ECR+M13: Group of embryos inoculated with ECR infected with phage M13. ECR: Group of embryos
293 inoculated with ECR not infected with phage M13. M13(5 PFU/uL): Group of embryos inoculated only
294 with the phage at a concentration of 5 PFU/uL. M13(11 PFU/uL): Group of embryos inoculated only with
295 the phage at the concentration of 11 PFU/uL. Nc: negative control (PBS). SP: control inoculated with SP.

296

297 **3.4. ECR can decrease the mortality of embryos challenged with SP**

298   According to Table 3, it was possible to observe that free phage M13 does not
299 reduce the mortality of embryos inoculated with SP. In contrast, when the ECR becomes
300 infected with phage M13, there is a significant reduction in the mortality rate in the face
301 of infection caused by SP, which was present in all groups except the negative controls.

302

303 Table 3. Mortality rate (%) in embryos infected with SP and treated with free M13 and
304 M13 infecting *E. coli*

NcPBS	NcM13	SP	SP (ECR)	SP (ECR+M13)	SP (M13)
0% (0/4)a	0% (0/4)a	75,0%(9/12)b	60,0%(3/5)b	25,0%(3/12)a	91,6% (11/12)b

305   __% (x/y): mortality rate (number of dead/number of alive). NcPBS: Negative control group with
306 PBS. NcM13: Negative control group with phage M13. SP: Control group inoculated with SP. SP
307 (ECR): Group challenged with SP and inoculated with ECR not infected with phage M13 one hour
308 later. SP (ECR+M13): Group challenged with SP and inoculated with ECR infected with phage
309 M13 one hour later. M13: Group infected with SP and treated with phage M13 one hour later.
310 Different letters show statistical difference between each group and SP group by chi-square test
311 followed by binomial between two proportions (p<0.05).

3.4.1 ECR prevents weight loss of SP treated embryos

313   According to the graph shown in Figure 2, it is possible to observe that the weight

314 of embryos tends to decrease due to infection caused by SP. However, in the presence of

315 ECR infected with phage M13, the embryos did not lose weight, and the values were

316 close to those of the negative controls.

317

318 **Figure 2. Weight of surviving embryos challenged with SP and treated or not with**

319 **ECR infected with M13**
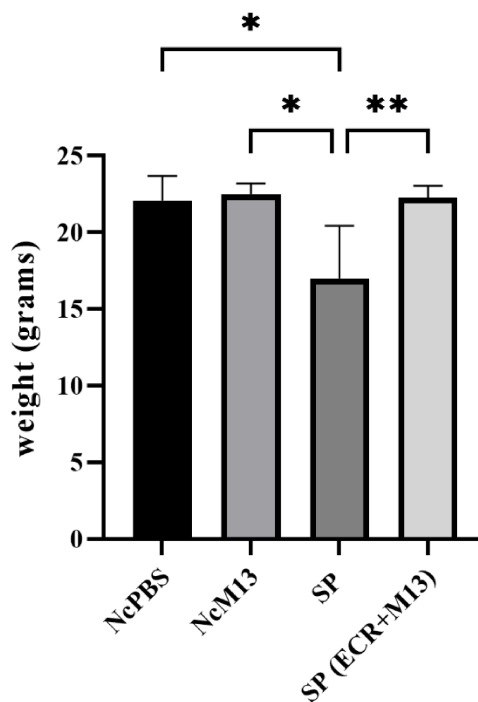
320
321

322 NcPBS: Negative control group with PBS. NcM13: Negative control group with phage M13. SP: Group

323 inoculated with SP. SP (ECR+M13): Infected by SP and treated with ECR infected with phage M13. M13:

324 phage M13 only. Symbol * shows a statistical difference ($p<0.05$). The weights referring to group M13 and

325 group ECR were not inserted in the graph because the embryos died, and the number of surviving embryos

326 was not sufficient for statistical analysis.

327

328 ### 3.4.2. Surviving embryos inoculated with SP and treated with ECR+M13

329 **have no severe lesions**

After 4 days of inoculation, we perform embryo diagnosis on the live embryos. In the group inoculated with SP, the 3 survivors showed excess excreta and thickening and greater redness of blood vessels, and 1 enlarged liver. In the group inoculated with SP and treated with the ECR bacteria infected with M13, only one embryo of the nine survivors had excess excreta. In the negative control group (embryo inoculated with M13), 2 of 4 embryos had excess excreta, while the negative control (inoculated with PBS) had no lesion.

3.4.3. Histopathological changes

We found no histomorphometry changes in the negative control. Granulopoietic cells were present in all livers in connective tissues of hepatic portal spaces. Nevertheless, not among hepatoblasts and not all connective tissue areas in portal spaces were occupied by granulopoiesis foci. We observed mild lipidosis in all livers, even in the controls. In positive control, we found 1 of the 3 live embryos with bleeding and congestion in the liver. In group infected by SP and inoculated with M13-infected ECR 1 of the and 4 live embryos presented bleeding and congestion in the liver and heart, respectively.

Table 4. Number of live chicken embryos with histomorphometric changes in liver and heart infected by SP or phage M13-infected ECR.

Change	Organ	NcPBS	SP	SP (ECR+M13)
Degeneration	Liver	np	np	np
	Heart	0/4	0/3	0/5
Inflammation	Liver	0/4	0/3	0/5
	Heart	0/4	0/3	0/5
Bleeding	Liver	0/4	1/3	1/5
	Heart	0/4	0/3	4/5
Congestion	Liver	0/4	1/3	1/5
	Heart	0/4	0/3	4/5
Lipidosis	Liver	0/4	0/3	0/5
	Heart	np	np	np

NcPBS: Negative control group with PBS. SP: Group inoculated with SP. SP (ECR+M13): Inoculated with SP and treated with ECR infected with phage M13. We performed only qualitative analysis.

3.4.3. Embryos challenged with SP increase IL-10 secretion four days after inoculation, but when treated with ECR+M13 there is no increase in IL-10

354   There was no difference between IFN-γ and IL-1β levels, when compared to CP
355   or CN (Figure 3A and 3B). In contrast, the cytokine IL-10 had a significant decrease
356   and a similar profile to the negative controls (Figure 3C).

357

358   **Figure 3. Dosage of inflammatory and anti-inflammatory cytokines in the serum of**
359   **embryos**
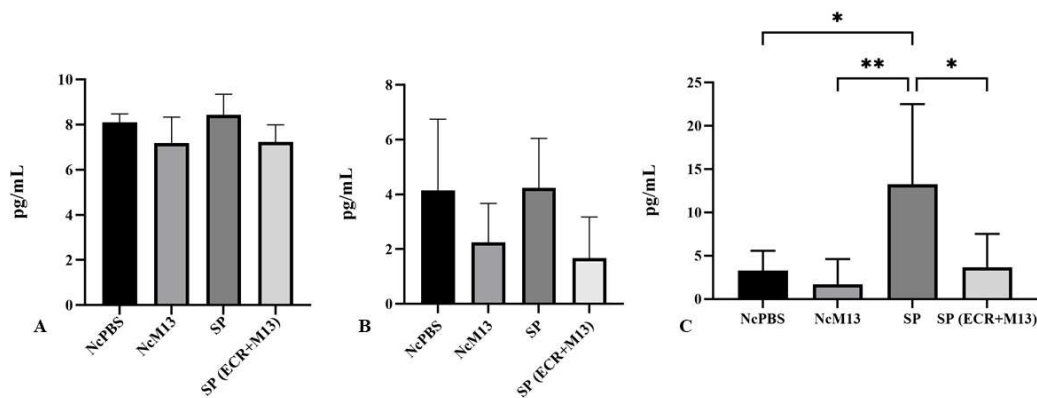
361   Levels (pg/mL) of IFN-γ (A); IL-1β (B), and IL-10 (C) in the serum of embryos. NcPBS: Negative control
362   group with PBS. NcM13: Negative control group with phage M13. SP: Group inoculated with SP. SP
363   (ECR+M13): Infected by SP and treated with ECR infected with phage M13. M13: phage M13 only.
364   Symbol * shows a statistical difference (p<0.05). The cytokines levels referring to group M13 and group
365   ECR were not inserted in the graph because the embryos died, and the number of surviving embryos was
366   not sufficient for statistical analysis.

367

4.   DISCUSSION

369

4.1. In infection tests with SP is not interesting to use ECR infected with phage M13

372   After selecting phage ligands or mimetics by the PD library, the phages can be
373   used as a screening test to choose the best targets by ELISA (da Silva Ribeiro et al. 2010).
374   It can be very useful since peptide synthesis is still costly and time-consuming. There are
375   still no studies of phages from the PD library that use screening tests for infection. It will
376   have many applications because, besides the time and cost issues, the phage being a larger
377   and more stable particle, could hit the target more successfully. To enable the use of

phages, we have done an *in vitro* test inoculating the SP with the free phage or infected with the ECR. We noticed a decrease in the amount of SP when inoculated with ECR (Table 1). This fact allows us to propose that in future works, if phages are used, they should be free of ECR so that the bacteria do not interfere with the tests. Although we only tested SP, it is possible that for other gram-negative bacteria, this event could also occur. The interaction between bacteria of different species happens through various mechanisms, such as competition for substrates and production of bacteriocins (Hawlena et al. 2012; Deng and Wang 2016). We cannot conclude what type of mechanism was used by ECR in inhibition of SP, but other works show that probiotic *E. coli* strains can inhibit pathogenic bacteria (Setia et al. 2009; Fang et al. 2018; Hrala et al. 2021).

The *in vitro* results were also observed in tests in an embryonic model. When we challenged embryos with SP and then treated them with phage-infected ECR it was possible to see a decrease in embryonic mortality. Embryos inoculated with SP showed a 75% mortality, while those inoculated with SP but treated with ECR had a 25% mortality (Table 3). This reduction was due to the presence of the bacteria since embryos challenged with SP and inoculated only with M13 showed no decrease in mortality. Lesions in embryos challenged with SP and treated with ECR infected with M13 were also mild. One embryo of the nine survivors showed increased excreta. However, 1 and 4 embryos in this group presented congestion and bleeding in liver and heart, respectively (table 4). The weight of surviving embryos and the level of cytokine IL-10 of the SP-challenged group treated with ECR infected with M13 was similar to the negative control showing that the ECR was probably able to control the multiplication of SP in these embryos.

4.2. Phage M13 does not lead to embryonic mortality or cause serious injury to embryos

Before we started testing, it was important to know if phage M13 caused damage or death in the embryos. Embryos inoculated with M13 at two doses (5 and 11PFU/embryo), ECR and ECR infected with M13 showed no mortality, and the only macroscopic change observed was excess uric acid (Table 2). Another experiment showed that phage M13 and ECR are harmless to hatchlings (de Almeida Araújo Santos et al. 2022). In our experiment, we found that tests with the phages can also be performed in chicken embryos as a potential infection model for evaluating PD-selected ligands.

4.3. SP can be a model of infection, and chicken embryos

SP is an avian-specific and vertically transmitted bacterium that causes severe injury to embryos, such as skin hemorrhage, subcutaneous edema, and increased mortality (Guo et al. 2017; Guo et al. 2019). Our intention was to find an embryonic period age and infective dose capable of not leading to the death of all embryos. We chose the ages of 13 and 14 days because before 11 days of incubation there is death of 100% of embryos (data not shown) and because from that age on the embryos already have a more active immunity (Stefaniak et al. 2020). Our results show that embryos inoculated with the 6 and 4 log CFU doses of SP showed a higher mortality rate when compared to the groups inoculated with the dose of 2 log CFU/embryo (Figure 1). At this dose, the mortality rate was similar, and thus, we decided to use the age of 13 days in the next phase to remove the biological material at 17 days of incubation. The intention was not to pass the age of 18 days of incubation because during this embryonic period, the embryo is already fully developed, becoming similar to an animal in experimental terms (Fonseca et al. 2021).

The decrease in weight of the SP-infected embryos (Figure 2) and the lesions in the surviving embryos, such as hemorrhage and membrane sticking (Table 2), excess excreta, and hepatomegaly (described in section 3.2.5), shows that these animals, although injured by the infection were able to survive trying to circumvent the inflammation caused by the bacteria. This result, together with the increase in the cytokine IL-10 in the surviving embryos (Figure 3C), may be an attempt by the embryo's immune system to modulate the inflammation caused by SP or the initiation of the Th2 type response similar to what occurs with the nascent animal (Tang et al. 2018; Foster et al. 2021). The inflammatory cytokines IFN-γ and IL-1β showed no increase (Figures 3A and 3B). It probably happened because these cytokines are released at the onset of inflammation, characterizing the resistance phase of the disease. As the blood collection was 4 days after inoculation, already changed to the induction phase of SP modulation, other cytokines are participating in the process, such as IL-10 (Kogut and Arsenault 2017). This fact reinforces the idea that this cytokine can inhibit the production of inflammatory cytokines (Th1 type) during systemic dissemination to limit the inflammatory response (Rothwell et al. 2004; Tang et al. 2018).

From the histopathological analysis, we observed granulopoietic cells in all livers in connective tissues of hepatic portal spaces. Nevertheless, not among hepatoblasts and

442   not all connective tissue areas in portal spaces were occupied by granulopoiesis foci.

443   Despite the, chicken fetal liver is not considered a relevant hematopoietic organ, as is the

444   fetal liver in mammals (Wong and Cavey 1992; Wong and Cavey 1993) the presence of

445   these granulopoietic foci was considered normal. Granulocytic differentiation in the

446   connective tissue of portal spaces on the 15th day of incubation and onwards was reported

447   by (Guedes et al. 2014).

448   Even without showing inflammatory changes in the heart and liver, the chicks

449   challenge with SP were smaller and depressed with an increase in the vessels showing

450   that it had a systemic inflammation that did not reach the tissues. In born animals, the

451   histopathological lesions generated by SP are evident (Cheng et al. 2020), and the survival

452   of the embryos in this study combined with the absence of liver and kidney damage (table

453   4) together with the increase in serious IL-10 (Figure 3) shows that embryos surviving

454   the challenge with SP have a better response immune than those who died.

455   We observed mild lipidosis in all livers, even in the controls. Wong and Cavey

456   1992 reported that by 14th day of incubation all hepatoblasts possess lipid and glycogen.

457   The amount of fat in the hepatoblasts was considered at normal level. The absence of any

458   accompanying cytopathic effects in the liver allows the determination their individual

459   characteristics, not resulting from drug administration.

460   We also observed some chicken embryos, in group treated with SP, hepatic

461   congestion and haemorrhage. This event is common in born animal (Shen et al. 2022).

462   Our results indicate that SP is an interesting model of systemic infection in CE, and some

463   embryo can be resistant to the disease progression.

464

465

466   **4.4. Phage M13 from the PD library can be used in chicken embryo model tests**

467   The PD technology presents numerous advantages in the selection of ligands and

468   structure mimetics of microorganisms, thus allowing both diagnosis and development of

469   molecules for disease control (Sioud 2019). However, depending on the microorganism,

470   the number of clones selected in the PD technology is high and the need for screening to

471   choose the best ligands is essential. Although phage-ELISA can determine good ligands

472   for diagnostic purposes (da Silva Ribeiro et al. 2010), this technique may not be

interesting for understanding the ligand:host relationship, such as the infection and inflammation process for example. In this sense, cell culture is a useful tool, but considering the chicken embryo a more complex organism that allows the replication of numerous microorganisms such as viruses and bacteria (Farzaneh et al. 2017), this model has several advantages.

The advantages of chicken embryos over hatchlings are mainly related to cost, space, and some ease of handling (Garcia et al. 2021) and are currently accepted by the FDA in testing with some drugs (Kue et al. 2014). Based on the importance of the PD and the embryo as an experimental model, we propose a model of infection and suggest the embryo's use in testing with the PD. Research with any system, whether organic or inorganic molecules, needs to be well standardized and to present guarantees of harmlessness so that the changes are well known. In this sense, this work clarifies that there are interferences of the ECR on the SP bacteria and that this may occur for other bacteria. Thus, our results show *in vitro* and *in vivo* models that in tests with infection, it is important that the M13 amplified in the ECR is purified. Another aspect that warrants the use of phage M13 from the purified PD library in tests with embryos is that M13 does not interfere with bacterial multiplication, or the response generated by the embryo. This is seen when embryos inoculated with M13 alone did not lead to embryo mortality (Table 2) and when the mortality rate of the SP-inoculated and M13-treated embryo groups was equal to the SP-only inoculated group (Table 3). Unfortunately, the number of surviving embryos of the group challenged with SP and treated with M13 or ECR, although statistically similar to the group only challenged with SP, did not allow the analysis of the weight and level of cytokines produced as only one or two embryos survived, respectively. One can consider that the number of embryos for the ECR group was low, and a larger quantity is need for better evaluation. However, the set of results allowed inferring that it is possible to use clones selected by the PD technology in embryo testing since M13 is innocuous and does not interfere with multiplication or bacterial action.

5. CONCLUSION

The SP-infected chicken embryo can be a helpful model of systemic infection for different tests, including screening tests for selecting ligand-binding peptides from M13 phages selected from the PD library.

511

512

6. REFERENCES

514 Bednarczyk M, Dunislawska A, Stadnicka K, Grochowska E (2021) Chicken embryo as
515 a model in epigenetic research. Poult Sci 100:101164.
516 https://doi.org/10.1016/j.psj.2021.101164

517 Behmer OA, Tolosa EMC (2003) Manual de técnicas para histologia normal e patológica.
518 Man técnicas para Histol Norm e patológica 331–331

519 Berhanu G, Fulasa A (2020) Pullorum Disease and Fowl Typhoid in Poultry: A Review.
520 Br J Poult Sci 9:48–56. https://doi.org/10.5829/idosi.bjps.2020.48.56

521 Blanco AE, Cavero D, Icken W, Voss M, Schmutz M, Preisinger R, Sharifi AR (2018)
522 Genetic approach to select against embryo mortality caused by Enterococcus faecalis
523 infection in laying hens. Poult Sci 97:4177–4186. https://doi.org/10.3382/ps/pey310

524 Cheng Y, Sihua Z, Lu Q, Zhang W, Wen G, Luo Q, Shao H, Zhang T (2020) Evaluation
525 of young chickens challenged with aerosolized Salmonella Pullorum. Avian Pathol
526 49:507–514. https://doi.org/10.1080/03079457.2020.1783433

527 da Silva Ribeiro V, Manhani MN, Cardoso R, Vieira CU, Goulart LR, Costa-Cruz JM
528 (2010) Selection of high affinity peptide ligands for detection of circulating
529 antibodies in neurocysticercosis. Immunol Lett 129:94–99.
530 https://doi.org/10.1016/j.imlet.2010.01.008

531 de Almeida Araújo Santos F, Valadares Junior EC, Goulart LR, Nunes PLF, Mendonça
532 EP, Girão LVC, da Hora AS, Ferreira TB, Bastos LM, Medeiros-Ronchi AA,
533 Fonseca BB (2022) Alternative use of phage display: phage M13 can remain viable
534 in the intestines of poultry without causing damage. AMB Express 12.
535 https://doi.org/10.1186/s13568-022-01407-9

536 Deng YJ, Wang SY (2016) Synergistic growth in bacteria depends on substrate
537 complexity. J Microbiol 54:23–30. https://doi.org/10.1007/s12275-016-5461-9

538 díaz-Valdés N, Manterola L, Belsúe V, Riezu-Boj JI, Larrea E, Echeverria I, Llópiz D,
539 López-Sagaseta J, Lerat H, Pawlotsky JM, Prieto J, Lasarte JJ, Borrás-Cuesta F,
540 Sarobe P (2011) Improved dendritic cell-based immunization against hepatitis C
541 virus using peptide inhibitors of interleukin 10. Hepatology 53:23–31.
542 https://doi.org/10.1002/hep.23980

543 Dong X, Pan P, Zheng DW, Bao P, Zeng X, Zhang XZ (2020) Bioinorganic hybrid
544 bacteriophage for modulation of intestinal microbiota to remodel tumor-immune
545 microenvironment against colorectal cancer. Sci Adv 6.

546   https://doi.org/10.1126/sciadv.aay1497

547 Ebrahimizadeh W, Rajabibazl M (2014) Bacteriophage vehicles for phage display:
548   Biology, mechanism, and application. Curr Microbiol 69:109–120.
549   https://doi.org/10.1007/s00284-014-0557-0

550 Fang K, Jin X, Hong SH (2018) Probiotic Escherichia coli inhibits biofilm formation of
551   pathogenic E. coli via extracellular activity of DegP. Sci Rep 8:1–12.
552   https://doi.org/10.1038/s41598-018-23180-1

553 Farzaneh M, Hassani SN, Mozdziak P, Baharvand H (2017) Avian embryos and related
554   cell lines: A convenient platform for recombinant proteins and vaccine production.
555   Biotechnol J 12:1–10. https://doi.org/10.1002/biot.201600598

556 Fonseca BB, da Silva MV, de Morais Ribeiro LN (2021) The chicken embryo as an in
557   vivo experimental model for drug testing: Advantages and limitations. Lab Anim
558   (NY) 50:138–139. https://doi.org/10.1038/s41684-021-00774-3

559 Foster N, Tang Y, Berchieri A, Geng S, Jiao X, Barrow P (2021) Revisiting persistent
560   salmonella infection and the carrier state: What do we know? Pathogens 10.
561   https://doi.org/10.3390/pathogens10101299

562 Garcia P, Wang Y, Viallet J, Macek Jilkova Z (2021) The Chicken Embryo Model: A
563   Novel and Relevant Model for Immune-Based Studies. Front Immunol 12:1–16.
564   https://doi.org/10.3389/fimmu.2021.791081

565 Ge H, Hu M, Zhao G, Du Y, Xu N, Chen X, Jiao X (2020) The "fighting wisdom and
566   bravery" of tailed phage and host in the process of adsorption. Microbiol Res 230.
567   https://doi.org/10.1016/j.micres.2019.126344

568 Ghimire S, Zhang X, Zhang J, Wu C (2022) Use of Chicken Embryo Model in Toxicity
569   Studies of Endocrine-Disrupting Chemicals and Nanoparticles. Chem Res Toxicol
570   7:17703–17712. https://doi.org/10.1021/acs.chemrestox.1c00399

571 Gibbs PS, Maurer JJ, Nolan LK, Wooley RE (2003) Prediction of chicken embryo
572   lethality with the avian Escherichia coli traits complement resistance, Colicin V
573   production, and presence of the increased serum survival gene cluster (iss). Avian
574   Dis 47:370–379. https://doi.org/10.1637/0005-
575   2086(2003)047[0370:POCELW]2.0.CO;2

576 Guedes PT, Oliveira BCEPD de, Manso PP de A, Caputo LFG, Cotta-Pereira G, Pelajo-
577   Machado M (2014) Histological analyses demonstrate the temporary contribution of
578   yolk sac, liver, and bone marrow to hematopoiesis during chicken development.
579   PLoS One 9:e90975. https://doi.org/10.1371/journal.pone.0090975

580 Guo R, Li Z, Jiao Y, Geng S, Pan Z, Chen X, Li Q, Jiao X (2017) O-polysaccharide is
581   important for Salmonella Pullorum survival in egg albumen, and virulence and
582   colonization in chicken embryos. Avian Pathol 46:535–540.
583   https://doi.org/10.1080/03079457.2017.1324197

584 Guo R, Li Z, Zhou X, Huang C, Hu Y, Geng S, Chen X, Li Q, Pan Z, Jiao X (2019)
585   Induction of arthritis in chickens by infection with novel virulent Salmonella
586   Pullorum strains. Vet Microbiol 228:165–172.
587   https://doi.org/10.1016/j.vetmic.2018.11.032

588 Hawlena H, Bashey F, Lively CM (2012) Bacteriocin-mediated interactions within and

589   between coexisting species. Ecol Evol 2:2521–2526.
590   https://doi.org/10.1002/ece3.354

591 Hrala M, Bosák J, Micenková L, Křenová J, Lexa M, Pirková V, Tomáštíková Z,
592   Koláčková I, Šmajs D (2021) Escherichia coli Strains Producing Selected
593   Bacteriocins Inhibit Porcine Enterotoxigenic Escherichia coli (ETEC) under both In
594   Vitro and In Vivo Conditions. Appl Environ Microbiol 87.
595   https://doi.org/10.1128/AEM.03121-20

596 Jamal M, Bukhari SMAUS, Andleeb S, Ali M, Raza S, Nawaz MA, Hussain T, Rahman
597   S u., Shah SSA (2019) Bacteriophages: an overview of the control strategies against
598   multiple bacterial infections in different fields. J Basic Microbiol 59:123–133.
599   https://doi.org/10.1002/jobm.201800412

600 Jiang H, Li Y, Cosnier S, Yang M, Sun W, Mao C (2022) Exploring phage engineering
601   to advance nanobiotechnology. Materials Today Nano 19.
602   https://doi.org/10.1016/j.mtnano.2022.100229

603 Kogut MH, Arsenault RJ (2017) Immunometabolic phenotype alterations associated with
604   the induction of disease tolerance and persistent asymptomatic infection of
605   Salmonella in the chicken intestine. Front Immunol 8:1–7.
606   https://doi.org/10.3389/fimmu.2017.00372

607 Kosecka-Strojek M, Trzeciak J, Homa J, Trzeciak K, Władyka B, Trela M,
608   Międzobrodzki J, Lis MW (2021) Effect of Staphylococcus aureus infection on the
609   heat stress protein 70 (HSP70) level in chicken embryo tissues. Poult Sci 100.
610   https://doi.org/10.1016/j.psj.2021.101119

611 Kue CS, Tan KY, Lam ML, Lee HB (2014) Chick embryo chorioallantoic membrane
612   (CAM): An alternative predictive model in acute toxicological studies for anti-
613   cancer drugs. Exp Anim 64:129–138. https://doi.org/10.1538/expanim.14-0059

614 Li Q, Li Y, Xia J, Wang X, Yin K, Hu Y, Yin C, Liu Z, Jiao X (2019) Virulence of
615   Salmonella enterica serovar Pullorum isolates compared using cell-based and
616   chicken embryo infection models. Poult Sci 98:1488–1493.
617   https://doi.org/10.3382/ps/pey482

618 Molina ED, Balander R, Fitzgerald SD, Giesy JP, Kannan K, Mitchell R, Bursian SJ
619   (2006) Effects of air cell injection of perfluorooctane sulfonate before incubation on
620   development of the white leghorn chicken (Gallus domesticus) embryo. Environ
621   Toxicol Chem An Int J 25:227–232. https://doi.org/10.1897/04-414R.1

622 Nakakido M, Tanaka N, Shimojo A, Miyamae N, Tsumoto K (2022) Development of a
623   high-throughput method to screen novel antiviral materials. PLoS One 17:1–8.
624   https://doi.org/10.1371/journal.pone.0266474

625 Oh JY, Kang MS, Yoon H, Choi HW, An BK, Shin EG, Kim YJ, Kim MJ, Kwon JH,
626   Kwon YK (2012) The embryo lethality of Escherichia coli isolates and its
627   relationship to the presence of virulence-associated genes. Poult Sci 91:370–375.
628   https://doi.org/10.3382/ps.2011-01807

629 Polláková M, Petrilla V, Andrejčáková Z, Petrillová M, Sopková D, Petrovová E (2021)
630   Spitting cobras: Experimental assay employing the model of chicken embryo and
631   the chick chorioallantoic membrane for imaging and evaluation of effects of venom
632   from African and Asian species (Naja ashei, Naja nigricollis, Naja siamensis, Naja

sumatrana). Toxicon 189:79–90. https://doi.org/10.1016/j.toxicon.2020.10.025

Rahbarnia L, Farajnia S, Babaei H, Majidi J, Veisi K, Ahmadzadeh V, Akbari B (2017) Evolution of phage display technology: from discovery to application. J Drug Target 25:216–224. https://doi.org/10.1080/1061186X.2016.1258570

Rashidi H, Sottile V (2009) The chick embryo: Hatching a model for contemporary biomedical research. BioEssays 31:459–465. https://doi.org/10.1002/bies.200800168

Rezaee MS, Liebhart D, Hess C, Hess M, Paudel S (2021) Bacterial Infection in Chicken Embryos and Consequences of Yolk Sac Constitution for Embryo Survival. Vet Pathol 58:71–79. https://doi.org/10.1177/0300985820960127

Ribeiro LN de M, de Paula E, Rossi DA, Monteiro GP, Júnior ECV, Silva RR, Franco R, Espíndola FS, Goulart LR, Fonseca BB (2020) Hybrid pectin-liposome formulation against multi-resistant bacterial strains. Pharmaceutics 12:1–15. https://doi.org/10.3390/pharmaceutics12080769

Rothwell L, Young JR, Zoorob R, Whittaker CA, Hesketh P, Archer A, Smith AL, Kaiser P (2004) Cloning and Characterization of Chicken IL-10 and Its Role in the Immune Response to Eimeria maxima . J Immunol 173:2675–2682. https://doi.org/10.4049/jimmunol.173.4.2675

Setia A, Bhandari SK, House JD, Nyachoti CM, Krause DO (2009) Development and in vitro evaluation of an Escherichia coli probiotic able to inhibit the growth of pathogenic Escherichia coli K88. J Anim Sci 87:2005–2012. https://doi.org/10.2527/jas.2008-1400

Seto F (1981) Early development of the avian immune system. Poult Sci 60:1981–1995. https://doi.org/10.3382/ps.0601981

Shen X, Zhang A, Gu J, Zhao R, Pan X, Dai Y, Yin L, Zhang Q, Hu X, Wang H, Zhang D (2022) Evaluating Salmonella pullorum dissemination and shedding patterns and antibody production in infected chickens. BMC Vet Res 18:240. https://doi.org/10.1186/s12917-022-03335-z

Sioud M (2019) Phage Display Libraries: From Binders to Targeted Drug Delivery and Human Therapeutics. Mol Biotechnol 61:286–303. https://doi.org/10.1007/s12033-019-00156-8

Stefaniak T, Madej JP, Graczyk S, Siwek M, Łukaszewicz E, Kowalczyk A, Sieńczyk M, Maiorano G, Bednarczyk M (2020) Impact of prebiotics and synbiotics administered in ovo on the immune response against experimental antigens in chicken broilers. Animals 10:1–15. https://doi.org/10.3390/ani10040643

Tang Y, Foster N, Jones MA, Barrow PA (2018) Model of persistent Salmonella infection: Salmonella enterica serovar Pullorum modulates the immune response of the chicken from a Th17-type response towards a Th2-type response Response. Infect Immun 86. https://doi.org/10.1128/IAI.00307-18

Van Belleghem JD, Dąbrowska K, Vaneechoutte M, Barr JJ, Bollyky PL (2019) Interactions between bacteriophage, bacteria, and the mammalian immune system. Viruses 11. https://doi.org/10.3390/v11010010

Wachholz GE, Rengel BD, Vargesson N, Fraga LR (2021) From the Farm to the Lab:

676   How Chicken Embryos Contribute to the Field of Teratology. Front Genet 12:1–11.
677   https://doi.org/10.3389/fgene.2021.666726

678 Wong GK, Cavey MJ (1992) Development of the liver in the chicken embryo. I. Hepatic
679   cords and sinusoids. Anat Rec 234:555–567. https://doi.org/10.1002/ar.1092340411

680 Wong GK, Cavey MJ (1993) Development of the liver in the chicken embryo. II.
681   Erythropoietic   and   granulopoietic   cells.   Anat   Rec   235:131–143.
682   https://doi.org/10.1002/ar.1092350114

683 Zosen D, Hadera MG, Lumor JS, Andersen JM, Paulsen RE (2021) Chicken embryo as
684   animal model to study drug distribution to the developing brain. J Pharmacol Toxicol
685   Methods 112:0–4. https://doi.org/10.1016/j.vascn.2021.107105

686

617

618   **Can a phospholipase inhibitor peptide be used to control**

619   **inflammation?**

620

621   Jessica Brito de Souza[1*], Emília Rezende Vaz[1], Simone Sommerfeld[2], Hebréia Oliveira

622   Almeida Souza[1], Fabiana Almeida Araújo Santos[1], Lucas Ian Veloso Correia[1], Sarah

623   Natalie Cirilo Gimenes[3], Luciana Machado Bastos[1], Belchiolina Beatriz Fonseca[1,2],

624   Luiz Ricardo Goulart[1ţ]

625

626   1. Postgraduate Program in Genetics and Biochemistry, Institute of Biotechnology,

627   Federal University of Uberlândia, Brazil

628   2. Postgraduate Program in Veterinary Sciences, Faculty of Veterinary Medicine,

629   Federal University of Uberlândia, Brazil

630   3. Laboratory of Immunopathology, Institute Butantan, SP, Brazil

631

632   *Corresponding author: souzajessicab34@gmail.com

633   Alternative corresponding author: biafonseca@ufu.br

634   ţ: in memoriam

635

636

637

638

639

640

641

ABSTRACT

Phage display (PD) is a technique and is considered efficient, robust and low-cost to select target-specific ligands that are exposed on the surface of a filamentous phage. Among the several existing phospholipases, phospholipase A2 (PLA$_2$s) are the enzymes mostly found in the venoms of several snake species. Since phospholipases play a relevant role in the progression of several inflammatory diseases, we selected by PD a peptide mimetic to phospholipase inhibitor and evaluated its effects *in vitro* and *in vivo*. We used peripheral blood mononuclear cells (PBMC) stimulated with lipopolysaccharide (LPS), to evaluate if F7 peptide interferes in cytokine levels of IL-1β, TNF-α and IL-10. As an animal model, we used chicken embryos inoculated with *Salmonella* Pullorum (SP) to also dose cytokines and evaluate mortality. It was found that the synthetic peptide F7 and phage were able to interfere with the expression of inflammatory cytokines, and that another *in vivo* model is needed to better understand the mechanism of action.

KEY WORDS: bacteriophage, biopanning, inflammation, immune response

1. INTRODUCTION

669

670   Phage display (PD) technology allows specific antigen ligands to be selected from
671 large combinatorial libraries of antibodies. Among its advantages are the ease of
672 execution, low cost, and robustness of the method (Ledsgaard et al. 2018). It is considered
673 the most widely used in screening technique, enabling the development of a wide range
674 of drugs by the ability to bring peptide therapeutics into the clinic (Mimmi et al. 2019).
675 Peptides originating from PD are applied in the treatment of some diseases, such as
676 hereditary angioedema (Perego et al. 2019), immune thrombocytopenia purpura
677 (Hamzeh-Mivehroud et al. 2013), anemia in chronic kidney disease (Macdougall 2008)
678 and blood glucose control in type 2 diabetes mellitus (Fala 2015).

679   Phages used in PD are viral particles that use bacterial cells, most notably
680 *Escherichia coli* (*E.coli*), as hosts for replication. They consist of a protein coat that coats
681 their genetic material, and these proteins can be conjugated or genetically modified to
682 display peptides, proteins, or antibodies (Barderas and Benito-Peña 2019). The most used
683 filamentous phage are M13, and the minor coating protein pIII is the most commonly
684 used peptide display. After selection by phage display, these peptides are sequenced,
685 characterized, and synthesized for further use (Barbas et al. 2001).

686   The phospholipases consist of hydrolase enzymes and their classification is
687 determined according to some factors, among them the site where these enzymes cleave
688 the phospholipid molecule. The phospholipase A_2 (PLA$_2$) superfamily corresponds to an
689 acylhydrolase that can hydrolyze the sn-2 position of glycerophospholipids, releasing
690 fatty acids and lysophospholipids (Murakami and Taketomi 2015). PLA$_2$ is one of the
691 main enzymes found in the venoms of almost all snake species, and in the families
692 Elapidae and Viperidae it is the most abundant (Hiu and Yap 2020). The PD may be a
693 useful technology to select phospholipase binding or mimetic and aid in understanding
694 and controlling injuries.

695   There are several types of human PLA$_2$'s, such as lipoprotein-associated, calcium-
696 independent, cytosolic and secreted. They are already proven to play an essential role in
697 the pathophysiology and progression of various inflammatory diseases (Vasquez et al.
698 2018), such as atherosclerosis (Zhang et al. 2020), bronchitis (Mruwat et al. 2013), asthma
699 (Nolin et al. 2019) and gout (Ha et al. 2020). The inflammation caused by snake venom
700 PLA2's stems from the activation of innate immune cells and endothelial cells that recruit

leukocytes into the tissues. In adition, releasing various inflammatory mediators and increasing oxidative stress, causing vascular dynamics and edema formation (Moreira et al. 2021).

Recently, the search for PLA$_2$ inhibitors has been increasing, especially for the treatment of inflammatory diseases, due to their ability to regulate the catalytic activity of the enzyme, making them excellent agents for therapeutic purposes (Chinnasamy et al. 2020; Mahmud et al. 2020; Batsika et al. 2021). In addition, they are considered a great tool to understand in more detail the function each PLA2 plays in cells and *in vivo* (Nikolaou et al. 2019). In view of this, this work aimed to select, a peptide mimetic to PLA$_2$ inhibitor by PD, and evaluate its effect on the inflammatory process.

2. METHODOLOGY

2.1. Phage Display

To select mimetic peptides to phospholipase inhibitor was used a PhD-7mer kits (New England Biolabs) according to the manufacturer's instructions. Three rounds of selection were performed. The amount of 1 μg of PLA$_2$, isolated from *Bothrops pauloensis* venom (BpPLA$_2$-TXI) (Ferreira et al. 2013), was incubated with $1x10^{11}$ infectious phage particles of PhD-7mer for 1 hour at 4°C. The phages that did not bind to the BpPLA$_2$- TXI was discarded by washes. In the first round, phages were washed five times with PBS-T 0,05% (137mM NaCl, 10mM phosphate, 2.7 mM KCl, and pH 7.4) and then eluted by competition elution using isolate from snake serum of *Crotalus durissus collilineatus* (γCdcPLI) (Gimenes et al. 2014). The second and third rounds the phages were washed ten times with PBS-T 0,05% and then eluted with γCdcPLI. Selected phages were amplified and purified using *E.Coli* ER2738 (ECR) and PEG-800/NaCl respectively.

2.2. DNA Sequencing

A total of twenty phages were submitted for DNA sequencing. Phages clones were re-solved in 100 μL of sodium-iodide buffer (10mmol/L TrisHCl, pH 8.0, 1mmol/L EDTA, 4 mol/L NaI) and precipitated with absolute ethanol. Phage DNA was centrifuged

at 10.000 rpm for 10 minutes, washed with 70% ethanol, and re-solved in 30 μL of ddH$_2$O. The sequencing primer (5'-OH CCC TCA TAG TTA GCG TAA CG-3, Biolabs) was mixed with 50 ng of phage DNA and the sequencing mix (DYEnamic ETDye Terminator Cycle Sequencing Kit, Amersham Biosciences). Sequences analysis was performed in a MegaBace 1000 Genetic Analyzer (Amersham Biosciences). DNA sequences were deduced by Expasy Translate tool (http://web.expasy.org/translate/). After DNA sequence analysis only twelve clones had valid sequences.

2.3. Synthesis of F7 peptide

The chemical synthesis of the F7 peptide was performed by FastBio (SP, Brazil) following manual phage display (Barbas et al. 2001). Its sequence presents 20 amino acids (ACNPILKEACGGGSAETVES), and after synthesis, it was reconstituted and prepared in aliquots of 20 mg/mL concentration, with a molarity of 10.126 uM.

2.4. Inhibition of phospholipase activity

Evaluation of the phospholipase activity of the PD-selected clones, phage and F7 peptide was performed according to the method of De Haas et al. (1968). Briefly, each of the clones (10^{11} pfu) were pre-incubated with 5μg of BpPLA$_2$-TXI. In addition, phage F7 and peptide F7 were incubated with 5μg of PLA$_2$, isolated from *Bothrops leucurus* venom with aspartic acid in position 49 (BlD-PLA$_2$) (Cecilio et al. 2013) for 30 minutes at 37°C. The amounts used for the F7 phage were 10^{11} pfu and the F7 peptide was 100 ug (1:20) and 200 ug (1:40). Then, all samples were quantified by potentiometric titration. The substrate used contained an egg yolk emulsion in the presence of 0.03M sodium deoxycholate and 0.6M CaCl$_2$. The results were expressed as percentage of inhibition.

2.5. Evaluation of the effect of F7 peptide *in vitro* inflammation model

2.5.1. Isolation of mononuclear cells from human peripheral blood

Blood was collected from healthy volunteers who had not taken any anti-inflammatory medication in the previous 15 days and had no inflammatory symptoms in

762   vacuum tubes containing heparin. Peripheral blood mononuclear cells (PBMC) were

763   isolated by Ficoll-Hypaque 1077 density gradient centrifugation (Sigma) following the

764   manufacturer's protocol. The cells were resuspended in an incomplete RPMI 1640

765   (Gibco) medium to analyze cell viability and perform cell counting by trypan blue

766   staining in a Neubauer chamber. The project was certificate by the Ethics and Research

767   (4.532.791). Approved by the Universidade Federal de Uberlândia.

768

769   2.5.2. Cell viability by MTT assay

770   Briefly, PBMC (2×10^4 cells/well) were seeded into 96-well microplates and

771   treated with different concentrations of the synthetic F7 peptide (1, 10 and 100 µM) for

772   24 hours under standard culture conditions (37°C, 95% humidified air, and 5% CO_2).

773   Control group cells were incubated in the absence of F7. Subsequently, cells were

774   incubated with 3-(4,5-dimethylthiazol-2-yl)-2,5-diphenyltetrazolium bromide (MTT)

775   (Invitrogen, USA) solution (5 mg/ml) for 4 h at 37°C. Formazan crystals were dissolved

776   by 50 µL of a solution containing 10% SDS and 0.01 M HCl in phosphate buffered saline

777   (PBS) for 18 h. The absorbance of each well was determined on a microplate reader at

778   570 nm (Multiskan GO Thermo Scientific, Waltham, MA, USA). The relative cell

779   viability (%) was calculated using the formula: % Viability = [(A570 –treated

780   cells)/(A570 –untreated cells)] x 100. Negative control cells were treated with RPMI

781   1640.

782   2.5.3. Stimulus with LPS

783   The impact of synthetic F7 peptide on cell inflammation was tested in PBMC.

784   Then, 1×10^6 cells/well were seeded into 24-well plates and treated with three

785   concentrations of the synthetic F7 peptide (1, 10 and 100 µM) for 1 hour at 37°C in 5%

786   CO_2. After this, lipopolysaccharide (LPS) (1 mg/mL) was added and the cells were

787   incubated for 24 hours at 37°C and 5% CO_2. PBMCs were centrifuged for 5 min at 1250g

788   and the supernatants was stored at -80°C for cytokine analysis.

789

790   2.5.4. Cytokines Assay in cells

791   To measure the levels of the cytokines IL-1β, tumour necrosis factor-alpha (TNF-

792   α) and IL-10, involved in the inflammation process, the supernatants of PBMC's were

selected for the assay of sandwich enzyme-linked immunosorbent assay (ELISA) using BD OptEIA Sets Human (BD, San Diego, CA). All samples were measured in triplicate. Briefly, after coating with primary anti-human IL-1β, TNF-α and IL-10 antibodies (BD) and blocking, 50 uL of supernatant samples was loaded, and biotinylated secondary anti-human IL-1B, TNF-α and IL-10 monoclonal antibodies (BD) were added, respectively. The wells were incubated with streptavidin horseradish peroxidase conjugate, and colorimetric reaction was developed with 3,3′,5,5′-tetramethylbenzidine (TMB) substrate solution (Thermo Scientific) and terminated with 2 N H_2SO_4. Then, plates were read at an absorbance of 450 nm by a plate reader (Titertek Multiskan Plus, Flow Laboratories, USA). The serum cytokine levels were determined by comparison with a standard curve obtained using recombinant human IL-1β, TNF-α and IL-10, respectively.

2.6. Evaluation of the effect of F7 peptide *in vivo* inflammation model

2.6.1. Chicken Embryos

The eggs line Hy-Line W36 were donated by Incubatório Novo Mundo (Uberlândia, Brazil). The eggs were incubated in an artificial incubator (Premium Ecológica®) at 37 °C, 58% humidity, being turned at a two -hour interval until 13 days of incubation (DI) when the tests started. The project was certificated by the Ethics and Research with Animals Committee of the Universidade Federal de Uberlândia (Nº 45/2022/CEUA/PROPP/REITO, process Nº23117.043271/2022-61).

2.6.2. Evaluation of the effect of phage F7 on embryos

To evaluate whether phage F7 interferes in the mortality rate caused by *Salmonella* Pullorum (SP), embryos were infected with ~2.13 log CFU/embryo of SP via allantoic fluid at 13 days of incubation. After 1 hour, the embryos were treated with 11 log CFU/embryo of the phage F7 or wild-type M13 (control), ECR infected by F7 or M13 (control). SP inoculated as a positive control and negative control (treated with PBS, ECR or M13) groups were entered. Each group had 12 embryos except for negative control treated with M13, or PBS, which had 5 embryos. The embryos were evaluated

823 daily for viability by ovoscopy. At 17 days of incubation, beside the mortality rate, the
824 blood of surviving embryos was collected via the allantoic vessel to cytokine analysis.

825

2.6.2.1. Cytokine analysis of chicken embryo serum

826

827 The levels of Interferon Gamma (IFN-γ), Interleukin-1 beta (IL-1β) and
828 Interleukin 10 (IL-10) in the chicken embryo serum were measured by the Elisa
829 technique. High-binding plates (Greiner Bio-One) were sensitized with embryo serum
830 diluted (1:1) in 50 mM bicarbonate buffer (pH 8.6) for 1 hour at 37°C. After 3 washes
831 with PBS-T (PBS+Tween 20 at 0.05%), the plates were blocked with 3% BSA in PBS
832 for 1 hour at 37°C. After the time, they were washed again with PBS-T for 4 times. Then
833 the plates were incubated with the antibodies, rabbit anti chicken IFN-γ IgG antibody
834 (BioRad), rabbit anti chicken IL-1β IgG antibody (BioRad) or IL-10 Polyclonal IgG
835 antibody (Thermo), diluted (1:500) in 3% BSA + PBS for 1 hour at 37oC. After 4 washes
836 with PBS-T, all plates were incubated with secondary goat anti rabbit IgG HRP (Sigma)
837 diluted (1:5000) in 3% BSA + PBS. Then washed 4 times again with PBS-T and
838 antibody/antigen binding was detected by adding the 3,3′,5,5′-tetramethylbenzidine
839 (TMB) substrate (Thermo Scientific). The reaction was stopped by the addition of 2 N
840 H_2SO_4. Reactivity was determined in a plate reader (Titertek Multiskan Plus, Flow
841 Laboratories, USA) at a wavelength of 450 nm. During the reaction, different
842 concentrations of the recombinant proteins IFN-γ, IL-1β e IL-10 (BD Biosciences, San
843 Diego, CA) were used to construct the standard curve.

844

2.6.3. Evaluation of the effect of F7 peptide *in vivo* model

845

846 To evaluate the effect of the synthetic peptide F7, each peptide control group
847 contained 5 embryos, which were inoculated with 10 and 100 uM of F7, separately
848 without the presence of SP. The negative control group was only inoculated with PBS.
849 The groups with the presence of SP, on the other hand, contained 10 embryos each and
850 were inoculated with ~3,5 log UFC/embrião of SP via allantoic fluid and after 1 hour, 10
851 or 100 uM of the F7 peptide via chorioallantoic membrane. The positive control group
852 was treated with PBS. After 24 hours, all groups with the peptide received boosters of the
853 corresponding dose. The mortality of the embryos was evaluated for 48 hours.

2.11. Statistical Analysis

Statistical analyzes were performed using GraphPad Prism 5.0 software. The data normality test (Shapiro-wilk) was carried out and non-parametric for variables without normal distribution were applied. The statistical test used was One-Way ANOVA, Kruskal-Wallis. To analysis of cytokine in chicken embryo, a relative standard curve was constructed from the absorbance values according to the respective control cytokine. The data were interpolated using Graph pad prism 9.1. So the cytokine level in chicken embryo was performed using One-Way ANOVA followed by the Tukey test. For mortality analysis we used the chi-square test followed by the binomial between two proportions. The significance was considered when $p < 0.05$ with a confidence interval (CI) of 0.95.

3.   RESULTS

3.1. Peptide Selection by Phage Display

After three rounds of selection, 20 peptides mimetic to the phospholipase inhibitor were obtained, but only 12 showed valid sequences, which we named A6, A9, A10, A11, B5, B6, C5, C6, C10, D10, E11 and F7. All of these clones consist of bacteriophages of the M13 filamentous type. What is distinctive about them is the sequence referring to the peptide to which each one is fused.

3.2. Phospholipase activity

3.2.1. Inhibition of phospholipase activity of selected phages

To evaluate the effectiveness of phage selected by PD, since such selection targeted a phospholipase inhibitor, the inhibitory profile of BpPLA$_2$-TXI was obtained through phospholipase activity. Phages B6 ($P < 0.05$) and F7 ($P < 0.005$) showed the ability to inhibit the phospholipase activity when compared to BpPLA$_2$-TXI activity. However, clone F7 obtained the highest percentage of inhibition, corresponding to 27% (Figure 1). In view of this, F7 phage was chosen as the target for the next experiments in this work.

884

885 **Figure 1. Inhibition of PLA₂ activity of phages selected by phage display**
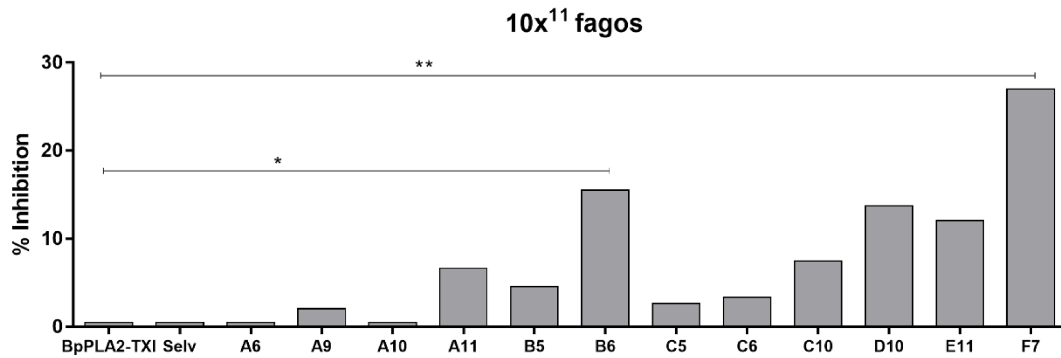
886

887 The assay was done according to De Haas and Postema (1968) and the enzyme used was BpPLA$_2$-TXI.
888 The amount of phage used in the experiment was 10^{11}. Clones B6 (p<0.05) and F7 (p<0.005) showed ability
889 to decrease phospholipase activity compared to PLA$_2$. The result of phospholipase activity was expressed
890 as % inhibition. *P<0.05; **P<0.005; ***P<0.0005 indicate statistical significance compared with the
891 control group (BpPLA$_2$-TXI).

892

893 ### 3.2.2. Inhibition of phospholipase activity of synthetic peptide and phage F7

894 In order to confirm the F7 phage and synthetic peptide ability to inhibit the PLA$_2$
895 activity, inhibition activity was performed. When compared to BlD-PLA$_2$, both were able
896 to inhibit its activity, corroborating the characteristic for which they were selected.
897 However, the phage presented a higher percentage of Inhibition than the peptide,
898 corresponding to approximately 60% (Figure 2).

899

900

901

902

903

904

905

906

907

Figure 2. Inhibition of PLA₂ activity of phage and synthetic peptide F7
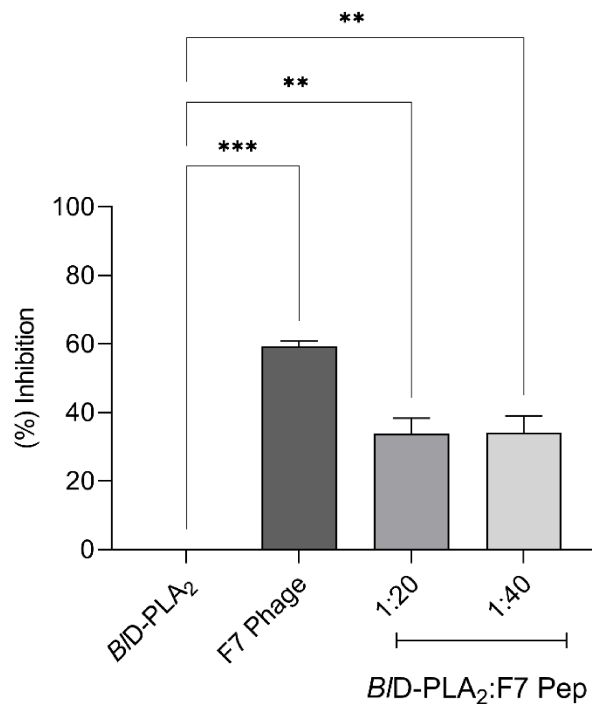
910   The assay was done according to De Haas and Postema (1968) and the enzyme used was BlD-PLA₂. The

911   amount of phage used in the experiment was 10^{11} and the synthetic peptide F7 was tested in the proportions

912   1:20 and 1:40 (enzyme:peptide, w/w). There was inhibition of the activity in all samples tested, with respect

913   to phospholipase. The highest inhibition rate corresponded to phage ($P<0.0005$). The result of

914   phospholipase activity was expressed as % inhibition. *$P<0.05$; **$P<0.005$; ***$P<0.0005$ indicate

915   statistical significance compared with the control group (BlD-PLA₂).

916

917   3.3. Effect of F7 peptide *in vitro* inflammation model

918

919   3.3.1. Cell viability of F7 in PBMC

920   To demonstrate that the F7 peptide has no cytotoxic action, we performed the

921   MTT assays using PBMC. It was shown that the F7 peptide tested at 1 µM, 10 µM and

922   100 µM concentrations did not affect cells viability and presented no significant

923   differences from controls (Figure 3).

924

925

926

927   **Figure 3. Cytotoxicity analysis of the synthetic peptide F7 in PBMC**
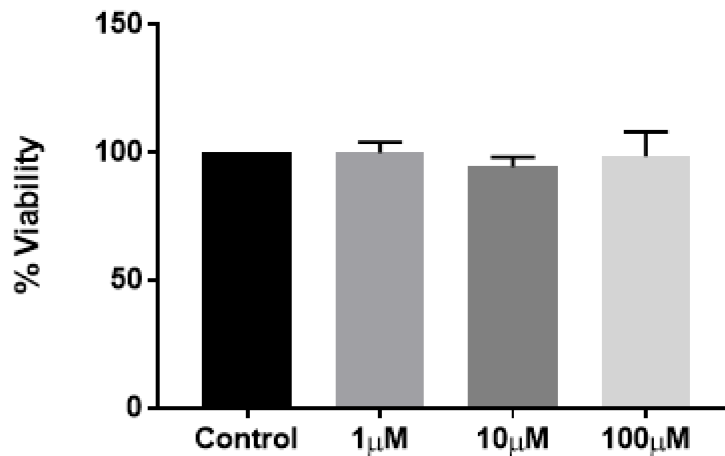
928

929   The F7 peptide showed no statistical difference when compared to control (PBMC without treatment)
930   indicating that the tested concentrations did not have a cytotoxic effect at 24 hours.

931

932   **3.3.2. Analysis of inflammatory and anti-inflammatory cytokines in the**
933   **supernatants of PBMCs**

934   To verify whether the F7 peptide can modulate an immune response, we have
935   stimulated PBMCs, and measured TNF-α, IL1β and IL-10 production. It was shown that
936   the peptide tested at 1 μM, 10 μM and 100 μM concentrations did not affect cells viability
937   (Fig 4A, 4C and 4E).

938

939   **3.3.2.1. IL-1β cytokine concentration**

940   In order to demonstrate that the F7 peptide alone could not induce a significant
941   expression of IL-1β in PBMC cells, we performed an assay in which cells were only
942   treated with F7, at three different concentrations (1, 10 and 100 uM). And in this same
943   assay, we put a positive control (LPS) that corresponds to the cell in contact only with
944   LPS, to demonstrate that the cell was susceptible to stimulation. From the results
945   obtained, we observed that the F7 peptide is not able to increase the levels of IL-1β in the
946   cells. At the three concentrations tested, the cells showed significantly low levels of
947   expression compared to cells with LPS (Figure 4A).

948   When the effect of F7 peptide on inflammation, represented by the presence of
949   LPS, was evaluated, it was able to significantly reduce IL-1β expression at concentrations
950   of 10 and 100 uM (P<0.05) (Figure 4B).

951

952   **3.3.2.2. TNF-α cytokine concentration**

953   The F7 peptide was not able to induce TNF-α (Fig 4C) production in the absence
954   of inflammatory stimulus. PBMC pretreated with the F7 synthetic peptide followed by
955   LPS stimulation for 24 hours presented significant decrease in TNF-α production (10 µM,
956   P<0,05) when compared to LPS-treated cells (Fig 4D).

957

958   **3.3.2.3. IL-10 cytokine concentration**

959   The F7 peptide was not able to induce IL-10 production in the absence of
960   inflammatory stimulus (Fig 4E) or or followed by LPS stimulation (Fig 4F).

961

962
963
964
965
966
967
968
969
970
971
972
973
974
975
976
977
978
979
980
981
982
983
984

Figure 4. Cytokines levels in supernatants of PBMC's
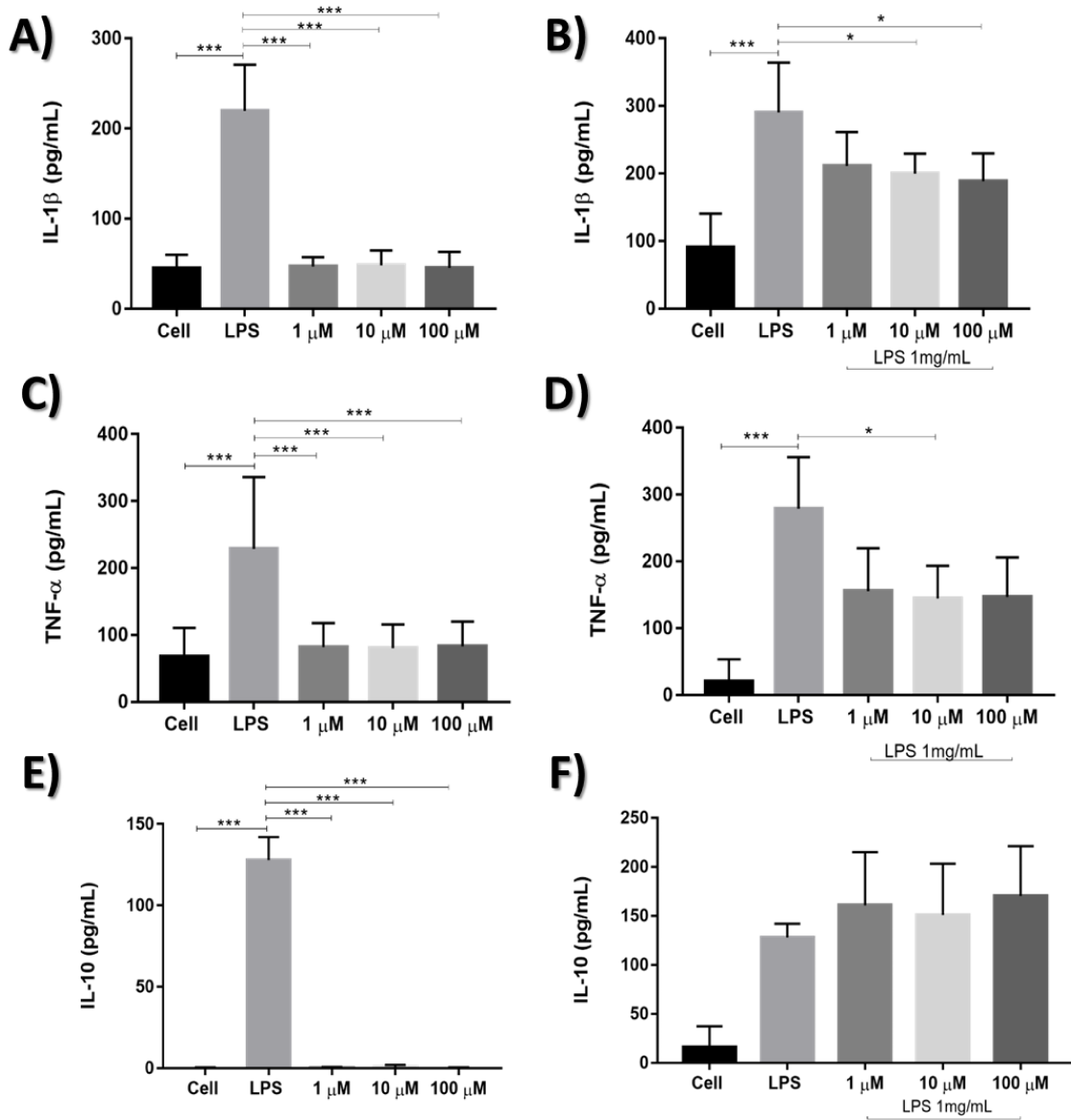
987 (A, C and E) The cells were treated with 1, 10 and 100 uM of F7 peptide for 24 hours. There was no increase

988 at the level of any cytokine with the addition of the different concentrations of the peptide tested. (B, D and

989 F) The cells were treated with 1, 10 and 100 uM of F7 peptide and after 1 hour stimulated with LPS (1

990 mg/mL) for 24 hours. At concentrations of 10 uM ($P<0,05$) and 100 uM ($P<0,05$) a reduction of IL-1β was

991 shown. At concentration of 10 uM ($P<0,05$) a reduction of TNF-α was shown. 1×10^6cells/well was used

992 and only PBMC was used for negative control (Cell); PBMC with 1 mg/mL of LPS was used for the positive

993 control (LPS). *$P<0.05$; **$P<0.005$; ***$P<0.0005$ indicate statistical significance compared with the

994 positive group (LPS).

995

996 **3.4. Effect of F7 phage and peptide chicken embryo**

3.4.1. Mortality of embryos infected with SP and treated with phage F7 or ECR infected by F7

F7 didn't raise the viability of embryos challenged with SP. However, when we treated CE with ECR infected by F7 or M13, the mortality was lower than the positive control. In positive control, 66,66% and 8.33% of embryos died after 48 and 72 hours of SP inoculation, respectively (Figure 5). On the other hand, chicken embryos challenged with SP and treated with ECR infected by F7 or M13 presented mortality rate of 8,33% after 48 hours and 41,6% (ECR+F7) and 50% (ECR+M13) after 72 horas (Figure 5).

Figure 5. Mortality of embryos challenge with SP and treated with F7 or ECR infected by F7
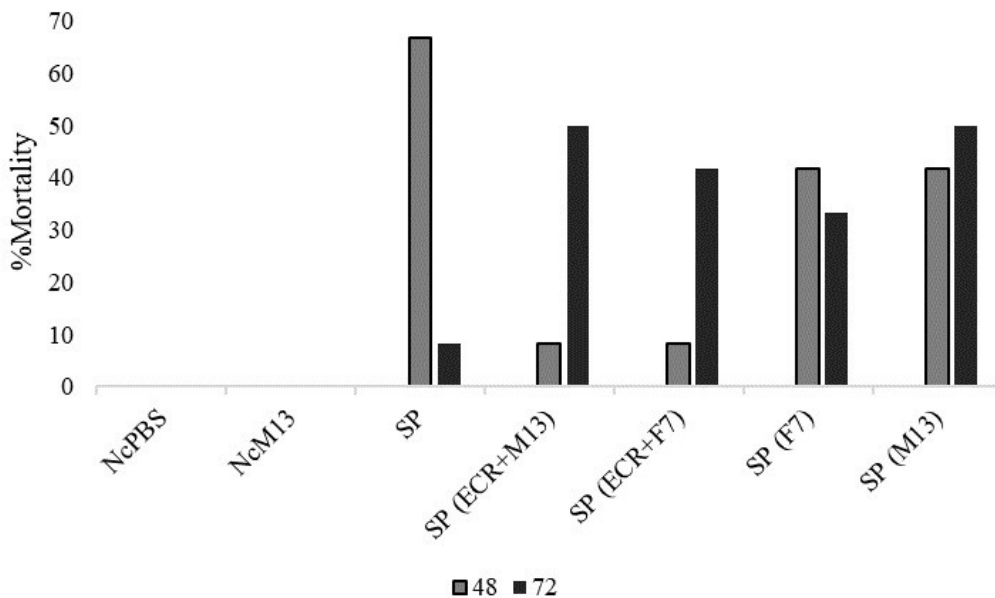
Mortality rate (%). NcPBS: Negative control group with PBS. NcM13: Negative control group with phage M13. SP: Group inoculated with SP. ECR+M13: *E.Coli* ER2738 infected by M13. ECR+F7: *E.Coli* ER2738 infected by F7. F7: phage F7. M13: Phage M13.

3.4.2. Cytokine levels in embryos challenged with SP and treated with phage F7

To evaluate the effect of phage F7 on the inflammatory profile, we quantified three cytokines that are mediators of inflammation, IFN-γ, IL-1β and IL-10 in the serum of chicken embryos. As the embryos treated with purified phage died, we tested the embryos treated with ECR infected by F7 or M13. The group treated with phage F7 reduced the expression levels of the two inflammatory cytokines (IFN-γ and IL-1β) compared to the positive control, which was the embryos in the presence of SP. However, the embryos treated with M13 or negative control didn't change the evaluated cytokines (Figure 6). Phage F7 didn't change IL-10 levels in the treated group (Figure 6C).

Figure 6. Quantification of inflammatory and anti-inflammatory cytokines in the serum of embryos
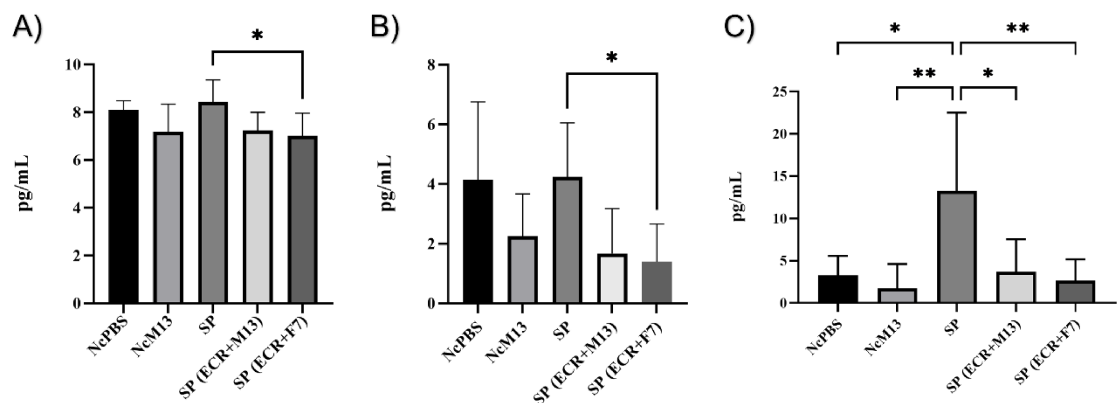
Levels (pg/mL) of IFN-γ (A); IL-1β (B) and IL-10 (C) in the serum of embryos. NcPBS: Negative control group with PBS. NcM13: Negative control group with phage M13. SP: Group inoculated with SP. ECR+M13: ECR infected with phage M13. ECR + F7: phage F7 with the presence of ECR. *P<0.05; **P<0.005 indicate statistical significance compared with the control group (SP).

3.4.3. Evaluation of the effect of F7 peptide on chicken embryos

In this assay, we found that the F7 peptide was not toxic to the embryos. However, when inflamed with SP, it was not able to prevent death during the 48 hours observed (Figure 7).

1041 **Figure 7. Percentage of embryo mortality with F7 peptide**
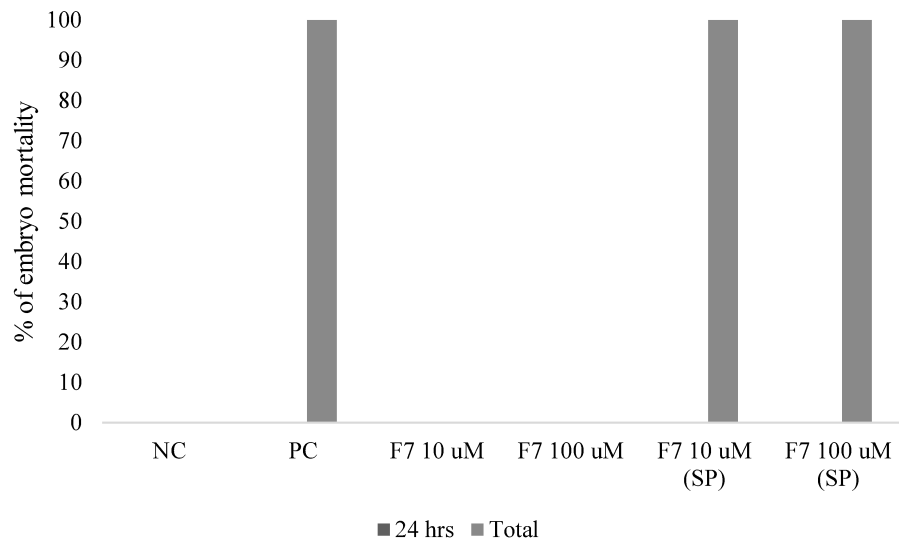
1042

1043 NC: Negative control group with PBS. PC: Positive control group with SP. F7 10 uM: Group with synthetic

1044 peptide F7 at a concentration of 10 uM. F7 100 uM: Group with synthetic peptide F7 at 100 uM

1045 concentration. F7 10 uM (SP): Group inoculated with SP and treated with synthetic peptide F7 at a

1046 concentration of 10 uM. F7 100 uM (SP): Group inoculated with SP and treated with synthetic peptide F7

1047 at 100 uM concentration.

1048

1049

1050

1051 ## 3. DISCUSSION

1052 Potential PLA_2 inhibitors were selected by phage display as it is considered an

1053 efficient molecular technique in which desirable peptides are displayed on the surface of

1054 a bacteriophage, which in this work was M13 (Zambrano-Mila et al. 2020).

1055 Phospholipase inhibition peptides were selected by phage display resulting in 20 clones,

1056 but only 12 showed valid sequences. The activity of phospholipase can be evaluated and

1057 measured in egg yolk emulsion because it provides phosphatidylcholine as a substrate.

1058 When hydrolyzed, it releases products such as fatty acids that can be titrated (De Haas et

1059 al. 1968). Among the 12 clones selected with valid sequences, clone F7 was the most

1060 successful in inhibiting $BpPLA_2$-TXI activity (Figure 1) and was therefore considered the

1061 target of study in this work.

1062 Snake venom PLA_2s belong to the group of type of secreted enzymes that are Ca^{2+}-

1063 dependent and have the catalytic site residues well conserved among different species

(Valentin and Lambeau 2000; Gutiérrez and Lomonte 2013). For a better understanding of the action and effects of clone F7, the peptide was synthesized and again tested for activity under BlD-PLA$_2$. When compared to the enzyme, the peptide showed approximately 35% inhibition of activity. This value was maintained in both concentrations analyzed. However, when the phage activity was evaluated, it was more efficient and managed to inhibit around 60% (Figure 2). This may be due to the difference in quantity between phage and peptide since they have different measurement units despite having the same sequence.

We performed test it *in vitro* in PBMCwich include lymphocytes (T cells, B cells and NK cells), monocytes and dendritic cells. In humans, the majority of cells that make up are lymphocytes, specifically CD3$^+$ T cells (Kleiveland 2015). These cells are primarily responsible for the cellular and humoral immune response (Vitetta et al. 1989) and were therefore chosen. The cytotoxicity assay showed that the F7 peptide does not cause any change in cell viability and can be used as a study model (Figure 3). To evaluate the action of the peptide on the inflammatory profile, we used LPS as a stimulus because it constitutes the cell wall of gram-negative bacteria and can induce the activation of inflammatory cytokines through toll-like receptor signaling pathways (Cui et al. 2014). For all the cytokines analyzed, LPS was able to increase the expression levels, so that it was proven that the unstimulated F7 peptide showed similar behavior to the negative control that only contained cell (Figure 4A, 4C and 4E).

In the inflammatory process, PLA$_2$'s perform hydrolysis of phospholipids, releasing arachidonic acid. This is modified into compounds called eicosanoids, which include prostaglandins and leukotrienes, which are the main mediators of inflammation (Khan and Hariprasad 2020). When evaluating two inflammatory cytokines, IL-1β and TNF-α, F7 peptide reduced their expression level at concentrations of 10µM and 100µM for the first one and 10µM for the last one (Figure 4B and 4D). In inflammation, these cytokines are positively regulated and can promote the expression of secreted PLA$_2$s through the involvement of the transcription factor NF-kB (Dore and Boilard 2019). LPS treated increased expression of the cytokine IL-10 because it prevents excessive inflammatory responses, positively regulates innate immunity, and promotes tissue repair mechanisms (Ouyang and O'Garra 2019). However, the F7 peptide did not increase the levels of IL-10 in PBMC's inoculated with LPS (Figure 4F).

From a therapeutic point of view, the use of bacteriophage has numerous advantages, among them low development cost, relatively free of side effects, high host specificity, can be considered natural antibiotic and potential impact on inflammatory response to infection (Moghadam et al. 2020). In view of this and the good inhibitory activity of phage F7, we used the model of inflammation with SP in chicken embryos proposed in the previous work to evaluate its effect. Then we tested both phage F7 and peptide F7.

The phage F7 could not lower the mortality rate of embryos challenged with SP while the ECR infected by F7 did (Figure 5). However, this event was not a result of the presence of F7 as the group treated with ECR infected with M13 had a similar effect. The ECR can inhibit the amount of SP (date don't published yet), which was probably the cause of the lower mortality in the phage-infected ECR groups.

Even with the high mortality of F7 phage-treated embryos, we quantified cytokines from F7-infected ECR-treated embryos. This is justified by the fact that the presence of the ECR allows the replication of phages, which may help in their action. Interestingly, the group challenged with SP and treated with F7-infected ECR showed a decrease in the pro-inflammatory cytokines IFN-γ and IL-1β in relation to the positive control group (Figure 6A and 6B). Despite this assay having the presence of the ECR bacteria along with the phages, the result remains significant as the embryos that were inoculated with the wild-type phage M13 also with the presence of the bacteria had no effect on the cytokines.

Another interesting event is that IFN-γ and IL-1β levels of negative control were similar to the positive control levels. This probably happened because these cytokines are released at the beginning of inflammation, characterizing the disease resistance phase, and as the blood collection was after 3 days of inoculation, a modulation induction phase is present (Kogut and Arsenault 2017). In any case, the results make clear an action of the F7 phage on the level of pro-inflammatory cytokines, similar to what happened *in vitro*.

The post-inflammation modulation phase is supported by the increase in IL-10 only in positive control embryos (Figure 6C). However the presence of F7 didn't increase the IL-10. Phospholipase has an early action in the inflammatory cycle. Thus, one explanation for this event is that the phospholipase inhibitor would only act in the initial phases of the inflammatory process.

We tested the peptide F7 in chicken embryo challenged with SP. However, the peptide couldn't avoid the high mortality (Figure 7). It is essential to mention that we quantify the SP on the McFarland scale, which is a visual tool that is often imprecise but widely used since the titration on plate takes approximately 24 hours. Then, after the inoculation, we titrate the exact amount of SP on the plate. Using ~2 log UFC/embrião of SP at 13 days of incubation, there is high mortality, but some chicken embryos survive. However, we used ~3.5 log UFC/embryo and they all died. Up to 12 days of incubation mortality caused by SP can be high. As the embryo has a fast metabolism, the difference in hours of the developmental stage can interfere with its response. So, in addition to the greater amount of bacteria, a small difference in embryonic age can be the cause of greater mortality in a shorter time.

Salmonella Pullorum causes severe systemic effects on embryos and chicks in the first days of life, leading to high mortality and damage. Although useful to many researchers, embryos infected with SP may not be the best alternative to evaluate the F7 peptide since SP causes a serious systemic disease. While the phospholipase inhibitor F7 acts at an early stage of inflammation and probably a mild and localized model of inflation may be more interesting. Thus, although the phage F7 has shown effects on the levels of inflammatory cytokines in chicken embryos, it is important to look for another model of local and mild inflammation to assess the real effect of F7 *in vivo*.

4. CONCLUSION

The peptide mimetic to the phospholipase inhibitor that was selected by PD was able to modulate the immune response such that both phage F7 and the peptide interfered with the expression of inflammatory cytokines. A *in vivo* model of local and mild inflammation should be tested to assess the effects of F7 *in vivo*.

5.   REFERENCES

Barbas C, Burton D, Scott J, Silverman G (2001) Phage display: a laboratory manual. Cold Spring Harbor Laboratory Press, New York

Barderas R, Benito-Peña E (2019) The 2018 Nobel Prize in Chemistry: phage display of peptides and antibodies. Anal Bioanal Chem 411:2475–2479. https://doi.org/10.1007/s00216-019-01714-4

Batsika CS, Gerogiannopoulou ADD, Mantzourani C, Vasilakaki S, Kokotos G (2021) The design and discovery of phospholipase A2 inhibitors for the treatment of inflammatory diseases. Expert Opin Drug Discov 16:1287–1305. https://doi.org/10.1080/17460441.2021.1942835

Cecilio AB, Caldas S, De Oliveira RA, Santos ASB, Richardson M, Naumann GB, Schneider FS, Alvarenga VG, Estevão-Costa MI, Fuly AL, Eble JA, Sanchez EF (2013) Molecular characterization of Lys49 and Asp49 phospholipases A2 from snake venom and their antiviral activities against Dengue virus. Toxins (Basel) 5:1780–1798. https://doi.org/10.3390/toxins5101780

Chinnasamy S, Selvaraj G, Selvaraj C, Kaushik AC, Kaliamurthi S, Khan A, Singh SK, Wei DQ (2020) Combining in silico and in vitro approaches to identification of potent inhibitor against phospholipase A2 (PLA2). Int J Biol Macromol 144:53–66. https://doi.org/10.1016/j.ijbiomac.2019.12.091

Cui J, Chen Y, Wang HY, Wang RF (2014) Mechanisms and pathways of innate immune activation and regulation in health and cancer. Hum Vaccines Immunother 10:3270–3285. https://doi.org/10.4161/21645515.2014.979640

De Haas G, Postema N, Nieuwenhuize W, Van Deenen L (1968) Purification and properties of an anionic zymogen of phospholipase A from porcine pancreas. Biochim Biophys Acta. https://doi.org/10.1016/0005-2744(68)90249-0

Dore E, Boilard E (2019) Roles of secreted phospholipase A 2 group IIA in inflammation and host defense. Biochim Biophys Acta - Mol Cell Biol Lipids 1864:789–802. https://doi.org/10.1016/j.bbalip.2018.08.017

Fala L (2015) Trulicity (Dulaglutide): A New GLP-1 Receptor Agonist Once-Weekly Subcutaneous Injection Approved for the Treatment of Patients with Type 2 Diabetes. Am Heal drug benefits 8:131–4

Ferreira FB, Gomes MSR, de Souza DLN, Gimenes SNC, Castanheira LE, Borges MH, Rodrigues RS, Yoneyama KAG, Brandeburgo MIH, Rodrigues VM (2013) Molecular cloning and pharmacological properties of an acidic PLA2 from Bothrops pauloensis snake venom. Toxins (Basel) 5:2403–2419. https://doi.org/10.3390/toxins5122403

Gimenes SNC, Ferreira FB, Silveira ACP, Rodrigues RS, Yoneyama KAG, Izabel Dos Santos J, Fontes MRDM, De Campos Brites VL, Santos ALQ, Borges MH, Lopes DS, Rodrigues VM (2014) Isolation and biochemical characterization of a γ-type phospholipase A2 inhibitor from Crotalus durissus collilineatus snake serum. Toxicon 81:58–66. https://doi.org/10.1016/j.toxicon.2014.01.012

Gutiérrez JM, Lomonte B (2013) Phospholipases A2: Unveiling the secrets of a functionally versatile group of snake venom toxins. Toxicon 62:27–39.

1202   https://doi.org/10.1016/j.toxicon.2012.09.006

1203 Ha VT, Lainscek D, Gesslbauer B, Jarc-Jovicic E, Hyotylainen T, Ilc N, Lakota K,
1204   Tomsic M, Van De Loo FAJ, Bochkov V, Petan T, Jerala R, Mancek-Keber M
1205   (2020) Synergy between 15-lipoxygenase and secreted PLA2promotes
1206   inflammation by formation of TLR4 agonists from extracellular vesicles. Proc Natl
1207   Acad Sci U S A 117:25679–25689. https://doi.org/10.1073/pnas.2005111117

1208 Hamzeh-Mivehroud M, Alizadeh AA, Morris MB, Bret Church W, Dastmalchi S (2013)
1209   Phage display as a technology delivering on the promise of peptide drug discovery.
1210   Drug Discov Today 18:1144–1157. https://doi.org/10.1016/j.drudis.2013.09.001

1211 Hiu JJ, Yap MKK (2020) Cytotoxicity of snake venom enzymatic toxins: Phospholipase
1212   A2 and L-amino acid oxidase. Biochem Soc Trans 48:719–731.
1213   https://doi.org/10.1042/BST20200110

1214 Khan MI, Hariprasad G (2020) Human secretary phospholipase a2 mutations and their
1215   clinical implications. J Inflamm Res 13:551–561.
1216   https://doi.org/10.2147/JIR.S269557

1217 Kleiveland CR (2015) Peripheral blood mononuclear cells. In: The impact of food
1218   bioactives on health. pp 161–167. https://doi.org/10.1007/978-3-319-16104-4_15

1219 Kogut MH, Arsenault RJ (2017) Immunometabolic phenotype alterations associated with
1220   the induction of disease tolerance and persistent asymptomatic infection of
1221   Salmonella in the chicken intestine. Front Immunol 8:1–7.
1222   https://doi.org/10.3389/fimmu.2017.00372

1223 Ledsgaard L, Kilstrup M, Karatt-Vellatt A, McCafferty J, Laustsen AH (2018) Basics of
1224   antibody phage display technology. Toxins (Basel) 10.
1225   https://doi.org/10.3390/toxins10060236

1226 Macdougall IC (2008) Novel erythropoiesis-stimulating agents: A new era in anemia
1227   management. Clin J Am Soc Nephrol 3:200–207.
1228   https://doi.org/10.2215/CJN.03840907

1229 Mahmud S, Parves MR, Riza YM, Sujon KM, Ray S, Tithi FA, Zaoti ZF, Alam S, Absar
1230   N (2020) Exploring the potent inhibitors and binding modes of phospholipase A2
1231   through in silico investigation. J Biomol Struct Dyn 38:4221–4231.
1232   https://doi.org/10.1080/07391102.2019.1680440

1233 Mimmi S, Maisano D, Quinto I, Iaccino E (2019) Phage Display: An Overview in Context
1234   to Drug Discovery. Trends Pharmacol Sci 40:87–91.
1235   https://doi.org/10.1016/j.tips.2018.12.005

1236 Moghadam MT, Amirmozafari N, Shariati A, Hallajzadeh M, Mirkalantari S,
1237   Khoshbayan A, Jazi FM (2020) How phages overcome the challenges of drug
1238   resistant bacteria in clinical infections. Infect Drug Resist 13:45–61.
1239   https://doi.org/10.2147/IDR.S234353

1240 Moreira V, Leiguez E, Janovits PM, Maia-Marques R, Fernandes CM, Teixeira C (2021)
1241   Inflammatory Effects of Bothrops Phospholipases A2: Mechanisms Involved in
1242   Biosynthesis of Lipid Mediators and Lipid Accumulation. Toxins (Basel) 13.
1243   https://doi.org/10.3390/toxins13120868

1244 Mruwat R, Yedgar S, Lavon I, Ariel A, Krimsky M, Shoseyov D (2013) Phospholipase

A2 in experimental allergic bronchitis: A lesson from mouse and rat models. PLoS One 8:2–10. https://doi.org/10.1371/journal.pone.0076641

Murakami M, Taketomi Y (2015) Phospholipase A 2. Bioact Lipid Mediat Curr Rev Protoc 23–42. https://doi.org/10.1007/978-4-431-55669-5_2

Nikolaou A, Kokotou MG, Vasilakaki S, Kokotos G (2019) Small-molecule inhibitors as potential therapeutics and as tools to understand the role of phospholipases A2. Biochim Biophys Acta - Mol Cell Biol Lipids 1864:941–956. https://doi.org/10.1016/j.bbalip.2018.08.009

Nolin JD, Murphy RC, Gelb MH, Altemeier WA, Henderson WR, Hallstrand TS (2019) Function of secreted phospholipase A 2 group-X in asthma and allergic disease. Biochim Biophys Acta - Mol Cell Biol Lipids 1864:827–837. https://doi.org/10.1016/j.bbalip.2018.11.009

Ouyang W, O'Garra A (2019) IL-10 Family Cytokines IL-10 and IL-22: from Basic Science to Clinical Translation. Immunity 50:871–891. https://doi.org/10.1016/j.immuni.2019.03.020

Perego F, Wu MA, Valerieva A, Caccia S, Suffritti C, Zanichelli A, Bergamaschini L, Cicardi M (2019) Current and emerging biologics for the treatment of hereditary angioedema. Expert Opin Biol Ther 19:517–526. https://doi.org/10.1080/14712598.2019.1595581

Valentin E, Lambeau G (2000) What can venom phospholipases A2 tell us about the functional diversity of mammalian secreted phospholipases A2? Biochimie 82:815–831. https://doi.org/10.1016/S0300-9084(00)01168-8

Vasquez AM, Mouchlis VD, Dennis EA (2018) Review of four major distinct types of human phospholipase A2. Adv Biol Regul 67:212–218. https://doi.org/10.1016/j.jbior.2017.10.009

Vitetta ES, Fernandez-Botran R, Myers CD, Sanders VM (1989) Cellular Interactions in the Humoral Immune Response. Adv Immunol 45:1–105. https://doi.org/10.1016/S0065-2776(08)60692-6

Zambrano-Mila MS, Blacio KES, Vispo NS (2020) Peptide Phage Display: Molecular Principles and Biomedical Applications. Ther Innov Regul Sci 54:308–317. https://doi.org/10.1007/s43441-019-00059-5

Zhang H, Gao Y, Wu D, Zhang D (2020) The relationship of lipoprotein-associated phospholipase A2 activity with the seriousness of coronary artery disease. BMC Cardiovasc Disord 20:1–6. https://doi.org/10.1186/s12872-020-01580-4

ExPASy Translate tool. http://web.expasy.org/translate/